2005

Solution Of Electromagnetic Scattering Parameters And Radiation Patterns Of Arbitrary Body Of Revolution Radiators

Wendell Brokaw
University of Central Florida

SOLUTION OF ELECTROMAGNETIC SCATTERING PARAMETERS AND RADIATION PATTERNS OF ARBITRARY BODY OF REVOLUTION RADIATORS

by

WENDELL A. BROKAW
B.S. University of Central Florida, 2000
M.S. University of Central Florida, 2003

A dissertation submitted in partial fulfillment of the requirements
for the degree of Doctor of Philosophy
in the School of Electrical Engineering and Computer Science
in the College of Engineering and Computer Science
at the University of Central Florida
Orlando, Florida

Fall Term
2005

Major Professor: Thomas X. Wu

ABSTRACT

A novel full wave analysis method to determine the scattering parameters and the radiation field intensities of arbitrary Body of Revolution (BOR) radiators consisting of impenetrable media is explored through derived components of modal analysis and the method of moments (MoM). Modal excitation is utilized to excite the structural feed; allowing for a more accurate measure of the scattering parameters of the total structure as opposed to the use of external excitation sources. The derivation of the mode matching method introduces a novel approach to achieving a frequency independent coupling matrix that will reduce the computational requirements for iterations utilized in the solution of multi-step discontinuous junctions. An application of interpolation functions across a single element of the MoM's traditional basis function approach allows for the ability to facilitate the meshing of complex structures. The combined field integral equation method is implemented in the analysis method to assure the mitigation of spurious solutions that can be problematic for electric field integral equation solutions that are predominant in many MoM based codes. The structures of interest represent bodies of revolution (BOR), which maintains that the structures must exhibit rotational symmetry about the longitudinal, or directional, axis. The complexity of the domain of structures that can be treated with the analysis method will be significantly reduced

through the use of BOR symmetry of the structure. The proposed method for the solution of structures will include the comprehensive treatment of Boundary Value Problems (BVP's) through modal analysis, aperture treatment, and an application of the method of moments.

Solutions for BOR radiating structures can be divided into two regions of analytical concern, the inner guided wave region and the outer radiating region. Modal analysis will be used to determine the scattering matrix of the inner guided wave region. The modal analysis will consist of subdividing the inner region into a number of finite step discontinuities, and the method of mode matching will be implemented to numerically solve the BVP's at each step discontinuity for a finite number of modal field distributions. The surface field equivalence principle will be applied to treat the aperture in order to produce an equivalent problem that supplants a source magnetic current density and an induced electric current density across the aperture that will radiate in the presence of the outer structural material of the BOR radiator. An algorithm utilizing the MoM is applied to solve integral equations that are defined to treat the surfaces of the BOR structure using electromagnetic boundary conditions. The application of the MoM will develop the field intensities on the aperture with complete consideration of the outer structural boundaries of the BOR radiator. The field intensities on the aperture will be related to the inner guided wave region through electromagnetic boundary conditions, and an admittance matrix will be numerically calculated. The admittance matrix will then apply to the inner guided wave region's scattering matrix to determine the reflection and transmission coefficients at the input of the BOR radiator.

The comprehensive solution method will be applied to a variety of BOR structures; the electromagnetic solutions of the structures as obtained by the proposed method shall be verified for accuracy against comparative analysis of the structures using known computational packages that have been generally accepted throughout industry with respect to design capabilities.

ACKNOWLEDGMENTS

I would like to thank the many people that have contributed to this topic through their conversation and direction. I extend my deepest gratitude to Dr. Thomas Wu for his unyielding passion in the field of computational electromagnetics. His direction for this research topic has been invaluable. I would like to thank Jie Chen for his invaluable contribution to realizing this research in his conversation and effort. This research was realized through financial and technical assistance of Harris Corporation to whom I offer my gratitude and recognize Greg Showman, Rich Folio, Dennis Eaton, and Joe Marcoux for their support, for without their efforts this research could not have been undertaken. I would like to thank Gary Defauw for his coordination of modeling support as extended by the Ansoft Corporation through a general license that included the use of their full modeling packages. I would also like to thank the members of the advisory committee for their time and consideration of the topic of presentation. Finally, I dedicate this research to the memory of my father Paul Harry Brokaw.

TABLE OF CONTENTS

LIST OF FIGURES

LIST OF TABLES

CHAPTER 1 INTRODUCTION

Closed form analytical solutions that characterize electromagnetic scattering and radiation become increasingly more difficult to apply within the field of problems that are presented throughout industry and academia. The ability to produce the systems that exhibit stringent operating requirements with feasible cost efficiency is only made possible through the application of numerical methods to develop the fundamental models used to predict such systems. Applied numerical methods, with respect to electromagnetic applications [1-4], can be employed in such a way as to develop unique tools that characterize segments of the complete analysis of a system. These tools can be integrated to form comprehensive methods for treating subsets of systems to approximate scattering and radiation characteristics as defined through electromagnetic field theory [5-13]. Approximations which include both scattering and radiation problems that occupy interest in the present day design endeavors are arbitrarily shaped three dimensional structures. The complexity of the domain of structures that can be treated with a general solver will be significantly reduced through the use of symmetries that are present in the structure [14-21]. Structures that exhibit rotational symmetry are defined as bodies of revolution (BOR). Through the use of BOR symmetry, a novel methodical treatment to determine the scattering parameters and the radiation field intensities from circular

symmetric feed horns consisting of impenetrable media will be explored. A prescribed method will be introduced that will significantly reduce the computational time required to solve arbitrarily shaped three dimensional structures exhibiting BOR symmetry.

Conical horn radiators continue to be a mainstay component in many terrestrial and space-borne antenna systems [22-27] due to the inherent advantages of symmetry, polarization diversity, and adaptability for utilization as feed components in antenna systems that require design frequencies that span the electromagnetic spectrum. The symmetry of conical horns introduces an opportunity to treat the family of radiators as BOR, which will reduce the dimensional complexity with respect to operations in any particular coordinate system. It has been shown that the methods employed through modal analysis [28-32] and aperture treatments [33-37] have produced physical systems whose radiation patterns correlate closely with predicted formulations. It is a contention that a novel procedure can be implemented to decrease the time necessary for computational convergence of structures that would otherwise go untreated by the majority of commercially available simulation packages. This procedure would effectively quantify both scattering parameters and radiation patterns of an aperture including the external contributions of the outer surface of the structure. The procedure can be extended to characterize scattering and radiation when the complete antenna system is a BOR structure (i.e. a reflector antenna system) containing 200,000 unknowns (linear systems of equations) or less. Several theoretical treatments will be applied to obtain solutions enveloped in the proposed procedure. The applied procedure will include modal analysis and excitation, equivalence models for the treatment of apertures,

and the method of moments for the solution of simultaneous systems of equations.

Mode matching, a subset of modal analysis [38-45], is a method for solving successive junctions for scattering parameters within a structure by satisfying electromagnetic boundary conditions. The application to the conical horn will be through the division of the continuous taper section of the horn into a finite number of step discontinuities. Electromagnetic boundary conditions are established at each of the step discontinuities and the junction is subsequently solved [53-56]. A novel approach to determine a frequency independent coupling matrix is developed to reduce the successive re-calculation that would be necessary at each step discontinuity. The mode matching procedure will ultimately yield the scattering matrix [30, 41] that provides the relation of the forward and backward propagating modes at the feed and aperture planes of the conical horn structure. Typically, an external source such as a dipole is used for the excitation of the internal region of a guided wave structure. Resultant to this external excitation method, the voltage to standing wave ratio (VSWR) is estimated using a method that extends the structural geometry by a wavelength, and probes the current along this segment which can deliver only the magnitude of the return loss with respect to scattering parameters. A novel approach of using modal quantities as the excitation of the inner region allows for an accurate resolution of scattering parameters in both magnitude and phase. Construction of a terminating admittance matrix that can be related to the outer conducting boundaries will be utilized to relate the outer radiating environment to the inner guided wave propagation. A relationship of the scattering matrix of the radiator to the aperture and outer boundary coupled impedance values will allow

for the determination of reflection and transmission at the input of the BOR radiator.

The surface equivalence principle [5, 7, 8] is applied to facilitate the analysis of the aperture of the radiating BOR structure. The application of the equivalence principle allows for the field analysis of the outer unbounded region of the BOR structure, which is external to the radiating aperture. Knowledge of the tangential field components at the aperture is required in order to satisfy the definition of the uniqueness theorem [5, 7]. The surface equivalence principle follows from the uniqueness theorem, and allows for the simplification of a problem when the equivalent problem preserves the boundary conditions of the original problem for the radiated fields external to a defined surface. The application of the surface equivalence principle will allow for establishment of an equivalent magnetic current distribution across the aperture, and the aperture will be replaced by a perfect electric conductor (PEC) segment. Utilizing Love's equivalence principle, the electric and magnetic field intensities within the inner region of the horn will be set equal to zero, and the problem is now reduced to an equivalent magnetic current distribution radiating in the presence of the closed impenetrable surfaces of the conical horn [7, 8, 46]. An electric surface current is then induced to maintain zero tangential electric field on the external surfaces of the horn. A set of combined field integral equations (CFIE) can be used to solve for the eigenvalues that will lead to the assembly of an input admittance matrix at the aperture of the horn.

The moment method is a general procedure for the solution of linear electromagnetic field problems based on the transformation of field equations into a system of linear equations in terms of unknown currents [46-52]. The MoM procedure

will be used to develop the CFIE into a system of linear equations to be solved through the use of an iterative solution algorithm. A novel approach using two linear interpolation functions over a single element as opposed to the traditional use of basis functions that span two elements is implemented in this treatment used to discretize the two dimensional BOR geometry for current resolution. The advantage to this approach is to facilitate fitting the interpolation functions to complex geometries as opposed to considerations that must be taken when fitting basis functions and weighting functions that span two elements of a discretized geometry.

Future applications of the detailed procedure will include integration of the method with additional treatments that afford the functionality of modeling electromagnetically large structures. The combination of methods will allow for the practical modeling of large scale phased arrays, reflector antenna system systems, and planar antenna systems that would encapsulate solution of problems that exhibit unknowns in excess of one billion. Future applications that will be further investigated for integration with the proposed method, adding the functionalities previously mentioned, will include iterative methods [58-62], the domain decomposition method [63-65], preconditioning techniques [66, 67], and fast multipole methods [68-70].

CHAPTER 2 MODAL ANALYSIS

Salient issues that will be presented in this chapter includes the equivalent transmission line theory, which correlates field equations with circuit equations, and the derivation of mode matching inclusive of a novel approach to the development of a frequency independent coupling matrix, $\mathbf{P}$, that will negate the necessity to re-calculate the matrix at successive step discontinuities.

2.1 Electromagnetic Metallic Waveguide Theory

Consider a uniform homogeneous and isotropic hollow metallic waveguide. We can establish Maxwell's equations for time harmonic fields without impressed sources as:

$$\nabla \times \mathbf{E} = -j\omega\mu\mathbf{H} \tag{2.1}$$

$$\nabla \times \mathbf{H} = j\omega\varepsilon\mathbf{E} \tag{2.2}$$

The general solution of Maxwell's equations can be obtained as the superposition of the normal modes that belong to H modes, or Transverse Electric (TE) modes, and E modes, or Transverse Magnetic (TM) modes. The electric and magnetic field components of each mode, assuming propagation in the z direction, can be expressed through vector potentials that can be decomposed into transverse and longitudinal components. To assist

in the decomposition of the transverse and longitudinal components we introduce the following:

$$\nabla = \nabla_t + \nabla_z \tag{2.3}$$

where $\nabla_z = \frac{\partial}{\partial z}\hat{\mathbf{a}}_z$, and ∇_t is the gradient operator that is transverse to the z-axis. The vector field intensities that are defined over the cross-section of the waveguide can be quantified as the superposition of the modal eigenfunctions, with the constraint that the vector function is considered to be well-behaved [31].

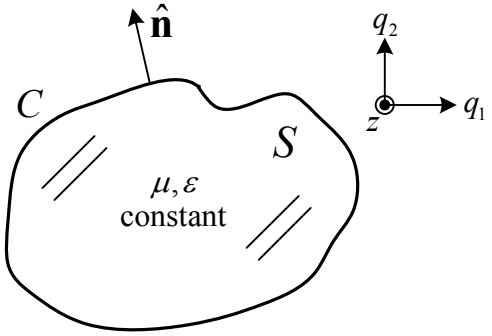

Figure 2-1 Metallic waveguide of arbitrary cross-section and reference coordinates.

2.1.1 TE and TM Modes in Hollow Waveguides

Maxwell's equations can be used to establish that the electromagnetic field components that are transverse to the direction of propagation can be expressed as a series of modal field quantities:

$$\mathbf{E}_t\left(q_1,q_2,z\right)=\sum_{n=1}^{\infty}\mathbf{E}_{t,n}\left(q_1,q_2,z\right) \tag{2.4}$$

$$\mathbf{H}_t\left(q_1,q_2,z\right)=\sum_{n=1}^{\infty}\mathbf{H}_{t,n}\left(q_1,q_2,z\right) \tag{2.5}$$

$\mathbf{E}_{t,n},\mathbf{H}_{t,n}$ being the transverse electric and magnetic fields of the *n*-th mode, q_1,q_2 are the coordinates in the transverse plane, and z is defined as the direction of propagation, as shown in Figure 2-1. The entire modal set can be decomposed into TE or H modes, and TM or E modes.

Considering H modes, the condition $\mathbf{E}_z=0$ exists. Using (2.1), (2.3), and decomposing the electromagnetic fields into transverse and longitudinal components, we can express

$$\left(\nabla_t+\nabla_z\right)\times\mathbf{E}_t=-j\omega\mu\left(\mathbf{H}_t+\mathbf{H}_z\right) \tag{2.6}$$

Consequently, for boundary value problems (BVP) will be of consequence to modal analysis, we only need to consider the transverse field components which results as

$$\nabla_z\times\mathbf{E}_t=-j\omega\mu\mathbf{H}_t \tag{2.7}$$

Similarly, substituting (2.3) into (2.2) and decomposing the magnetic term yields

$$\left(\nabla_t+\nabla_z\right)\times\left(\mathbf{H}_t+\mathbf{H}_z\right)=j\omega\varepsilon\mathbf{E}_t \tag{2.8}$$

and for the transverse field components

$$\nabla_t\times\mathbf{H}_z+\nabla_z\times\mathbf{H}_t=j\omega\varepsilon\mathbf{E}_t \tag{2.9}$$

Mathematical operations on (2.7) and the insertion of equation (2.9) produce

$$\mathbf{E}_t = \frac{j\omega\mu}{k_c^2}\hat{\mathbf{a}}_z \times \nabla_t H_z \tag{2.10}$$

Similarly, mathematical operations on (2.7) and the insertion of equation (2.10) produce

$$\mathbf{H}_t = \frac{1}{k_c^2}\nabla_t\left(\frac{\partial H_z}{\partial z}\right) \tag{2.11}$$

where

$$k = \omega\sqrt{\mu\varepsilon} \tag{2.12}$$

is the wave number of the the media, and the cutoff wave number, k_c, is related to the cutoff frequency as

$$k_c = \omega_c\sqrt{\mu\varepsilon} \tag{2.13}$$

Also, the cutoff wave number and the guide wave number, k_z, have the following relationship to the wave number of the media

$$k_c = \sqrt{k^2 - k_z^2} \tag{2.14}$$

Considering E modes, $\mathbf{H}_z = 0$ exists. Using (2.1), (2.3), and decomposing the electromagnetic fields into transverse and longitudinal components, we can express

$$\left(\nabla_t + \nabla_z\right)\times\left(\mathbf{E}_t + \mathbf{E}_z\right) = -j\omega\mu\mathbf{H}_t \tag{2.15}$$

Again, for BVP's consequential to modal analysis, we only need to consider the transverse field components which results as

$$\nabla_t \times \mathbf{E}_z + \nabla_z \times \mathbf{E}_t = -j\omega\mu\mathbf{H}_t \tag{2.16}$$

Similarly, substituting (2.3) into (2.2) and decomposing the magnetic term yields

$$\left(\nabla_t + \nabla_z\right) \times \mathbf{H}_t = j\omega\varepsilon\left(\mathbf{E}_t + \mathbf{E}_z\right) \tag{2.17}$$

and for the transverse field components

$$\nabla_z \times \mathbf{H}_t = j\omega\varepsilon\mathbf{E}_t \tag{2.18}$$

Mathematical operations on (2.18) and insertion into (2.16) produce

$$\mathbf{H}_t = \frac{-j\omega\varepsilon}{k_c^2}\hat{\mathbf{a}}_z \times \nabla_t E_z \tag{2.19}$$

Similarly, mathematical operations on (2.18) and insertion into (2.19) produce

$$\mathbf{E}_t = \frac{1}{k_c^2}\nabla_t\left(\frac{\partial E_z}{\partial z}\right) \tag{2.20}$$

2.2 Equivalent Transmission Lines

Evaluation of the modal field quantities can be difficult when applying Maxwell's Equations directly. The use of equivalent transmission line theory can reduce the complexity of the field relations that must be solved. The transmission line theory is used to produce a more palatable conceptual representation for field manipulations through relationships that correlate field equations to circuital equations.

Consider the H modes, we establish the following equation

$$H_z = h_z\left(q_1, q_2\right)\left[Ae^{-jk_z z} + Be^{jk_z z}\right] \tag{2.21}$$

Inserting (2.21) into (2.10) and (2.11) yields

$$\mathbf{E}_t = \frac{j\omega\mu}{k_c^2}\hat{\mathbf{a}}_z \times \nabla_t h_z \left[Ae^{-jk_z z} + Be^{jk_z z} \right]$$
$$= \hat{\mathbf{a}}_z \times \nabla_t h_z \left[\frac{j\omega\mu}{k_c^2}\left(Ae^{-jk_z z} + Be^{jk_z z} \right) \right]$$

and

$$\mathbf{H}_t = \frac{1}{k_c^2}\left(-jk_z\right)\nabla_t h_z \left[Ae^{-jk_z z} - Be^{jk_z z} \right]$$
$$= -\nabla_t h_z \left[\frac{jk_z}{k_c^2}\left(Ae^{-jk_z z} - Be^{jk_z z} \right) \right]$$

We can establish the transverse vectors

$$\mathbf{e}_t = \hat{\mathbf{a}}_z \times \nabla_t h_z \tag{2.22}$$

$$\mathbf{h}_t = -\nabla_t h_z \tag{2.23}$$

We can also define

$$V\left(z\right) = \frac{j\omega\mu}{k_c^2}\left(Ae^{-jk_z z} + Be^{jk_z z} \right) \tag{2.24}$$

$$I\left(z\right) = \frac{jk_z}{k_c^2}\left(Ae^{-jk_z z} - Be^{jk_z z} \right) \tag{2.25}$$

Similarly, for E modes, we obtain the following equation

$$E_z = e_z\left(q_1, q_2\right)\left[Ae^{-jk_z z} - Be^{jk_z z} \right] \tag{2.26}$$

Inserting (2.26) into (2.19) and (2.20) leads to

$$\begin{aligned}\mathbf{E}_t &= \frac{1}{k_c^2}\left(-jk_z\right)\nabla_t e_z\left[Ae^{-jk_z z}+Be^{jk_z z}\right]\\ &= \nabla_t e_z\left[\frac{-jk_z}{k_c^2}\left(Ae^{-jk_z z}+Be^{jk_z z}\right)\right]\end{aligned}$$

and

$$\begin{aligned}\mathbf{H}_t &= \frac{-j\omega\varepsilon}{k_c^2}\hat{\mathbf{a}}_z\times\nabla_t e_z\left[Ae^{-jk_z z}-Be^{jk_z z}\right]\\ &= \hat{\mathbf{a}}_z\times\nabla_t e_z\left[\frac{-j\omega\varepsilon}{k_c^2}\left(Ae^{-jk_z z}-Be^{jk_z z}\right)\right]\end{aligned}$$

We can establish the transverse vectors

$$\mathbf{e}_t = \nabla_t e_z \tag{2.27}$$

$$\mathbf{h}_t = \hat{\mathbf{a}}_z\times\nabla_t e_z \tag{2.28}$$

We can also define

$$V\left(z\right) = \frac{-jk_z}{k_c^2}\left(Ae^{-jk_z z}+Be^{jk_z z}\right) \tag{2.29}$$

$$I\left(z\right) = \frac{-j\omega\varepsilon}{k_c^2}\left(Ae^{-jk_z z}-Be^{jk_z z}\right) \tag{2.30}$$

Considering both H and E modes, $V(z)$ and $I\left(z\right)$ satisfy the transmission line equation

$$\begin{aligned}\frac{dV\left(z\right)}{dz} &= -jk_z Z_C I\left(z\right)\\ \frac{dI\left(z\right)}{dz} &= -jk_z Y_C V\left(z\right)\end{aligned} \tag{2.31}$$

where the corresponding characteristic impedance is

$$Z_C = \begin{cases} \dfrac{\omega\mu}{k_z} & \text{for H modes} \\ \dfrac{k_z}{\omega\varepsilon} & \text{for E modes} \end{cases} \tag{2.32}$$

A single mode can be characterized in the transverse direction as

$$\mathbf{E}_t(q_1, q_2, z) = V(z)\mathbf{e}_t(q_1, q_2)$$
$$\mathbf{H}_t(q_1, q_2, z) = I(z)\mathbf{h}_t(q_1, q_2)$$

A comprehensive characterization of the modal field quantities in a waveguide follows from (2.4) and (2.5) can be extended to allow the transverse field components to be factorized as follows

$$\mathbf{E}_t(q_1, q_2, z) = \sum_{n=1}^{\infty} V_n(z)\mathbf{e}_{t,n}(q_1, q_2)$$
$$\mathbf{H}_t(q_1, q_2, z) = \sum_{n=1}^{\infty} I_n(z)\mathbf{h}_{t,n}(q_1, q_2) \tag{2.33}$$

V_n and I_n represent measures of modal amplitudes of the *n*-th mode transverse electric and magnetic field intensities, respectively.

The transverse modal eigenvectors $\mathbf{e}_{t,n}$ and $\mathbf{h}_{t,n}$ are wave potentials of the Helmholtz wave equation

$$\nabla_t^2 \varphi_n + k_{c,n}^2 \varphi_n = 0 \tag{2.34}$$

as applied to the cross-section, S, of the waveguide surface. $k_{c,n}^2$ is the eigenvalue of the *n*-th mode and φ_n is the scalar eigenfunction.

The boundary conditions defined on the contour, C, of S is

$$\begin{aligned} &\frac{\partial \varphi_n}{\partial n} = 0, && \text{for H modes} \\ &\varphi_n = 0, && \text{for E modes} \end{aligned} \tag{2.35}$$

Figure 2-1 shows the cross-sectional surface S, the contour C of S, and the derivative $\frac{\partial}{\partial n}$ along the outwardly directed normal, $\hat{\mathbf{n}}$. We can establish the following relations for the derived scalar eigenfunctions for H and E modes

$$\text{H modes:} \quad \varphi_n = h_{z,n} \tag{2.36}$$

$$\text{E modes:} \quad \varphi_n = e_{z,n} \tag{2.37}$$

When the scalar eigenfunctions φ_n are calculated for the H and E modes, the transverse field vectors can be determined from

$$\mathbf{e}_{t,n} = \begin{cases} \hat{\mathbf{a}}_z \times \nabla_t h_{z,n} & \text{for H modes} \\ \nabla_t e_{z,n} & \text{for E modes} \end{cases} \tag{2.38}$$

$$\mathbf{h}_{t,n} = \hat{\mathbf{a}}_z \times \mathbf{e}_{t,n} \tag{2.39}$$

Extending (2.14) and (2.13) we have

$$k_{z,n} = \sqrt{k^2 - k_{c,n}^2} \tag{2.40}$$

as the guide wave number for the *n*-th mode,

$$k_{c,n} = \omega_{c,n}\sqrt{\mu\varepsilon} \tag{2.41}$$

as the *n*-th mode cutoff wave number. When $k_{c,n} > k$, the wave number and impedance are imaginary terms, and it follows that the mode attenuates and becomes evanescent. The attenuation constant can be defined as

$$\alpha_{z,n} = jk_{z,n} = \sqrt{k_{c,n}^2 - k^2} \tag{2.42}$$

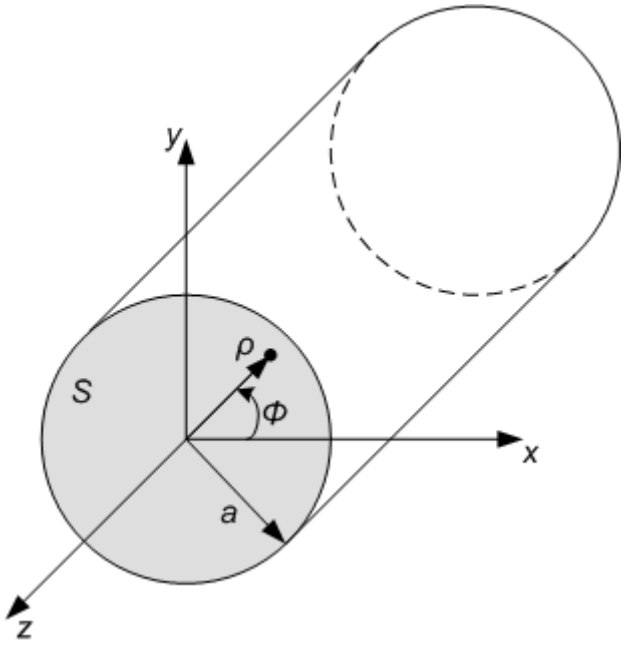

Figure 2-2 Cylindrical waveguide of circular cross section and reference coordinates.

2.3 Circular Cross-sectional Waveguide

The cylindrical waveguide is prevalent in many practical guided wave antenna structures [7]. The cylindrical waveguide follows from the previous section, and supports TE and TM modes within the structure. Figure 2-2 shows a general cylindrical waveguide with circular cross-section S. We shall consider the extension of the general hollow waveguide theory to the circular waveguide.

Considering H modes, we shall express the transverse vectors

$$h_{z,n} = C_n J_m\left(k_{\rho,n}\rho\right)\cos\left(m\phi\right) \tag{2.43}$$

where

$$k_{\rho,n} = \frac{\chi'_{m,n}}{a} \tag{2.44}$$

Establishing (2.38) and(2.39), we have

$$\mathbf{e}_{t,n} = \hat{\mathbf{a}}_z \times \nabla_t h_{z,n} \tag{2.45}$$

$$\mathbf{h}_{t,n} = -\nabla_t h_{z,n} \tag{2.46}$$

We can express

$$\begin{aligned}\nabla_t h_{z,n} &= \hat{\mathbf{a}}_\rho \frac{\partial h_{z,n}}{\partial \rho} + \hat{\mathbf{a}}_\phi \frac{1}{\rho}\frac{\partial h_{z,n}}{\partial \phi} \\ &= \hat{\mathbf{a}}_\rho C_n k_{\rho,n} J'_m\left(k_{\rho,n}\rho\right)\cos\left(m\phi\right) + \hat{\mathbf{a}}_\phi C_n \frac{-m}{\rho} J_m\left(k_{\rho,n}\rho\right)\sin\left(m\phi\right)\end{aligned} \tag{2.47}$$

$$\hat{\mathbf{a}}_z \times \nabla_t h_{z,n} = \hat{\mathbf{a}}_\phi C_n k_{\rho,n} J'_m\left(k_{\rho,n}\rho\right)\cos\left(m\phi\right) + \hat{\mathbf{a}}_\rho C_n \frac{m}{\rho} J_m\left(k_{\rho,n}\rho\right)\sin\left(m\phi\right) \tag{2.48}$$

Let

$$e_{\rho,n} = C_n \frac{m}{\rho} J_m\left(k_{\rho,n}\rho\right)\sin\left(m\phi\right) \tag{2.49}$$

$$e_{\phi,n} = C_n k_{\rho,n} J'_m\left(k_{\rho,n}\rho\right)\cos\left(m\phi\right) \tag{2.50}$$

where applying the boundary condition

$$e_{\phi,n}\Big|_{\rho=a} = 0$$

yields

$$J'_m\left(k_{\rho,n}a\right) = k_{\rho,n} = \frac{\chi'_{m,n}}{a} \tag{2.51}$$

$$\begin{aligned} h_{\rho,n} &= -C_n k_{\rho,n} J'_m\left(k_{\rho,n}\rho\right)\cos\left(m\phi\right) \\ &= -e_{\phi,n} \end{aligned} \tag{2.52}$$

$$\begin{aligned} h_{\phi,n} &= C_n \frac{m}{\rho} J_m\left(k_{\rho,n}\rho\right)\sin\left(m\phi\right) \\ &= e_{\rho,n} \end{aligned} \tag{2.53}$$

Normalization:

$$\iint\left(\mathbf{e}_{t,n}\times\mathbf{h}_{t,n}\right)\bullet d\mathbf{S} = 1 \tag{2.54}$$

Establishes

$$\int_0^{2\pi}\int_0^{a}\left(e_{\rho,n}h_{\phi,n} - e_{\phi,n}h_{\rho,n}\right)\rho d\rho d\phi = 1 \tag{2.55}$$

It follows

$$C_n^H = \sqrt{\frac{2}{\pi\left(1+\delta_{0,m}\right)}}\frac{1}{\sqrt{\chi'^2_{m,n} - m^2}J_m\left(\chi'_{m,n}\right)} \tag{2.56}$$

where

$$\delta_{0,m} = \begin{cases} 1 & \text{m} = 0 \\ 0 & \text{m} \neq 0 \end{cases} \tag{2.57}$$

Considering E modes, we shall express the transverse vectors

$$e_{z,n} = C_n J_m\left(k_{\rho,n}\rho\right)\sin\left(m\phi\right) \tag{2.58}$$

where

$$k_{\rho,n} = \frac{\chi_{m,n}}{a} \tag{2.59}$$

Establishing (2.38) and(2.39), we have

$$\mathbf{e}_{t,n} = \nabla_t e_{z,n} \tag{2.60}$$

$$\mathbf{h}_{t,n} = \hat{\mathbf{a}}_z \times \nabla_t e_{z,n} \tag{2.61}$$

We can express

$$\begin{aligned} \nabla_t e_{z,n} &= \hat{\mathbf{a}}_\rho \frac{\partial e_{z,n}}{\partial \rho} + \hat{\mathbf{a}}_\phi \frac{1}{\rho} \frac{\partial e_{z,n}}{\partial \phi} \\ &= \hat{\mathbf{a}}_\rho C_n k_{\rho,n} J'_m\left(k_{\rho,n}\rho\right)\sin\left(m\phi\right) + \hat{\mathbf{a}}_\phi C_n \frac{m}{\rho} J_m\left(k_{\rho,n}\rho\right)\cos\left(m\phi\right) \end{aligned} \tag{2.62}$$

$$\hat{\mathbf{a}}_z \times \nabla_t h_{z,n} = \hat{\mathbf{a}}_\phi C_n k_{\rho,n} J'_m\left(k_{\rho,n}\rho\right)\sin\left(m\phi\right) + \hat{\mathbf{a}}_\rho C_n \frac{-m}{\rho} J_m\left(k_{\rho,n}\rho\right)\cos\left(m\phi\right) \tag{2.63}$$

Let

$$e_{\rho,n} = C_n k_{\rho,n} J'_m\left(k_{\rho,n}\rho\right)\sin\left(m\phi\right) \tag{2.64}$$

$$e_{\phi,n} = C_n \frac{m}{\rho} J_m\left(k_{\rho,n}\rho\right)\cos\left(m\phi\right) \tag{2.65}$$

where applying the boundary condition

$$e_{\phi,n}\Big|_{\rho=a} = 0$$

yields

$$J'_m\left(k_{\rho,n}a\right) = k_{\rho,n} = \frac{\chi_{m,n}}{a} \tag{2.66}$$

$$\begin{aligned} h_{\rho,n} &= -C_n \frac{m}{\rho} J_m\left(k_{\rho,n}\rho\right)\cos\left(m\phi\right) \\ &= -e_{\phi,n} \end{aligned} \tag{2.67}$$

$$\begin{aligned} h_{\phi,n} &= -C_n k_{\rho,n} J'_m\left(k_{\rho,n}\rho\right)\sin\left(m\phi\right) \\ &= e_{\rho,n} \end{aligned} \tag{2.68}$$

Normalization:

$$\iint\left(\mathbf{e}_{t,n}\times\mathbf{h}_{t,n}\right)\bullet d\mathbf{S} = 1 \tag{2.69}$$

Establishes

$$\int_0^{2\pi}\int_0^{a}\left(e_{\rho,n}h_{\phi,n} - e_{\phi,n}h_{\rho,n}\right)\rho d\rho d\phi = 1 \tag{2.70}$$

It follows

$$C_n^E = \sqrt{\frac{2}{\pi\left(1+\delta_{0,m}\right)}}\frac{1}{\chi_{m,n}J_{m+1}\left(\chi_{m,n}\right)} \tag{2.71}$$

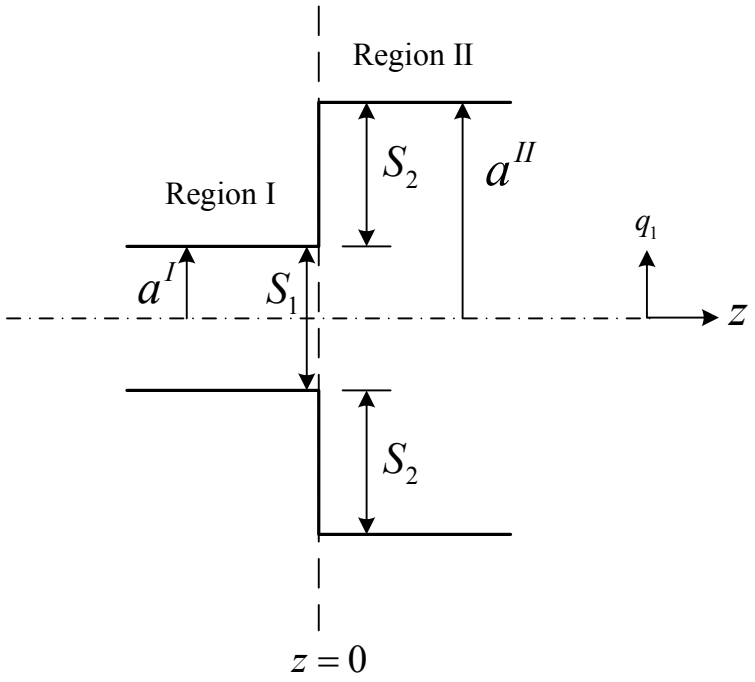

Figure 2-3 Step junction discontinuity.

2.4 Step Junction Discontinuity

Figure 2-3 illustrates a single step junction discontinuity of circular waveguides of two different radii, a^I and a^{II}, in which the condition $a^I < a^{II}$ is imposed. The step discontinuity separates two regions (waveguides) I and II to the left and right of the $z = 0$ reference, respectively.

Through boundary conditions

$$\left.\begin{array}{ll} \text{on } S_1 & \sum_n V_n^I \mathbf{e}_{t,n}^I \\ \text{on } S_2 & 0 \end{array}\right\} = \sum_n V_n^{II} \mathbf{e}_{t,n}^{II} \text{ on } S_1, S_2 \tag{2.72}$$

$$\left.\begin{array}{ll} \text{on } S_1 & \sum_n I_n^I \mathbf{h}_{t,n}^I \\ \text{on } S_2 & f(q_1, q_2) \end{array}\right\} = \sum_n I_n^{II} \mathbf{h}_{t,n}^{II} \text{ on } S_1, S_2 \tag{2.73}$$

where $f(q_1, q_2)$ is an unknown value.

Mode orthogonality relationships:

$$\iint_{S_1} \left(\mathbf{e}_{t,n}^I \times \mathbf{h}_{t,k}^I\right) \bullet d\mathbf{S} = \delta_{n,k} \tag{2.74}$$

$$\iint_{S_1+S_2} \left(\mathbf{e}_{t,n}^{II} \times \mathbf{h}_{t,k}^{II}\right) \bullet d\mathbf{S} = \delta_{n,k} \tag{2.75}$$

where

$$\delta_{n,k} = \begin{cases} 1 & \text{n = k} \\ 0 & \text{n} \neq \text{k} \end{cases} \tag{2.76}$$

Applying the cross-product of (2.72) and $\mathbf{h}_{t,k}^{II}$, and taking the surface integral over $S_1 + S_2$, and using (2.75) yields

$$\sum_n V_n^I \iint_{S_1} \left(\mathbf{e}_{t,n}^I \times \mathbf{h}_{t,k}^{II}\right) \bullet d\mathbf{S} = V_k^{II} \tag{2.77}$$

Similarly, applying the cross-product of $\mathbf{e}_{t,k}^{I}$ and (2.73), and taking the surface integral over $S_1 + S_2$, and using (2.74) yields

$$I_k^I = \sum_n I_n^{II} \iint_{S_1} \left(\mathbf{e}_{t,k}^I \times \mathbf{h}_{t,n}^{II} \right) \bullet d\mathbf{S} \tag{2.78}$$

Defining

$$\mathbf{P}_{k,n} = \iint_{S_1} \left(\mathbf{e}_{t,k}^I \times \mathbf{h}_{t,n}^{II} \right) \bullet d\mathbf{S} \tag{2.79}$$

We can express (2.77) and (2.78) in matrix form

$$\mathbf{P}^T \mathbf{V}^I = \mathbf{V}^{II} \tag{2.80}$$

$$\mathbf{I}^I = \mathbf{P}\mathbf{I}^{II} \tag{2.81}$$

where $\mathbf{P}^T$ represents the transpose of the $\mathbf{P}$ matrix.

The $\mathbf{P}$ matrix can be represented in detail as

$$\mathbf{P} = \begin{pmatrix} \mathbf{P}_{H,H} & \mathbf{P}_{H,E} \\ \mathbf{P}_{E,H} & \mathbf{P}_{E,E} \end{pmatrix}$$

where H denotes TE modes and E denotes TM modes. We can rewrite (2.73)

$$\left.\begin{array}{ll} \text{on } S_1 & \sum_n I_n^{H^I} \mathbf{h}_{t,n}^{H^I} + \sum_n I_n^{E^I} \mathbf{h}_{t,n}^{E^I} \\ \text{on } S_2 & f\left(q_1, q_2\right) \end{array}\right\} = \sum_n I_n^{H^{II}} \mathbf{h}_{t,n}^{H^{II}} + \sum_n I_n^{E^{II}} \mathbf{h}_{t,n}^{E^{II}} \text{ on } S_1, S_2 \tag{2.82}$$

Applying the cross-product of $\mathbf{e}_{t,k}^{H^I}$ and (2.82), and taking the surface integral over $S_1 + S_2$, and using (2.74) yields

$$I_k^{H^I} = \sum_n I_n^{H^{II}} \iint_{S_1} \left(\mathbf{e}_{t,k}^{H^I} \times \mathbf{h}_{t,n}^{H^{II}} \right) \bullet d\mathbf{S} + \sum_n I_n^{E^{II}} \iint_{S_1} \left(\mathbf{e}_{t,k}^{H^I} \times \mathbf{h}_{t,n}^{E^{II}} \right) \bullet d\mathbf{S} \tag{2.83}$$

Applying the cross-product of $\mathbf{e}_{t,k}^{E^I}$ and (2.82), and taking the surface integral over $S_1 + S_2$, and using (2.74) yields

$$I_k^{E^I} = \sum_n I_n^{H^{II}} \iint_{S_1} \left(\mathbf{e}_{t,k}^{E^I} \times \mathbf{h}_{t,n}^{H^{II}} \right) \bullet d\mathbf{S} + \sum_n I_n^{E^{II}} \iint_{S_1} \left(\mathbf{e}_{t,k}^{E^I} \times \mathbf{h}_{t,n}^{E^{II}} \right) \bullet d\mathbf{S} \tag{2.84}$$

We can write (2.83) and (2.84) in matrix form as follows

$$\mathbf{I}^{H^I} = \mathbf{P}_{H,H} \mathbf{I}^{H^{II}} + \mathbf{P}_{H,E} \mathbf{I}^{E^{II}} \tag{2.85}$$

$$\mathbf{I}^{E^I} = \mathbf{P}_{E,H} \mathbf{I}^{H^{II}} + \mathbf{P}_{E,E} \mathbf{I}^{E^{II}} \tag{2.86}$$

where

$$\begin{aligned}
\left(\mathbf{P}_{H,H} \right)_{k,n} &= \iint_{S_1} \left(\mathbf{e}_{t,k}^{H^I} \times \mathbf{h}_{t,n}^{H^{II}} \right) \bullet d\mathbf{S} \\
\left(\mathbf{P}_{H,E} \right)_{k,n} &= \iint_{S_1} \left(\mathbf{e}_{t,k}^{H^I} \times \mathbf{h}_{t,n}^{E^{II}} \right) \bullet d\mathbf{S} \\
\left(\mathbf{P}_{E,H} \right)_{k,n} &= \iint_{S_1} \left(\mathbf{e}_{t,k}^{E^I} \times \mathbf{h}_{t,n}^{H^{II}} \right) \bullet d\mathbf{S} \\
\left(\mathbf{P}_{E,E} \right)_{k,n} &= \iint_{S_1} \left(\mathbf{e}_{t,k}^{E^I} \times \mathbf{h}_{t,n}^{E^{II}} \right) \bullet d\mathbf{S}
\end{aligned} \tag{2.87}$$

Using (2.85) and (2.86), we have

$$\begin{pmatrix} I^{H^I} \\ I^{E^I} \end{pmatrix} = \begin{pmatrix} \mathbf{P}_{H,H} & \mathbf{P}_{H,E} \\ \mathbf{P}_{E,H} & \mathbf{P}_{E,E} \end{pmatrix} \begin{pmatrix} I^{H^{II}} \\ I^{E^{II}} \end{pmatrix} \tag{2.88}$$

We can express the analytical form for the $\mathbf{P}$ matrix in the circular waveguide junction

$$\begin{aligned}\left(\mathbf{P}_{\varphi,\varphi}\right)_{k,n} = \pi\left(1+\delta_{0,m}\right)\frac{a^I}{2}\frac{k^I_{\rho,k}k^{II}_{\rho,n}}{\left(k^I_{\rho,k}\right)^2-\left(k^{II}_{\rho,n}\right)^2}\Big[&k^{II}_{\rho,n}J_{m-1}\left(k^I_{\rho,k}a^I\right)J_{m-2}\left(k^{II}_{\rho,n}a^I\right)\\ &-k^I_{\rho,k}J_{m-2}\left(k^I_{\rho,k}a^I\right)J_{m-1}\left(k^{II}_{\rho,n}a^I\right)\\ &+k^{II}_{\rho,n}J_{m+1}\left(k^I_{\rho,k}a^I\right)J_m\left(k^{II}_{\rho,n}a^I\right)\\ &-k^I_{\rho,k}J_m\left(k^I_{\rho,k}a^I\right)J_{m+1}\left(k^{II}_{\rho,n}a^I\right)\Big]C^{\varphi}_k C^{\varphi}_n\end{aligned} \tag{2.89}$$

where φ assumes either *H* or *E* respectively.

$$\left(\mathbf{P}_{H,E}\right)_{k,n} = \pi\left(1+\delta_{0,m}\right)J_m\left(k^{H^I}_{\rho,k}a^I\right)J_{m+1}\left(k^{E^{II}}_{\rho,n}a^I\right)C^H_k C^E_n \tag{2.90}$$

$$\left(\mathbf{P}_{E,H}\right)_{k,n} = 0 \tag{2.91}$$

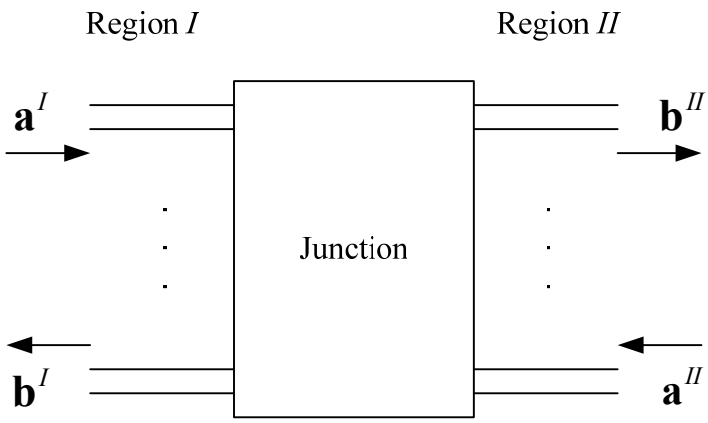

Figure 2-4 Step junction discontinuity N-port network model.

2.4.1 Determination of the Scattering Matrix

Obtaining the scattering matrix of the step junction discontinuity can be realized by using N-port network. Figure 2-4 exhibits an N-port network model of a step discontinuity. We can use (2.80) and (2.81) to obtain

$$\mathbf{P}^T\sqrt{\mathbf{Z}_C^I}\left(\mathbf{a}^I+\mathbf{b}^I\right)=\sqrt{\mathbf{Z}_C^{II}}\left(\mathbf{b}^{II}+\mathbf{a}^{II}\right) \tag{2.92}$$

$$\sqrt{\mathbf{Y}_C^I}\left(\mathbf{a}^I-\mathbf{b}^I\right)=\mathbf{P}\sqrt{\mathbf{Y}_C^{II}}\left(\mathbf{b}^{II}-\mathbf{a}^{II}\right) \tag{2.93}$$

which yields

$$\mathbf{P}^T\sqrt{\mathbf{Z}_C^I}\mathbf{b}^I-\sqrt{\mathbf{Z}_C^{II}}\mathbf{b}^{II}=-\mathbf{P}^T\sqrt{\mathbf{Z}_C^I}\mathbf{a}^I+\sqrt{\mathbf{Z}_C^{II}}\mathbf{a}^{II} \tag{2.94}$$

$$\sqrt{\mathbf{Y}_C^I}\mathbf{b}^I+\mathbf{P}\sqrt{\mathbf{Y}_C^{II}}\mathbf{b}^{II}=\sqrt{\mathbf{Y}_C^I}\mathbf{a}^I+\mathbf{P}\sqrt{\mathbf{Y}_C^{II}}\mathbf{a}^{II} \tag{2.95}$$

We can write (2.94) and (2.95) in matrix form

$$\begin{pmatrix} \mathbf{P}^T\sqrt{\mathbf{Z}_C^I} & -\sqrt{\mathbf{Z}_C^{II}} \\ \sqrt{\mathbf{Y}_C^I} & \mathbf{P}\sqrt{\mathbf{Y}_C^{II}} \end{pmatrix}\begin{pmatrix} \mathbf{b}^I \\ \mathbf{b}^{II} \end{pmatrix} = \begin{pmatrix} -\mathbf{P}^T\sqrt{\mathbf{Z}_C^I} & \sqrt{\mathbf{Z}_C^{II}} \\ \sqrt{\mathbf{Y}_C^I} & \mathbf{P}\sqrt{\mathbf{Y}_C^{II}} \end{pmatrix}\begin{pmatrix} \mathbf{a}^I \\ \mathbf{a}^{II} \end{pmatrix} \tag{2.96}$$

We can designate

$$\mathbf{E} = \begin{pmatrix} \mathbf{P}^T\sqrt{\mathbf{Z}_C^I} & -\sqrt{\mathbf{Z}_C^{II}} \\ \sqrt{\mathbf{Y}_C^I} & \mathbf{P}\sqrt{\mathbf{Y}_C^{II}} \end{pmatrix} \tag{2.97}$$

$$\mathbf{F} = \begin{pmatrix} -\mathbf{P}^T\sqrt{\mathbf{Z}_C^I} & \sqrt{\mathbf{Z}_C^{II}} \\ \sqrt{\mathbf{Y}_C^I} & \mathbf{P}\sqrt{\mathbf{Y}_C^{II}} \end{pmatrix} \tag{2.98}$$

It follows that we can determine the scattering matrix by

$$\mathbf{S} = \mathbf{E}^{-1}\mathbf{F} \tag{2.99}$$

Expression (2.99) will be valid when the number of modes in each waveguide is different.

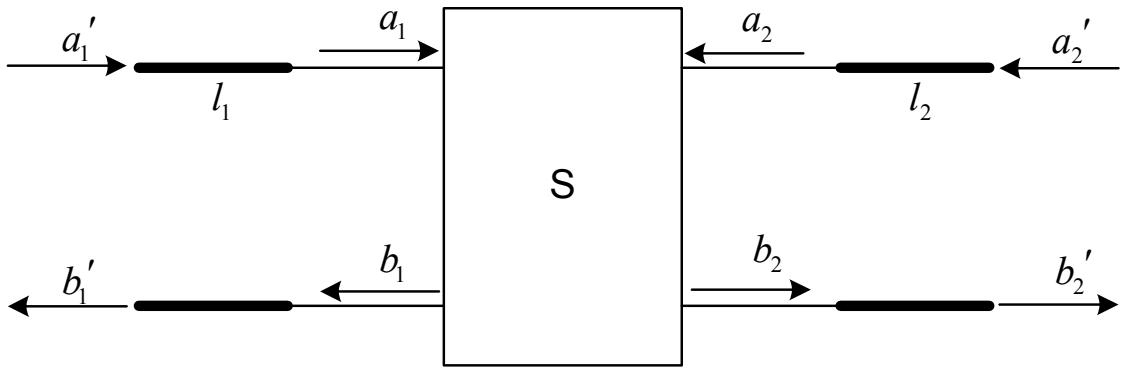

Figure 2-5 Phase compensation model.

2.5 Multi-mode Scattering Matrix Connection

A final scattering matrix can be obtained for a model that is composed of successive step discontinuities. The scattering parameters of each junction will have to be shifted in phase if transmission media lengths, l_n, exist on either side of the junction. Figure 2-5 displays a simplified illustration that would necessitate a reference plane shift for phase consideration. The scattering matrices of two junction discontinuities can then be combined through a cascading of the matrices. Figure 2-6 illustrates a simplified model for the cascading of scattering matrices.

2.5.1 Phase Compensation

The derivation for the phase compensation as exhibited by Figure 2-5 will be detailed. We can establish

$$\begin{pmatrix} \mathbf{b}_1 \\ \mathbf{b}_2 \end{pmatrix} = \begin{pmatrix} \mathbf{S}_{11} & \mathbf{S}_{12} \\ \mathbf{S}_{21} & \mathbf{S}_{22} \end{pmatrix} \begin{pmatrix} \mathbf{a}_1 \\ \mathbf{a}_2 \end{pmatrix} \tag{2.100}$$

and

$$\begin{pmatrix} \mathbf{b}_1 \\ \mathbf{b}_2 \end{pmatrix} = \begin{pmatrix} e^{j\mathbf{k}l_1} & \mathbf{0} \\ \mathbf{0} & e^{j\mathbf{k}l_2} \end{pmatrix} \begin{pmatrix} \mathbf{b}_1' \\ \mathbf{b}_2' \end{pmatrix} \tag{2.101}$$

$$\begin{pmatrix} \mathbf{a}_1 \\ \mathbf{a}_2 \end{pmatrix} = \begin{pmatrix} e^{-j\mathbf{k}l_1} & \mathbf{0} \\ \mathbf{0} & e^{-j\mathbf{k}l_2} \end{pmatrix} \begin{pmatrix} \mathbf{a}_1' \\ \mathbf{a}_2' \end{pmatrix} \tag{2.102}$$

It follows from insertion of (2.101) and (2.102) into (2.100)

$$\begin{pmatrix} \mathbf{b}_1' \\ \mathbf{b}_2' \end{pmatrix} = \begin{pmatrix} e^{-j\mathbf{k}l_1} & \mathbf{0} \\ \mathbf{0} & e^{-j\mathbf{k}l_2} \end{pmatrix} \begin{pmatrix} \mathbf{S}_{11} & \mathbf{S}_{12} \\ \mathbf{S}_{21} & \mathbf{S}_{22} \end{pmatrix} \begin{pmatrix} e^{-j\mathbf{k}l_1} & \mathbf{0} \\ \mathbf{0} & e^{-j\mathbf{k}l_2} \end{pmatrix} \begin{pmatrix} \mathbf{a}_1' \\ \mathbf{a}_2' \end{pmatrix} \tag{2.103}$$

Defining diagonal matrices $\mathbf{H}_1 = e^{-j\mathbf{k}l_1}$ and $\mathbf{H}_2 = e^{-j\mathbf{k}l_2}$, it is shown

$$\begin{pmatrix} \mathbf{b}_1' \\ \mathbf{b}_2' \end{pmatrix} = \begin{pmatrix} \mathbf{H}_1\mathbf{S}_{11}\mathbf{H}_1 & \mathbf{H}_1\mathbf{S}_{12}\mathbf{H}_2 \\ \mathbf{H}_2\mathbf{S}_{21}\mathbf{H}_1 & \mathbf{H}_2\mathbf{S}_{22}\mathbf{H}_2 \end{pmatrix} \begin{pmatrix} \mathbf{a}_1' \\ \mathbf{a}_2' \end{pmatrix} \tag{2.104}$$

Expressing (2.104) in another form

$$\begin{aligned}
\mathbf{S}_{11}' &= \mathbf{H}_1\mathbf{S}_{11}\mathbf{H}_1 \\
\mathbf{S}_{12}' &= \mathbf{H}_1\mathbf{S}_{12}\mathbf{H}_2 \\
\mathbf{S}_{21}' &= \mathbf{H}_2\mathbf{S}_{21}\mathbf{H}_1 \\
\mathbf{S}_{22}' &= \mathbf{H}_2\mathbf{S}_{22}\mathbf{H}_2
\end{aligned} \tag{2.105}$$

A special case where $l_1 = 0$ establishes that $\mathbf{H}_1 = \mathbf{I}$, where $\mathbf{I}$ is the identity matrix. We will express the following using (2.105)

$$\begin{aligned}
\mathbf{S}_{11}' &= \mathbf{S}_{11} \\
\mathbf{S}_{12}' &= \mathbf{S}_{12}\mathbf{H}_2 \\
\mathbf{S}_{21}' &= \mathbf{H}_2\mathbf{S}_{21} \\
\mathbf{S}_{22}' &= \mathbf{H}_2\mathbf{S}_{22}\mathbf{H}_2
\end{aligned} \tag{2.106}$$

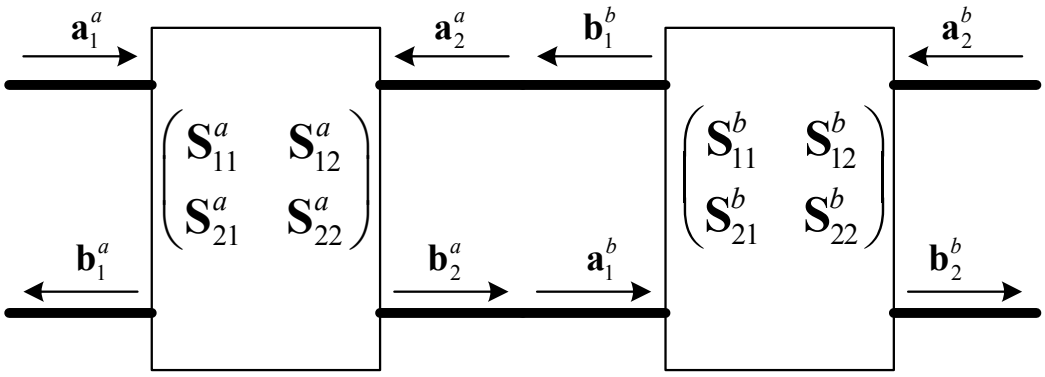

Figure 2-6 Model for cascading scattering matrices.

2.5.2 Cascading Scattering Matrices

Referring to Figure 2-6, we will express the following relationships

$$\begin{pmatrix} \mathbf{b}_1^a \\ \mathbf{b}_2^a \end{pmatrix} = \begin{pmatrix} \mathbf{S}_{11}^a & \mathbf{S}_{12}^a \\ \mathbf{S}_{21}^a & \mathbf{S}_{22}^a \end{pmatrix} \begin{pmatrix} \mathbf{a}_1^a \\ \mathbf{a}_2^a \end{pmatrix} \tag{2.107}$$

and

$$\begin{pmatrix} \mathbf{b}_1^b \\ \mathbf{b}_2^b \end{pmatrix} = \begin{pmatrix} \mathbf{S}_{11}^b & \mathbf{S}_{12}^b \\ \mathbf{S}_{21}^b & \mathbf{S}_{22}^b \end{pmatrix} \begin{pmatrix} \mathbf{a}_1^b \\ \mathbf{a}_2^b \end{pmatrix} \tag{2.108}$$

Expanding (2.107) and (2.108) establishes

$$\mathbf{b}_1^a = \mathbf{S}_{11}^a \mathbf{a}_1^a + \mathbf{S}_{12}^a \mathbf{a}_2^a \tag{2.109}$$

$$\mathbf{b}_2^a = \mathbf{S}_{21}^a \mathbf{a}_1^a + \mathbf{S}_{22}^a \mathbf{a}_2^a \tag{2.110}$$

$$\mathbf{b}_1^b = \mathbf{S}_{11}^b \mathbf{a}_1^b + \mathbf{S}_{12}^b \mathbf{a}_2^b \tag{2.111}$$

$$\mathbf{b}_2^b = \mathbf{S}_{21}^b \mathbf{a}_1^b + \mathbf{S}_{22}^b \mathbf{a}_2^b \tag{2.112}$$

Through inspection, the connection relationship can be expressed as

$$\mathbf{b}_2^a = \mathbf{a}_1^b \tag{2.113}$$

$$\mathbf{b}_1^b = \mathbf{a}_2^a \tag{2.114}$$

Applying (2.110) and (2.114) gives

$$\mathbf{b}_2^a = \mathbf{S}_{21}^a \mathbf{a}_1^a + \mathbf{S}_{22}^a \mathbf{b}_1^b \tag{2.115}$$

Similarly, from (2.111) and (2.113) we get

$$\mathbf{b}_1^b = \mathbf{S}_{11}^b \mathbf{b}_2^a + \mathbf{S}_{12}^b \mathbf{a}_2^b \tag{2.116}$$

Using (2.115) and applying (2.116), it follows

$$\begin{aligned} \mathbf{b}_1^b &= \mathbf{S}_{11}^b \left(\mathbf{S}_{21}^a \mathbf{a}_1^a + \mathbf{S}_{22}^a \mathbf{b}_1^b \right) + \mathbf{S}_{12}^b \mathbf{a}_2^b \\ \mathbf{b}_1^b - \mathbf{S}_{11}^b \mathbf{S}_{22}^a \mathbf{b}_1^b &= \mathbf{S}_{11}^b \mathbf{S}_{21}^a \mathbf{a}_1^a + \mathbf{S}_{12}^b \mathbf{a}_2^b \\ \mathbf{b}_1^b &= \left(\mathbf{I} - \mathbf{S}_{11}^b \mathbf{S}_{22}^a \right)^{-1} \mathbf{S}_{11}^b \mathbf{S}_{21}^a \mathbf{a}_1^a + \left(\mathbf{I} - \mathbf{S}_{11}^b \mathbf{S}_{22}^a \right)^{-1} \mathbf{S}_{12}^b \mathbf{a}_2^b \end{aligned} \tag{2.117}$$

Similarly, using (2.116) and applying (2.115), it can be shown

$$\begin{aligned} \mathbf{b}_2^a &= \mathbf{S}_{21}^a \mathbf{a}_1^a + \mathbf{S}_{22}^a \left(\mathbf{S}_{11}^b \mathbf{b}_2^a + \mathbf{S}_{12}^b \mathbf{a}_2^b \right) \\ \left(\mathbf{I} - \mathbf{S}_{22}^a \mathbf{S}_{11}^b \right) \mathbf{b}_2^a &= \mathbf{S}_{21}^a \mathbf{a}_1^a + \mathbf{S}_{22}^a \mathbf{S}_{12}^b \mathbf{a}_2^b \\ \mathbf{b}_2^a &= \left(\mathbf{I} - \mathbf{S}_{22}^a \mathbf{S}_{11}^b \right)^{-1} \mathbf{S}_{21}^a \mathbf{a}_1^a + \left(\mathbf{I} - \mathbf{S}_{22}^a \mathbf{S}_{11}^b \right)^{-1} \mathbf{S}_{22}^a \mathbf{S}_{12}^b \mathbf{a}_2^b \end{aligned} \tag{2.118}$$

Collectively, (2.109) , (2.114), and (2.117) resolves to

$$\begin{aligned}\mathbf{b}_1^a &= \mathbf{S}_{11}^a\mathbf{a}_1^a + \mathbf{S}_{12}^a\mathbf{b}_1^b \\ &= \mathbf{S}_{11}^a\mathbf{a}_1^a + \mathbf{S}_{12}^a\left(\mathbf{I}-\mathbf{S}_{11}^b\mathbf{S}_{22}^a\right)^{-1}\mathbf{S}_{11}^b\mathbf{S}_{21}^a\mathbf{a}_1^a + \mathbf{S}_{12}^a\left(\mathbf{I}-\mathbf{S}_{11}^b\mathbf{S}_{22}^a\right)^{-1}\mathbf{S}_{12}^b\mathbf{a}_2^b\end{aligned} \tag{2.119}$$

Combining (2.112), (2.113), and (2.118)

$$\begin{aligned}\mathbf{b}_2^b &= \mathbf{S}_{21}^b\mathbf{b}_2^a + \mathbf{S}_{22}^b\mathbf{a}_2^b \\ &= \mathbf{S}_{21}^b\left(\mathbf{I}-\mathbf{S}_{22}^a\mathbf{S}_{11}^b\right)^{-1}\mathbf{S}_{21}^a\mathbf{a}_1^a + \mathbf{S}_{21}^b\left(\mathbf{I}-\mathbf{S}_{22}^a\mathbf{S}_{11}^b\right)^{-1}\mathbf{S}_{22}^a\mathbf{S}_{12}^b\mathbf{a}_2^b + \mathbf{S}_{22}^b\mathbf{a}_2^b\end{aligned} \tag{2.120}$$

Using (2.119) and (2.120), we obtain

$$\begin{aligned}\mathbf{S}_{11}^C &= \mathbf{S}_{11}^a + \mathbf{S}_{12}^a\left(\mathbf{I}-\mathbf{S}_{11}^b\mathbf{S}_{22}^a\right)^{-1}\mathbf{S}_{11}^b\mathbf{S}_{21}^a \\ \mathbf{S}_{12}^C &= \mathbf{S}_{12}^a\left(\mathbf{I}-\mathbf{S}_{11}^b\mathbf{S}_{22}^a\right)^{-1}\mathbf{S}_{12}^b \\ \mathbf{S}_{21}^C &= \mathbf{S}_{21}^b\left(\mathbf{I}-\mathbf{S}_{22}^a\mathbf{S}_{11}^b\right)^{-1}\mathbf{S}_{21}^a \\ \mathbf{S}_{21}^C &= \mathbf{S}_{22}^b + \mathbf{S}_{21}^b\left(\mathbf{I}-\mathbf{S}_{22}^a\mathbf{S}_{11}^b\right)^{-1}\mathbf{S}_{22}^a\mathbf{S}_{12}^b\end{aligned} \tag{2.121}$$

Allowing the following definition

$$\begin{aligned}\mathbf{G} &= \mathbf{S}_{12}^a\left(\mathbf{I}-\mathbf{S}_{11}^b\mathbf{S}_{22}^a\right)^{-1} \\ \mathbf{H} &= \mathbf{S}_{21}^b\left(\mathbf{I}-\mathbf{S}_{22}^a\mathbf{S}_{11}^b\right)^{-1}\end{aligned} \tag{2.122}$$

it follows that the cascaded matrices will take the form

$$\begin{aligned}\mathbf{S}_{11}^C &= \mathbf{S}_{11}^a + \mathbf{G}\mathbf{S}_{11}^b\mathbf{S}_{21}^a \\ \mathbf{S}_{12}^C &= \mathbf{G}\mathbf{S}_{12}^b \\ \mathbf{S}_{21}^C &= \mathbf{H}\mathbf{S}_{21}^a \\ \mathbf{S}_{21}^C &= \mathbf{S}_{22}^b + \mathbf{H}\mathbf{S}_{22}^a\mathbf{S}_{12}^b\end{aligned} \tag{2.123}$$

CHAPTER 3 INTEGRAL EQUATIONS AND THE METHOD OF MOMENTS

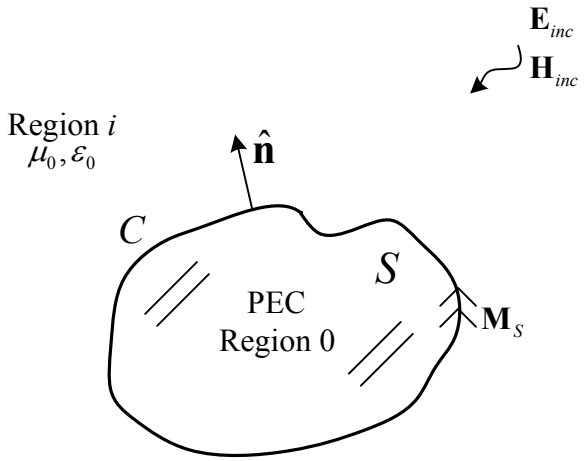

Figure 3-1 Original problem under investigation.

3.1 Integral Equations for Scattering by Perfect Electric Conductor

Consider Figure 3-1, the body of the object is consistent of perfect electric conductor (PEC). The incident electromagnetic fields, $\mathbf{E}_{inc}, \mathbf{H}_{inc}$, can originate from a uniform plane wave, cylindrical wave, spherical wave, and/or some external current(s). We will designate the PEC body as region 0, and the region of interest as *i*. Applying the surface equivalence principle, the problem defined in Figure 3-1 is equivalent to

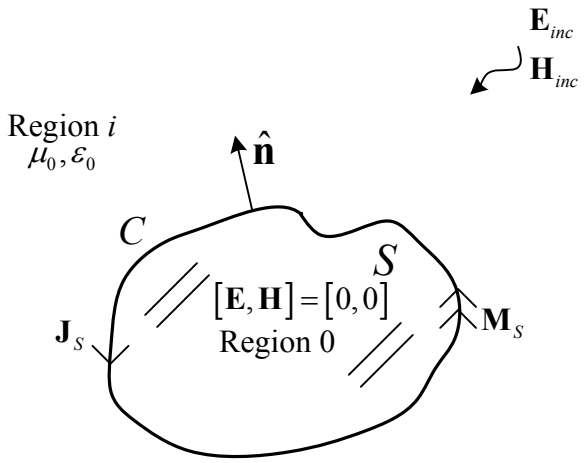

Figure 3-2 Equivalent model for the original problem.

replacing the PEC body with a medium that defines zero electromagnetic fields within a surface contour *C*, signified as region 0, as shown in Figure 3-2. The surface current $\mathbf{J}_S$ is also introduced on the boundary through the use of the surface equivalence principle, and the current is defined as

$$\mathbf{J}_S = \hat{\mathbf{n}} \times \mathbf{H}^i \tag{3.1}$$

where $\mathbf{H}^i$ represents the magnetic field in region *i*. Further application of the surface equivalence principle permits the replacement of the medium in region 0 with μ_0, ε_0, such that the entire space is characterized as free-space, as shown in Figure 3-3. The electromagnetics fields of region *i* can be determined from the equivalence model as shown in Figure 3-3; it is important to note that the electromagnetic fields in region 0 of the equivalence model shown in Figure 3-3 are not equivalent to the fields presented in

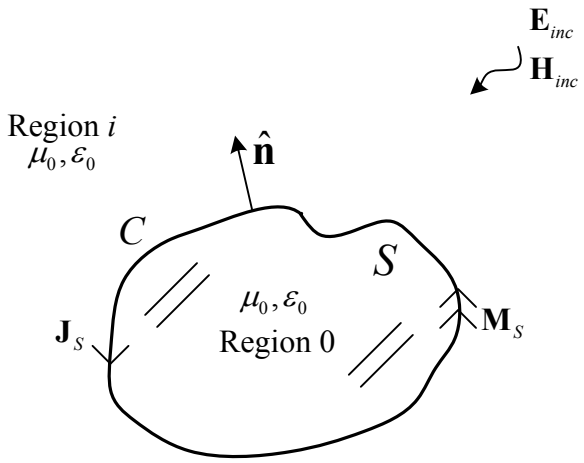

Figure 3-3 Free-Space equivalence model with material replacement in region 0.

region 0 of the original problem, as defined by Figure 3-1. The fields generated by $\mathbf{J}_S$ are the scattered fields that will be present in the original problem. The solution of the electromagnetic fields can be determined for the free-space equivalence model by the following

$$\mathbf{E}^i = \mathbf{E}^i_J\left(\mathbf{J}_S\right) + \mathbf{E}^i_M\left(\mathbf{M}_S\right) + \mathbf{E}_{inc} \tag{3.2}$$

$$\mathbf{H}^i = \mathbf{H}^i_J\left(\mathbf{J}_S\right) + \mathbf{H}^i_M\left(\mathbf{M}_S\right) + \mathbf{H}_{inc} \tag{3.3}$$

where on the boundary

$$\mathbf{E}_J^i\left(\mathbf{J}_S\right) = -Z_0 L_0\left(\mathbf{J}_S\right) + \frac{\rho_S^E}{2\varepsilon_0}\hat{\mathbf{n}} \tag{3.4}$$

$$\mathbf{E}_M^i\left(\mathbf{M}_S\right) = K_0\left(\mathbf{M}_S\right) + \frac{1}{2}\hat{\mathbf{n}}\times\mathbf{M}_S \tag{3.5}$$

$$\mathbf{H}_J^i\left(\mathbf{J}_S\right) = -K_0\left(\mathbf{J}_S\right) - \frac{1}{2}\hat{\mathbf{n}}\times\mathbf{J}_S \tag{3.6}$$

$$\mathbf{H}_M^i\left(\mathbf{M}_S\right) = -Y_0 L_0\left(\mathbf{M}_S\right) - \frac{\rho_S^H}{2\mu_0}\hat{\mathbf{n}} \tag{3.7}$$

where Z_0 and Y_0 are the intrinsic impedance and admittance of the medium in region *i*, L_0 and K_0 are principle values of L and K operators, and ρ_S^E, ρ_S^H are the density of electric and magnetic charges, respectively, placed over the surface boundary. The L and K operators are defined as [51]

$$L\left(\mathbf{F}_S\right) = jk_0\iint_S \mathbf{F}_S\left(\mathbf{r}'\right)G\left(R\right)dS' - \frac{1}{jk_0}\iint_S\left[\nabla'_S\bullet\mathbf{F}_S\left(\mathbf{r}'\right)\right]\nabla G\left(R\right)dS' \tag{3.8}$$

$$K\left(\mathbf{F}_S\right) = \iint_S \mathbf{F}_S\left(\mathbf{r}'\right)\times\nabla G\left(R\right)dS' \tag{3.9}$$

where $\mathbf{F}_S$ can represent either $\mathbf{J}_S$ or $\mathbf{M}_S$.

Region *i* of Figure 3-3 can not represent zero fields at the surface boundary; therefore, by applying boundary conditions to the equivalence model of Figure 3-2, boundary conditions can be defined that will determine the basic integral equations.

3.1.1 Electric Field Integral Equation (EFIE)

The electric field boundary condition applied in Figure 3-2 will define $\mathbf{E}_C^0 = 0$, where *C* represents the contour boundary of the surface *S*. The electric boundary condition establishes

$$\hat{\mathbf{n}} \times \left[\mathbf{E}_C^i - \mathbf{E}_C^0 \right] = -\mathbf{M}_S \tag{3.10}$$

Using (3.2) it follows

$$\hat{\mathbf{n}} \times \left[\mathbf{E}_{J,C}^i \left(\mathbf{J}_S \right) + \mathbf{E}_{M,C}^i \left(\mathbf{M}_S \right) + \mathbf{E}_{inc,C} \right] = -\mathbf{M}_S \tag{3.11}$$

where *C* designates the quantities on the contour boundary. (3.11) can be re-written as

$$\hat{\mathbf{n}} \times \mathbf{E}_{J,C}^i \left(\mathbf{J}_S \right) = -\mathbf{M}_S - \hat{\mathbf{n}} \times \mathbf{E}_{M,C}^i \left(\mathbf{M}_S \right) - \hat{\mathbf{n}} \times \mathbf{E}_{inc,C} \tag{3.12}$$

The application of (3.12) to a generalized problem introduces a concern that must be addressed with respect to the uniqueness of the solution. The use of the electric field boundary condition forces $\hat{\mathbf{n}} \times \mathbf{E}_C^0 = 0$; however, there was no imposition of boundary conditions for $\hat{\mathbf{n}} \times \mathbf{H}_C^0 = 0$. Due to the non-existent boundary condition for the magnetic field in region 0, the solution may not be unique, indicating spurious resonance can occur.

Addressing spurious resonance, (3.12) can be used to derive a MoM matrix equation of the form

$$\mathbf{ZJ} = \mathbf{V} \tag{3.13}$$

Given frequencies where the $\mathbf{Z}$ matrix exhibits singularity implies $\det(\mathbf{Z}) = 0$; therefore,

there can not be a determination of the solutions for $\mathbf{J}$, since $\mathbf{J}$ will approach infinity.

An alternative form of the EFIE can be derived through the cross-product of the normal vector with (3.12)

$$\mathbf{E}^i_{J,C}\left(\mathbf{J}_S\right) = -\hat{\mathbf{n}} \times \mathbf{M}_S - \mathbf{E}^i_{M,C}\left(\mathbf{M}_S\right) - \mathbf{E}_{inc,C} \tag{3.14}$$

3.1.2 Magnetic Field Integral Equation (MFIE)

Similar to the previous section, the magnetic field boundary condition applied in Figure 3-2 will define $\mathbf{H}^0_C = 0$. The magnetic boundary condition establishes

$$\hat{\mathbf{n}} \times \left[\mathbf{H}^i_C - \mathbf{H}^0_C\right] = \mathbf{J}_S \tag{3.15}$$

Using (3.3) it follows

$$\hat{\mathbf{n}} \times \left[\mathbf{H}^i_{J,C}\left(\mathbf{J}_S\right) + \mathbf{H}^i_{M,C}\left(\mathbf{M}_S\right) + \mathbf{H}_{inc,C}\right] = \mathbf{J}_S \tag{3.16}$$

where *C* designates the quantities on the contour boundary. (3.16) can be re-written as

$$\hat{\mathbf{n}} \times \mathbf{H}^i_{J,C}\left(\mathbf{J}_S\right) - \mathbf{J}_S = -\hat{\mathbf{n}} \times \mathbf{H}^i_{M,C}\left(\mathbf{M}_S\right) - \hat{\mathbf{n}} \times \mathbf{H}_{inc,C} \tag{3.17}$$

Likewise, the application of (3.17) to a generalized problem introduces a concern that must be addressed with respect to the uniqueness of the solution. The use of the magnetic field boundary condition forces $\hat{\mathbf{n}} \times \mathbf{H}^0_C = 0$; however, there was no imposition of boundary conditions for $\hat{\mathbf{n}} \times \mathbf{E}^0_C = 0$. Due to the non-existent boundary condition for the electric field in region 0, the solution may not be unique, indicating spurious

resonance can occur.

An alternative form of the MFIE can be derived through the cross-product of the normal vector with (3.17)

$$\mathbf{H}^i_{J,C}\left(\mathbf{J}_S\right)+\hat{\mathbf{n}}\times\mathbf{J}_S=-\mathbf{H}^i_{M,C}\left(\mathbf{M}_S\right)-\mathbf{H}_{inc,C} \tag{3.18}$$

3.1.3 Combined Field Integral Equation (CFIE)

The CFIE is a method used to mitigate the spurious resonances that are inherent to problems that are solved through the use of EFIE and MFIE application. The CFIE is an alternative method that is based on the combination of boundary conditions

$$\hat{\mathbf{n}}\times\mathbf{E}^i_S+\mathbf{M}_S=\hat{\mathbf{n}}\times\mathbf{E}^0_S \tag{3.19}$$

$$\hat{\mathbf{n}}\times\mathbf{H}^i_S-\mathbf{J}_S=\hat{\mathbf{n}}\times\mathbf{H}^0_S \tag{3.20}$$

The boundary conditions (3.19) and (3.20) are forced to zero by establishing

$$\alpha\left(\mathbf{E}^0_S\right)+\hat{\mathbf{n}}\times\mathbf{H}^0_S=0 \tag{3.21}$$

where α is an arbitrary coefficient with the requirement $\mathrm{Re}\left(\alpha\right)>0$.

The net power P flowing into region 0 is characterized by

$$P=\frac{1}{2}\mathrm{Re}\left[\oiint_S\left(\mathbf{E}^0_S\times\bar{\mathbf{H}}^0_S\right)\cdot\left(-\hat{\mathbf{n}}\right)dS\right] \tag{3.22}$$

where the overbar indicates the complex conjugate operator. Region 0 has no impressed sources, which implies

$$P \geq 0 \tag{3.23}$$

However, applying (3.21), we can establish

$$P = \frac{1}{2}\mathrm{Re}\left[\oiint_S \left(\hat{\mathbf{n}} \times \bar{\mathbf{H}}_S^0 \right) \cdot \left(\mathbf{E}_S^0 \right) dS \right] = -\frac{1}{2}\mathrm{Re}\left[\bar{\alpha} \left| \mathbf{E}_S^0 \right|^2 \right] \tag{3.24}$$

Asserting the requirement $\mathrm{Re}(\alpha) > 0$ indicates

$$P = \frac{1}{2}\mathrm{Re}\left[\oiint_S \left(\hat{\mathbf{n}} \times \bar{\mathbf{H}}_S^0 \right) \cdot \left(\mathbf{E}_S^0 \right) dS \right] = -\frac{1}{2}\mathrm{Re}\left[\bar{\alpha} \left| \mathbf{E}_S^0 \right|^2 \right] \leq 0 \tag{3.25}$$

Using (3.23) and (3.25), it must follow that $P = 0$, which in turn yields $\mathbf{E}_S^0 = 0$. Substitution of $\mathbf{E}_S^0 = 0$ into (3.21) validates that $\mathbf{E}_S^0 = \mathbf{H}_S^0 = 0$ is guaranteed.

Applying the cross product of the normal vector and (3.19), (3.20), and (3.21), respectively, yields alternative forms of integral equations as

$$\text{EFIE: } \mathbf{E}_S^i - \hat{\mathbf{n}} \times \mathbf{M}_S = \mathbf{E}_S^0 = 0 \tag{3.26}$$

$$\text{MFIE: } \mathbf{H}_S^i + \hat{\mathbf{n}} \times \mathbf{J}_S = \mathbf{H}_S^0 = 0 \tag{3.27}$$

$$\text{CFIE: } \alpha\left(\hat{\mathbf{n}} \times \mathbf{E}_S^0 \right) - \mathbf{H}_S^0 = 0 \tag{3.28}$$

Inserting (3.20) and (3.26) into (3.21) produces

$$\alpha\left(\mathbf{E}_S^i - \hat{\mathbf{n}} \times \mathbf{M}_S \right) + \left(\hat{\mathbf{n}} \times \mathbf{H}_S^i - \mathbf{J}_S \right) = 0 \tag{3.29}$$

Substituting (3.2) and (3.3) into (3.29) yields

$$\begin{aligned}&\alpha\left(\mathbf{E}_J^i\left(\mathbf{J}_S\right)+\mathbf{E}_M^i\left(\mathbf{M}_S\right)+\mathbf{E}_{inc}-\hat{\mathbf{n}}\times\mathbf{M}_S\right)\\&+\hat{\mathbf{n}}\times\left(\mathbf{H}_J^i\left(\mathbf{J}_S\right)+\mathbf{H}_M^i\left(\mathbf{M}_S\right)+\mathbf{H}_{inc}\right)-\mathbf{J}_S=0\end{aligned}\tag{3.30}$$

Re-writing (3.30) produces the CFIE expression

$$\begin{aligned}\alpha\mathbf{E}_J^i\left(\mathbf{J}_S\right)+\hat{\mathbf{n}}\times\mathbf{H}_J^i\left(\mathbf{J}_S\right)-\mathbf{J}_S=\alpha\hat{\mathbf{n}}\times\mathbf{M}_S-\alpha\mathbf{E}_M^i\left(\mathbf{M}_S\right)\\-\alpha\mathbf{E}_{inc}-\hat{\mathbf{n}}\times\mathbf{H}_M^i\left(\mathbf{M}_S\right)-\hat{\mathbf{n}}\times\mathbf{H}_{inc}\end{aligned}\tag{3.31}$$

Taking cross product of the normal vector and (3.31) yields alternatively

$$\begin{aligned}\alpha\hat{\mathbf{n}}\times\mathbf{E}_J^i\left(\mathbf{J}_S\right)-\mathbf{H}_J^i\left(\mathbf{J}_S\right)-\hat{\mathbf{n}}\times\mathbf{J}_S=-\alpha\mathbf{M}_S-\alpha\hat{\mathbf{n}}\times\mathbf{E}_M^i\left(\mathbf{M}_S\right)\\-\alpha\hat{\mathbf{n}}\times\mathbf{E}_{inc}+\mathbf{H}_M^i\left(\mathbf{M}_S\right)+\mathbf{H}_{inc}\end{aligned}\tag{3.32}$$

3.1.4 Operator Forms of Integral Equations

Substitution of the electromagnetic boundary solutions (3.4) – (3.7) into (3.14), (3.18), and (3.31) presents the operator form of the integral equations:

EFIE:

$$-Z_0L_{0,S}\left(\mathbf{J}_S\right)=\frac{1}{2}\hat{\mathbf{n}}\times\mathbf{M}_S-K_{0,S}\left(\mathbf{M}_S\right)-\mathbf{E}_{inc,S}\tag{3.33}$$

or

$$-Z_0\hat{\mathbf{n}}\times L_{0,S}\left(\mathbf{J}_S\right)=-\frac{1}{2}\mathbf{M}_S-\hat{\mathbf{n}}\times K_{0,S}\left(\mathbf{M}_S\right)-\hat{\mathbf{n}}\times\mathbf{E}_{inc,S}\tag{3.34}$$

MFIE:

$$-K_{0,S}\left(\mathbf{J}_S\right)+\frac{1}{2}\hat{\mathbf{n}}\times\mathbf{J}_S=Y_0L_{0,S}\left(\mathbf{M}_S\right)-\mathbf{H}_{inc,S} \tag{3.35}$$

or

$$-\hat{\mathbf{n}}\times K_{0,S}\left(\mathbf{J}_S\right)-\frac{1}{2}\mathbf{J}_S=Y_0\hat{\mathbf{n}}\times L_{0,S}\left(\mathbf{M}_S\right)-\hat{\mathbf{n}}\times\mathbf{H}_{inc,S} \tag{3.36}$$

CFIE:

$$\begin{aligned}-\alpha Z_0L_{0,S}\left(\mathbf{J}_S\right)-\hat{\mathbf{n}}\times K_{0,S}\left(\mathbf{J}_S\right)-\frac{1}{2}\mathbf{J}_S=\alpha\frac{1}{2}\hat{\mathbf{n}}\times\mathbf{M}_S-\alpha K_{0,S}\left(\mathbf{M}_S\right)-\alpha\mathbf{E}_{inc,S}\\ +Y_0\hat{\mathbf{n}}\times L_{0,S}\left(\mathbf{M}_S\right)-\hat{\mathbf{n}}\times\mathbf{H}_{inc,S}\end{aligned} \tag{3.37}$$

which is derived from $\alpha\cdot(3.33)+(3.36)$. Alternatively, by deriving the CFIE from $\alpha_1\cdot(3.33)+\alpha_2\cdot(3.36)$ yields

$$\begin{aligned}-\alpha_1Z_0L_{0,S}\left(\mathbf{J}_S\right)-\alpha_2\hat{\mathbf{n}}\times K_{0,S}\left(\mathbf{J}_S\right)-\alpha_2\frac{1}{2}\mathbf{J}_S=\alpha_1\frac{1}{2}\hat{\mathbf{n}}\times\mathbf{M}_S-\alpha_1K_{0,S}\left(\mathbf{M}_S\right)-\alpha_1\mathbf{E}_{inc,S}\\ +\alpha_2Y_0\hat{\mathbf{n}}\times L_{0,S}\left(\mathbf{M}_S\right)-\alpha_2\hat{\mathbf{n}}\times\mathbf{H}_{inc,S}\end{aligned} \tag{3.38}$$

3.2 General Method of Moment Solution of BOR Scattering

3.2.1 Solution Method with EFIE

Re-stating (3.33) presents the EFIE operator equation

$$-Z_0 L_{0,S}\left(\mathbf{J}_S\right) = \frac{1}{2}\hat{\mathbf{n}}\times\mathbf{M}_S - K_{0,S}\left(\mathbf{M}_S\right) - \mathbf{E}_{inc,S}$$

Initially examining the left hand side of (3.33), we will expand upon the components of the equation. Using (3.8), we can express

$$L_0\left(\mathbf{J}_S\right) = jk_0\iint_S \mathbf{J}_S\left(\mathbf{r}'\right)G\left(R\right)dS' - \frac{1}{jk_0}\iint_S\left[\nabla'_S\bullet\mathbf{J}_S\left(\mathbf{r}'\right)\right]\nabla G\left(R\right)dS' \tag{3.39}$$

where

$$dS' = t'\sin\theta' dt' d\phi' \tag{3.40}$$

The interest lies in evaluating $L_S = L_t \hat{\mathbf{a}}_t + L_\phi \hat{\mathbf{a}}_\phi$, therefore only L_t and L_ϕ are of consequence in (3.39). Expanding upon the components of (3.39), we can express

$$\nabla'_S \bullet \mathbf{J}_S(\mathbf{r}') = \frac{1}{t'}\frac{\partial}{\partial t'}(t' J_{t'}) + \frac{1}{t' \sin\theta'}\frac{\partial J_{\phi'}}{\partial \phi'} \tag{3.41}$$

$$\nabla G(R) = -\frac{1}{R}\left(jk_0 + \frac{1}{R}\right) G(R)\mathbf{R} \tag{3.42}$$

$$\mathbf{J}_S(\mathbf{r}') = J_t(\mathbf{r}')\hat{\mathbf{a}}_t + J_\phi(\mathbf{r}')\hat{\mathbf{a}}_\phi \tag{3.43}$$

$$\begin{aligned} J_t(\mathbf{r}') = {} & J_{t'}(\mathbf{r}')\left[\sin\theta\sin\theta'\cos(\phi-\phi') + \cos\theta\cos\theta'\right] \\ & + J_{\phi'}(\mathbf{r}')\left[\sin\theta\sin(\phi-\phi')\right] \end{aligned} \tag{3.44}$$

$$J_\phi(\mathbf{r}') = J_{t'}(\mathbf{r}')\left[-\sin\theta'\sin(\phi-\phi')\right] + J_{\phi'}(\mathbf{r}')\cos(\phi-\phi') \tag{3.45}$$

Inserting (3.41)-(3.45) into the left hand side of (3.33), we can develop

$$\begin{aligned} -Z_0 L_t(\mathbf{J}_S) &= -Z_0\left[L^A_{t,t'} + L^B_{t,t'} + L^A_{t,\phi'} + L^B_{t,\phi'}\right] \\ -Z_0 L_\phi(\mathbf{J}_S) &= -Z_0\left[L^A_{\phi,t'} + L^B_{\phi,t'} + L^A_{\phi,\phi'} + L^B_{\phi,\phi'}\right] \end{aligned} \tag{3.46}$$

where

$$\begin{aligned} L_t(\mathbf{J}_S) &= jk_0 \iint_S J_t(\mathbf{r}') G(R)\, dS' - \frac{1}{jk_0}\iint_S \left[\nabla'_S \bullet \mathbf{J}_S(\mathbf{r}')\right](\nabla G)_t\, dS' \\ &= jk_0 \iint_S \Big\{ J_{t'}(\mathbf{r}')\left[\sin\theta\sin\theta'\cos(\phi-\phi') + \cos\theta\cos\theta'\right] \\ &\quad + J_{\phi'}(\mathbf{r}')\left[\sin\theta\sin(\phi-\phi')\right]\Big\} G(R)\, dS' \\ &\quad - \frac{1}{jk_0}\iint_S \left[\frac{1}{t'}\frac{\partial}{\partial t'}(t' J_{t'}) + \frac{1}{t'\sin\theta'}\frac{\partial J_{\phi'}}{\partial \phi'}\right](\nabla G)_t\, dS' \\ &= L^A_{t,t'} + L^B_{t,t'} + L^A_{t,\phi'} + L^B_{t,\phi'} \end{aligned} \tag{3.47}$$

defining

$$L_{t,t'}^{A} = jk_0 \iint_S \left\{ J_{t'}(\mathbf{r}') \left[\sin\theta \sin\theta' \cos(\phi - \phi') + \cos\theta \cos\theta' \right] \right\} G(R)\, dS' \tag{3.48}$$

$$L_{t,t'}^{B} = -\frac{1}{jk_0} \iint_S \left[\frac{1}{t'} \frac{\partial}{\partial t'} (t' J_{t'}) \right] (\nabla G)_t \, dS' \tag{3.49}$$

$$L_{t,\phi'}^{A} = +jk_0 \iint_S \left\{ J_{\phi'}(\mathbf{r}') \left[\sin\theta \sin(\phi - \phi') \right] \right\} G(R)\, dS' \tag{3.50}$$

$$L_{t,\phi'}^{B} = -\frac{1}{jk_0} \iint_S \left[\frac{1}{t' \sin\theta'} \frac{\partial J_{\phi'}}{\partial \phi'} \right] (\nabla G)_t \, dS' \tag{3.51}$$

where

$$(\nabla G)_t = G_1(R) R_t \tag{3.52}$$

From (3.42), we can define

$$G_1(R) = -\frac{1}{R} \left(jk_0 + \frac{1}{R} \right) G(R) \tag{3.53}$$

and we can express the 3-D free-space Green's function

$$G(R) = \frac{e^{-jk_0 R}}{4\pi R} \tag{3.54}$$

We also define

$$R_t = \left[\rho - \rho' \cos(\phi - \phi') \right] \sin\theta + (z - z') \cos\theta \tag{3.55}$$

Similarly, we can express

$$\begin{aligned} L_{\phi}\left(\mathbf{J}_S\right) &= jk_0 \iint_S J_{\phi}\left(\mathbf{r}'\right) G\left(R\right) dS' - \frac{1}{jk_0} \iint_S \left[\nabla'_S \bullet \mathbf{J}_S\left(\mathbf{r}'\right)\right] \left(\nabla G\right)_{\phi} dS' \\ &= jk_0 \iint_S \left\{ J_{t'}\left(\mathbf{r}'\right) \left[-\sin\theta' \sin\left(\phi - \phi'\right)\right] + J_{\phi'}\left(\mathbf{r}'\right) \cos\left(\phi - \phi'\right) \right\} G\left(R\right) dS' \\ &\quad - \frac{1}{jk_0} \iint_S \left[\frac{1}{t'} \frac{\partial}{\partial t'} \left(t' J_{t'}\right) + \frac{1}{t' \sin\theta'} \frac{\partial J_{\phi'}}{\partial \phi'} \right] \left(\nabla G\right)_{\phi} dS' \\ &= L^A_{\phi,t'} + L^B_{\phi,t'} + L^A_{\phi,\phi'} + L^B_{\phi,\phi'} \end{aligned} \tag{3.56}$$

defining

$$L^A_{\phi,t'} = -jk_0 \iint_S \left\{ J_{t'}\left(\mathbf{r}'\right) \left[-\sin\theta' \sin\left(\phi - \phi'\right)\right] \right\} G\left(R\right) dS' \tag{3.57}$$

$$L^B_{\phi,t'} = -\frac{1}{jk_0} \iint_S \left[\frac{1}{t'} \frac{\partial}{\partial t'} \left(t' J_{t'}\right) \right] \left(\nabla G\right)_{\phi} dS' \tag{3.58}$$

$$L^A_{\phi,\phi'} = jk_0 \iint_S \left\{ J_{\phi'}\left(\mathbf{r}'\right) \cos\left(\phi - \phi'\right) \right\} G\left(R\right) dS' \tag{3.59}$$

$$L^B_{\phi,\phi'} = -\frac{1}{jk_0} \iint_S \left[\frac{1}{t' \sin\theta'} \frac{\partial J_{\phi'}}{\partial \phi'} \right] \left(\nabla G\right)_{\phi} dS' \tag{3.60}$$

where

$$\left(\nabla G\right)_{\phi} = G_1\left(R\right) R_{\phi} \tag{3.61}$$

and

$$R_{\phi} = \rho' \sin\left(\phi - \phi'\right) \tag{3.62}$$

Establishing

$$\begin{aligned} -Z_0 L_t\left(t,\phi\right) &= -Z_0 \left[L^A_{t,t'}\left(J_{t'}\right) + L^B_{t,t'}\left(J_{t'}\right) + L^A_{t,\phi'}\left(J_{\phi'}\right) + L^B_{t,\phi'}\left(J_{\phi'}\right) \right] \\ -Z_0 L_{\phi}\left(t,\phi\right) &= -Z_0 \left[L^A_{\phi,t'}\left(J_{t'}\right) + L^B_{\phi,t'}\left(J_{t'}\right) + L^A_{\phi,\phi'}\left(J_{\phi'}\right) + L^B_{\phi,\phi'}\left(J_{\phi'}\right) \right] \end{aligned} \tag{3.63}$$

Employing a moment method approach that uses interpolation functions as opposed to basis function expansions, we can obtain the impedance matrix of the developed tangential electric fields by using an inner product operation. The matrix will be of the form

$$\mathbf{Z}_{EFIE} = \begin{pmatrix} \mathbf{Z}^{A}_{t,t'} + \mathbf{Z}^{B}_{t,t'} & \mathbf{Z}^{A}_{t,\phi'} + \mathbf{Z}^{B}_{t,\phi'} \\ \mathbf{Z}^{A}_{\phi,t'} + \mathbf{Z}^{B}_{\phi,t'} & \mathbf{Z}^{A}_{\phi,\phi'} + \mathbf{Z}^{B}_{\phi,\phi'} \end{pmatrix} \tag{3.64}$$

If we assume

$$J_{t'} = \sum_{e'} \sum_{i'} N^{e'}_{t,i'} J^{e'}_{t',i'} \tag{3.65}$$

is the weighting interpolation function $W^{e}_{t,i}$, $N^{e'}_{t,i'}$ represents the linear interpolation function, and

$$J_{t'} = \sum_{e'} \sum_{i'} N^{e'}_{\phi,i'} J^{e'}_{\phi',i'} \tag{3.66}$$

is the weighting interpolation function $W^{e}_{\phi,i}$, $N^{e'}_{\phi,i'}$ represents the linear interpolation function.

It follows that we have $k \to (i,e), n \to (i',e')$

$$\mathbf{L}^{A}_{t,t'(k,n)} = \left\langle W^{e}_{t,i}, L^{A}_{t,t'}\left(N^{e'}_{t,i'}\right)\right\rangle, \mathbf{Z}^{A}_{t,t'} = -Z_0\mathbf{L}^{A}_{t,t'} \tag{3.67}$$

$$\mathbf{L}^{B}_{t,t'(k,n)} = \left\langle W^{e}_{t,i}, L^{B}_{t,t'}\left(N^{e'}_{t,i'}\right)\right\rangle, \mathbf{Z}^{B}_{t,t'} = -Z_0\mathbf{L}^{B}_{t,t'} \tag{3.68}$$

$$\mathbf{L}^{A}_{t,\phi'(k,n)} = \left\langle W^{e}_{t,i}, L^{A}_{t,\phi'}\left(N^{e'}_{\phi,i'}\right)\right\rangle, \mathbf{Z}^{A}_{t,\phi'} = -Z_0\mathbf{L}^{A}_{t,\phi'} \tag{3.69}$$

$$\mathbf{L}^{B}_{t,\phi'(k,n)} = \left\langle W^{e}_{t,i}, L^{B}_{t,\phi'}\left(N^{e'}_{\phi,i'}\right)\right\rangle, \mathbf{Z}^{B}_{t,\phi'} = -Z_0\mathbf{L}^{B}_{t,\phi'} \tag{3.70}$$

$$\mathbf{L}^{A}_{\phi,t'(k,n)} = \left\langle W^{e}_{\phi,i}, L^{A}_{\phi,t'}\left(N^{e'}_{t,i'}\right)\right\rangle, \mathbf{Z}^{A}_{\phi,t'} = -Z_0\mathbf{L}^{A}_{\phi,t'} \tag{3.71}$$

$$\mathbf{L}^{B}_{\phi,t'(k,n)} = \left\langle W^{e}_{\phi,i}, L^{B}_{\phi,t'}\left(N^{e'}_{t,i'}\right)\right\rangle, \mathbf{Z}^{B}_{\phi,t'} = -Z_0\mathbf{L}^{B}_{\phi,t'} \tag{3.72}$$

$$\mathbf{L}^{A}_{\phi,\phi'(k,n)} = \left\langle W^{e}_{\phi,i}, L^{A}_{\phi,\phi'}\left(N^{e'}_{\phi,i'}\right)\right\rangle, \mathbf{Z}^{A}_{\phi,\phi'} = -Z_0\mathbf{L}^{A}_{\phi,\phi'} \tag{3.73}$$

$$\mathbf{L}^{B}_{\phi,\phi'(k,n)} = \left\langle W^{e}_{\phi,i}, L^{B}_{\phi,\phi'}\left(N^{e'}_{\phi,i'}\right)\right\rangle, \mathbf{Z}^{B}_{\phi,\phi'} = -Z_0\mathbf{L}^{B}_{\phi,\phi'} \tag{3.74}$$

And on the left hand side of equation (3.33)

$$\mathbf{Z}_{EFIE}\mathbf{J} \tag{3.75}$$

where $\mathbf{J} = \begin{pmatrix} \mathbf{J}_t \\ \mathbf{J}_\phi \end{pmatrix}$.

Focusing on the right hand side of (3.33), we can assume $\mathbf{M}_S$ is expanded by a global basis function

$$\begin{aligned} \mathbf{M}_S &= \sum_n \mathbf{m}_{S,n} V_n \\ &= \sum_n m_{t,n}(t,\phi) V_n \hat{\mathbf{a}}_t + \sum_n m_{\phi,n}(t,\phi) V_n \hat{\mathbf{a}}_\phi \end{aligned} \tag{3.76}$$

Operations on (3.76) yield

$$\begin{aligned}\frac{1}{2}\hat{\mathbf{n}}\times\mathbf{M}_S &= \frac{1}{2}\hat{\mathbf{n}}\times\left[\sum_n m_{t,n}(t,\phi)V_n\hat{\mathbf{a}}_t + \sum_n m_{\phi,n}(t,\phi)V_n\hat{\mathbf{a}}_\phi\right] \\ &= \sum_n \frac{1}{2}m_{t,n}(t,\phi)V_n\hat{\mathbf{a}}_\phi + \sum_n\left[-\frac{1}{2}m_{\phi,n}(t,\phi)\right]V_n\hat{\mathbf{a}}_t\end{aligned} \tag{3.77}$$

where

$$\left(\frac{1}{2}\hat{\mathbf{n}}\times\mathbf{M}_S\right)_t = \left[-\frac{1}{2}m_{\phi,n}(t,\phi)\right]V_n \tag{3.78}$$

$$\left(\frac{1}{2}\hat{\mathbf{n}}\times\mathbf{M}_S\right)_\phi = \sum_n \frac{1}{2}m_{t,n}(t,\phi)V_n \tag{3.79}$$

It follows

$$\begin{aligned}-K_0(\mathbf{M}_S) &= -\iint_S \mathbf{M}_S(t',\phi')\times\nabla G(R)\,dS' \\ &= -\iint_S\left[\mathbf{M}_S(t',\phi')\times R\right]G_1(R)\,dS'\end{aligned} \tag{3.80}$$

where

$$\begin{aligned}\left[-K_0(\mathbf{m}_{S,n})\right]_t = -\iint_S \mathbf{m}_{t',n}\Big[&(\rho\sin\theta'\cos\theta - \rho'\sin\theta\cos\theta') \\ &+ (z'-z)\sin\theta\cos(\phi-\phi')\Big]\sin(\phi-\phi')G_1(R)\,dS' \\ -\iint_S \mathbf{m}_{\phi',n}\Big[&\rho'\cos\theta - \rho\cos\theta\cos(\phi-\phi') \\ &+ (z-z')\sin\theta'\cos(\phi-\phi')\Big]G_1(R)\,dS'\end{aligned} \tag{3.81}$$

and

$$\begin{aligned}\left[-K_0\left(\mathbf{m}_{S,n}\right)\right]_\phi = -\iint_S \mathbf{m}_{t',n}\Big[\rho\cos\theta' - \rho'\cos\theta'\cos\left(\phi-\phi'\right) \\ +\left(z'-z\right)\sin\theta'\cos\left(\phi-\phi'\right)\Big]G_1\left(R\right)dS' \\ -\iint_S \mathbf{m}_{\phi',n}\left(z'-z\right)\sin\left(\phi-\phi'\right)G_1\left(R\right)dS'\end{aligned} \tag{3.82}$$

The right hand side will become

$$\mathbf{P}_{EFIE}\mathbf{V} + \mathbf{V}_{EFIE}^{inc} \tag{3.83}$$

where

$$\mathbf{P}_{EFIE} = \begin{pmatrix}\mathbf{P}_t^A \\ \mathbf{P}_\phi^A\end{pmatrix} + \begin{pmatrix}\mathbf{P}_t^B \\ \mathbf{P}_\phi^B\end{pmatrix} \tag{3.84}$$

with

$$\mathbf{P}_t^A\left(k,n\right) = \left\langle W_{t,i}^e, -\frac{1}{2}m_{\phi,n}\right\rangle \tag{3.85}$$

$$\mathbf{P}_\phi^A\left(k,n\right) = \left\langle W_{\phi,i}^e, \frac{1}{2}m_{t,n}\right\rangle \tag{3.86}$$

$$\mathbf{P}_t^B\left(k,n\right) = \left\langle W_{t,i}^e, \left[-K_{0,S}\left(\mathbf{m}_{S,n}\right)\right]_t\right\rangle \tag{3.87}$$

$$\mathbf{P}_\phi^B\left(k,n\right) = \left\langle W_{\phi,i}^e, \left[-K_{0,S}\left(\mathbf{m}_{S,n}\right)\right]_\phi\right\rangle \tag{3.88}$$

and

$$\mathbf{V}_{EFIE}^{inc} = \begin{pmatrix}\mathbf{V}_{t,k}^{inc} \\ \mathbf{V}_{\phi,k}^{inc}\end{pmatrix} \tag{3.89}$$

with

$$\mathbf{V}_{t,k}^{inc} = \left\langle W_{t,i}^{e}, -E_{t}^{inc} \right\rangle \tag{3.90}$$

$$\mathbf{V}_{\phi,k}^{inc} = \left\langle W_{t,i}^{e}, -E_{\phi}^{inc} \right\rangle \tag{3.91}$$

The final form of the EFIE equation is

$$\mathbf{Z}_{EFIE}\mathbf{J} = \mathbf{P}_{EFIE}\mathbf{V} + \mathbf{V}_{EFIE}^{inc} \tag{3.92}$$

3.2.2 Solution Method with MFIE

Re-stating (3.36) presents the EFIE operator equation

$$-\hat{\mathbf{n}} \times K_{0,S}\left(\mathbf{J}_S\right) - \frac{1}{2}\mathbf{J}_S = Y_0 \hat{\mathbf{n}} \times L_{0,S}\left(\mathbf{M}_S\right) - \hat{\mathbf{n}} \times \mathbf{H}_{inc,S}$$

Initially examining the left hand side of (3.36), we will expand upon the components of the equation. Using (3.9), we can express

$$K_0\left(\mathbf{J}_S\right) = \iint_S \mathbf{J}_S\left(\mathbf{r}'\right) \times \nabla G\left(R\right) dS' \tag{3.93}$$

where

$$dS' = t' \sin\theta' dt' d\phi' \tag{3.94}$$

Similarly, to the EFIE Solution method, the interest lies in evaluating $K_S = K_t\hat{\mathbf{a}}_t + K_\phi\hat{\mathbf{a}}_\phi$, therefore only K_t and K_ϕ are of consequence in (3.93). Expanding (3.93), we can express

$$\begin{aligned} K_0(\mathbf{J}_S) &= \iint_S \left[\mathbf{J}_S(\mathbf{r}')\times\nabla G(R)\right]_t dS'\hat{\mathbf{a}}_t + \iint_S \left[\mathbf{J}_S(\mathbf{r}')\times\nabla G(R)\right]_\phi dS'\hat{\mathbf{a}}_\phi \\ &= K_t(\mathbf{J}_S)\hat{\mathbf{a}}_t + K_\phi(\mathbf{J}_S)\hat{\mathbf{a}}_\phi \end{aligned} \tag{3.95}$$

Further mathematical operations and manipulation extends

$$\begin{aligned} -\hat{\mathbf{n}}\times K_0(\mathbf{J}_S) &= -\iint_S \left[\mathbf{J}_S(\mathbf{r}')\times\nabla G(R)\right]_t dS'\hat{\mathbf{a}}_\phi + \iint_S \left[\mathbf{J}_S(\mathbf{r}')\times\nabla G(R)\right]_\phi dS'\hat{\mathbf{a}}_t \\ &= K_\phi(\mathbf{J}_S)\hat{\mathbf{a}}_t - K_t(\mathbf{J}_S)\hat{\mathbf{a}}_\phi \end{aligned} \tag{3.96}$$

where

$$\begin{aligned} \left[-\hat{\mathbf{n}}\times K_0(\mathbf{J}_S)\right]_t &= \iint_S \left[\mathbf{J}_S(\mathbf{r}')\times\nabla G(R)\right]_\phi dS' \\ &= K_\phi(\mathbf{J}_S) \\ &= \iint_S \{J_{t'}\left[\rho\cos\theta' - \rho'\cos\theta'\cos(\phi-\phi')\right. \\ &\quad \left.+(z'-z)\sin\theta'\cos(\phi-\phi')\right] + J_{\phi'}(z'-z)\sin(\phi-\phi')\} G_1(R)\,dS' \\ &= \overline{K}_{t,t'} + \overline{K}_{t,\phi'} \\ &= K_{\phi,t'} + K_{\phi,\phi'} \end{aligned} \tag{3.97}$$

Understanding that

$$\begin{aligned} \overline{K}_{t,t'} &= K_{\phi,t'} \\ \overline{K}_{t,\phi'} &= K_{\phi,\phi'} \end{aligned}$$

Similarly,

$$\begin{aligned}\left[-\hat{\mathbf{n}}\times K_0\left(\mathbf{J}_S\right)\right]_\phi &= -\iint_S\left[\mathbf{J}_S\left(\mathbf{r}'\right)\times\nabla G\left(R\right)\right]_t\,dS'\\ &= -K_t\left(\mathbf{J}_S\right)\\ &= -\iint_S\Big\{J_{t'}\Big[\left(\rho\sin\theta'\cos\theta-\rho'\sin\theta\cos\theta'\right)\\ &\quad+\left(z'-z\right)\sin\theta'\sin\theta\Big]\sin\left(\phi-\phi'\right)+J_{\phi'}\Big[\rho'\cos\theta\\ &\quad-\rho\cos\theta\cos\left(\phi-\phi'\right)+\left(z-z'\right)\sin\theta\cos\left(\phi-\phi'\right)\Big]\Big\}G_1\left(R\right)dS'\\ &= \bar{K}_{\phi,t'}+\bar{K}_{\phi,\phi'}\\ &= -K_{t,t'}-K_{t,\phi'}\end{aligned}\tag{3.98}$$

where

$$\begin{aligned}\bar{K}_{\phi,t'} &= -K_{t,t'}\\ \bar{K}_{\phi,\phi'} &= -K_{t,\phi'}\end{aligned}$$

The overbar in the previous equations indicates a cross-product of the normal operation. We further define

$$\begin{aligned}\bar{K}_{t,t'} = \iint_S J_{t'}\Big[&\rho\cos\theta'-\rho'\cos\theta'\cos\left(\phi-\phi'\right)\\ &+\left(z'-z\right)\sin\theta'\cos\left(\phi-\phi'\right)\Big]G_1\left(R\right)dS'\end{aligned}\tag{3.99}$$

$$\bar{K}_{t,\phi'} = \iint_S J_{\phi'}\left(z'-z\right)\sin\left(\phi-\phi'\right)G_1\left(R\right)dS'\tag{3.100}$$

$$\begin{aligned}-\bar{K}_{\phi,t'} = \iint_S J_{t'}\Big[&\left(\rho\sin\theta'\cos\theta-\rho'\sin\theta\cos\theta'\right)\\ &+\left(z'-z\right)\sin\theta'\sin\theta\Big]\sin\left(\phi-\phi'\right)G_1\left(R\right)dS'\end{aligned}\tag{3.101}$$

$$\begin{aligned}-\bar{K}_{\phi,\phi'} = \iint_S J_{\phi'}\Big[&\rho'\cos\theta-\rho\cos\theta\cos\left(\phi-\phi'\right)\\ &+\left(z-z'\right)\sin\theta\cos\left(\phi-\phi'\right)\Big]G_1\left(R\right)dS'\end{aligned}\tag{3.102}$$

Utilizing the weighting functions of (3.65) and (3.66) on (3.97) and (3.98), respectively, we obtain the matrix relation

$$\mathbf{Z}_{MFIE} = \begin{pmatrix} \bar{\mathbf{K}}_{t,t'} & \bar{\mathbf{K}}_{t,\phi'} \\ \bar{\mathbf{K}}_{\phi,t'} & \bar{\mathbf{K}}_{\phi,\phi'} \end{pmatrix} - \frac{1}{2}\begin{pmatrix} \mathbf{D}_{t,t} & \mathbf{0} \\ \mathbf{0} & \mathbf{D}_{\phi,\phi} \end{pmatrix} \tag{3.103}$$

where

$$\bar{\mathbf{K}}_{t,t'(k,n)} = \left\langle W^e_{t,i}, \bar{\mathbf{K}}_{t,t'}\left(N^{e'}_{t,i'}\right)\right\rangle \tag{3.104}$$

$$\bar{\mathbf{K}}_{t,\phi'(k,n)} = \left\langle W^e_{t,i}, \bar{\mathbf{K}}_{t,\phi'}\left(N^{e'}_{\phi,i'}\right)\right\rangle \tag{3.105}$$

$$\bar{\mathbf{K}}_{\phi,t'(k,n)} = \left\langle W^e_{\phi,i}, \bar{\mathbf{K}}_{\phi,t'}\left(N^{e'}_{t,i'}\right)\right\rangle \tag{3.106}$$

$$\bar{\mathbf{K}}_{\phi,\phi'(k,n)} = \left\langle W^e_{\phi,i}, \bar{\mathbf{K}}_{\phi,\phi'}\left(N^{e'}_{\phi,i'}\right)\right\rangle \tag{3.107}$$

We will also express

$$\mathbf{D}_{t,t(k,n)} = \left\langle W^e_{t,i}, N^e_{t,j}\right\rangle \tag{3.108}$$

$$\mathbf{D}_{\phi,\phi(k,n)} = \left\langle W^e_{\phi,i}, N^e_{\phi,j}\right\rangle \tag{3.109}$$

where the matrices of (3.108) and (3.109) are sparse and frequency independent. The left side of (3.36) can be represented by

$$\mathbf{Z}_{MFIE}\mathbf{J} \tag{3.110}$$

Focusing on the right hand side of (3.36), and maintaining the assumption of the basis function expansion in (3.76) we obtain

$$\begin{aligned} Y_0\hat{\mathbf{n}}\times L_{0,S}\left(\mathbf{M}_S\right) &= Y_0\sum_n \hat{\mathbf{n}}\times L_{0,S}\left(\mathbf{m}_{S,n}\right) \\ &= Y_0\sum_n L_t\left(\mathbf{m}_{S,n}\right)\hat{\mathbf{a}}_\phi - Y_0\sum_n L_\phi\left(\mathbf{m}_{S,n}\right)\hat{\mathbf{a}}_t \\ &= -Y_0 L_\phi\left(\mathbf{m}_{S,n}\right) \end{aligned} \tag{3.111}$$

Further

$$\begin{aligned} \left[Y_0\hat{\mathbf{n}}\times L_{0,S}\left(\mathbf{m}_{S,n}\right)\right]_t = -Y_0\Bigg\{ jk_0\Bigg[&\iint_S -m_{t',n}\left(\mathbf{r}'\right)\sin\theta'\sin\left(\phi-\phi'\right)G\left(R\right)dS' \\ &+\iint_S m_{\phi',n}\left(\mathbf{r}'\right)\cos\left(\phi-\phi'\right)G\left(R\right)dS'\Bigg] \\ &-\frac{1}{jk_0}\iint_S\left[\nabla'\bullet\mathbf{m}_{S,n}\left(\mathbf{r}'\right)\right]\left(\nabla G\right)_\phi\, dS'\Bigg\} \\ = Y_0 L_t\left(\mathbf{m}_{S,n}\right) \end{aligned} \tag{3.112}$$

$$\begin{aligned} \left[Y_0\hat{\mathbf{n}}\times L_{0,S}\left(\mathbf{m}_{S,n}\right)\right]_\phi = Y_0\Bigg\{ jk_0\Bigg[&\iint_S -m_{t',n}\left(\mathbf{r}'\right)\left[\sin\theta\sin\theta'\cos\left(\phi-\phi'\right)\right. \\ &\left.+\cos\theta\cos\theta'\right]G\left(R\right)dS' \\ &+\iint_S m_{\phi',n}\left(\mathbf{r}'\right)\sin\theta\sin\left(\phi-\phi'\right)G\left(R\right)dS'\Bigg] \\ &-\frac{1}{jk_0}\iint_S\left[\nabla'_S\bullet\mathbf{m}_{S,n}\left(\mathbf{r}'\right)\right]\left(\nabla G\right)_t\, dS'\Bigg\} \\ = Y_0 L_\phi\left(\mathbf{m}_{S,n}\right) \end{aligned} \tag{3.113}$$

The right hand side will become

$$\mathbf{P}_{MFIE}\mathbf{V}+\mathbf{V}^{inc}_{MFIE} \tag{3.114}$$

where

$$\mathbf{P}_{MFIE} = \begin{pmatrix} \mathbf{P}_t^M \\ \mathbf{P}_\phi^M \end{pmatrix} \tag{3.115}$$

with

$$\mathbf{P}_t^M (k,n) = \left\langle W_{t,i}^e, P_{t,n} \right\rangle \tag{3.116}$$

$$\mathbf{P}_\phi^M (k,n) = \left\langle W_{t,i}^e, P_{\phi,n} \right\rangle \tag{3.117}$$

The final form of the MFIE equation is

$$\mathbf{Z}_{MFIE}\mathbf{J} = \mathbf{P}_{MFIE}\mathbf{V} + \mathbf{V}_{MFIE}^{inc} \tag{3.118}$$

3.2.3 Solution Method with CFIE

The solution method of the CFIE can be seen as a combination of the EFIE and MFIE solution. We can concisely express the final forms through consideration of previous derivations as

$$\mathbf{Z}_{CFIE}\mathbf{J} = \mathbf{P}_{CFIE}\mathbf{V} + \mathbf{V}_{CFIE}^{inc} \tag{3.119}$$

Using (3.38), we can further state

$$\mathbf{Z}_{CFIE} = \alpha_1 \mathbf{Z}_{EFIE} + \alpha_2 \mathbf{Z}_{MFIE} \tag{3.120}$$

$$\mathbf{P}_{CFIE} = \alpha_1 \mathbf{P}_{EFIE} + \alpha_2 \mathbf{P}_{MFIE} \tag{3.121}$$

$$\mathbf{V}_{CFIE}^{inc} = \alpha_1 \mathbf{V}_{EFIE}^{inc} + \alpha_2 \mathbf{V}_{MFIE}^{inc} \tag{3.122}$$

3.2.4 Development of MoM Algorithm Using Interpolation Functions

Traditionally, the moment method is implemented through the use of basis and weighting functions. The use of basis functions contributes to the challenge of the meshing arbitrary structures. Expanding upon the theory of interpolation functions, element analysis, and global assembly as implemented in the finite element method (FEM), we can develop a convenient implementation of the method of moments. Beginning with the operator equation

$$L(J) = E \tag{3.123}$$

where L is a linear operator, J represents the unknown coefficients, and E represents the known excitation. Initially, the entire solution domain must be divided into $N_{element}$ number of elements. J can be expanded through interpolation functions such that

$$J = \sum_{e'}^{N_{element}} \sum_{i'} N_{i'}^{e'} J_{i'}^{e'} \tag{3.124}$$

where $i' = 1, 2, \ldots, N$. Inserting (3.124) into (3.123) yields

$$L\left(\sum_{e'}^{N_{element}} \sum_{i'} N_{i'}^{e'} J_{i'}^{e'} \right) = E \tag{3.125}$$

which yields

$$\sum_{e'}^{N_{element}} \sum_{i'} L\left(N_{i'}^{e'} \right) J_{i'}^{e'} = E \tag{3.126}$$

Assume W_i^e is another set of interpolation functions that may or may not be the same as

N_i^e. Taking the inner product of W_i^e and (3.126), results as

$$\sum_{e'}\sum_{i'}\left\langle W_i^e, L\left(N_{i'}^{e'}\right)\right\rangle J_{i'}^{e'} = \left\langle W_i^e, E\right\rangle \tag{3.127}$$

Defining the global number for the i^{th} local node in the e^{th} element is m, and the global number for the i'^{th} local node in the e'^{th} element is n. Consequently, we can add $\left\langle W_i^e, L\left(N_{i'}^{e'}\right)\right\rangle$ to (m,n) the element of the global impedance matrix, and as a result (3.127) can be written as

$$\mathbf{ZJ} = \mathbf{B} \tag{3.128}$$

Similarly, $\mathbf{B}$ is obtained by adding $\left\langle W_i^e, E\right\rangle$ to global $\mathbf{B}$ vector after element analysis.

Pseudo-code to realize this application is as follows:

```
A=zeros(N_nodes,N_nodes)
B=zeros(N_nodes,1)
for e1=1:N_elements
        for i1=1:N
                n=global(i1,e1)
                calculate L(N_{i'}^{e'}) (at each Gaussian interpolation point)
                calculate E(N_{i'}^{e'}) (if it is expanded by interpolation functions)
                for e=1:N_elements
                        for i=1:N
                                m=global(i,e) +a        !where a = <W_i^e, L(N_{i'}^{e'})>
                                A(m,n)=A(m,n)+a
                        end
                end
        b=function <W_i^e, E>
        B(m)=B(m)+b
        end
end
```

If $W_i^e = N_i^e$, the above procedure is the Galerkin method. If L is self-adjoint, the $\mathbf{Z}$ matrix exhibits symmetry.

If E is expanded by a global function $\phi_{i'}$, we have

$$E = \sum_{i'}^{N_\phi} \phi_{i'} E_{i'} \tag{3.129}$$

which can be inserted into (3.127), resulting as

$$\sum_{e'} \sum_{i'} \left\langle W_i^e, L\left(N_{i'}^{e'}\right) \right\rangle J_{i'}^{e'} = \sum_{i'} \left\langle W_i^e, \phi_{i'} \right\rangle E_{i'} \tag{3.130}$$

establishing

$$\mathbf{ZJ} = \mathbf{BE} \tag{3.131}$$

If E is expanded by an interpolation function, we have

$$E = \sum_{e'} \sum_{i'} \left\langle M_{i'}^{e'}, E_{i'}^{e'} \right\rangle \tag{3.132}$$

Inserting (3.132) into (3.127) results in

$$\sum_{e'} \sum_{i'} \left\langle W_i^e, L\left(N_{i'}^{e'}\right) \right\rangle J_{i'}^{e'} = \sum_{e'} \sum_{i'} \left\langle W_i^e, M_{i'}^{e'} \right\rangle E_{i'}^{e'} \tag{3.133}$$

establishing (3.131), where $\mathbf{B}$ is defined as the modal excitation matrix with dimensions $N\_nodes \times N_\phi$ matrix, and $\mathbf{E}$ is a vector with length N_ϕ.

CHAPTER 4 SOLUTION METHODOLOGY

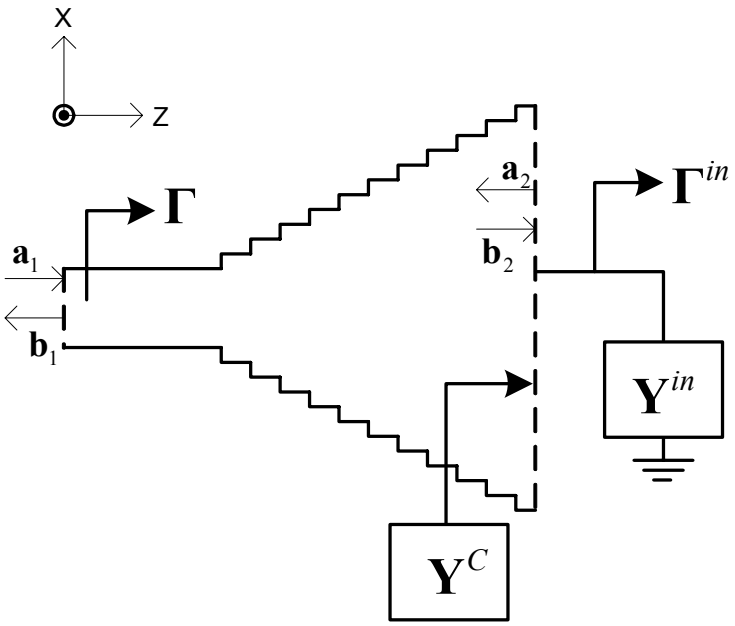

Figure 4-1 Input Admittance terminated model.

4.1 Admittance Matrix Formulation

The preceding chapters have detailed methods to be implemented in a solution methodology. Here, to solve the internal and external regions, we address solutions to establish the linkage of the two regions. The transmission line equivalence was introduced earlier will be used to establish the motivational theory for coupling the inner

modal scattering parameters and the external solutions and their contributions to the common aperture. Essentially, it is necessary to terminate the aperture with an input modal admittance matrix that is collectively representative of the solution of the external region. When the admittance matrix is solved, the reflection coefficient matrix at the input port can be subsequently derived. The following derivations will detail the formulation of the admittance matrix.

The boundary conditions that are defined exactly incident on the aperture of the internal and external regions must satisfy Maxwell's equations. Therefore, we will define the following conditions across region transverse to the aperture.

$$\begin{aligned} \mathbf{E}^{(0)} &= \mathbf{E}^{I} = \mathbf{E}^{II} \\ \mathbf{H}^{(0)} &= \mathbf{H}^{I} = \mathbf{H}^{II} \end{aligned} \tag{4.1}$$

Furthermore, of interest is the equation

$$\mathbf{H}^{II} = \mathbf{H}_{F}^{S} + \mathbf{H}_{A}^{S} \tag{4.2}$$

Here we will define region *I* as the internal region and region *II* as the external region. The 0 superscript denotes the boundary separating region *I* and *II*; A and F subscripts denote the magnetic fields attributed by the magnetic and electric vector potentials, respectively. Given (4.2), we can establish a modal expression accounting for *N* number of modes that takes the form

$$\sum_{n=1}^{N} h_{F,n}^{S} V_n + \sum_{n=1}^{N} h_{A,n}^{S} V_n = \sum_{n=1}^{N} h_{t,n} I_n \tag{4.3}$$

V and I represent modal voltages and currents, respectively. Collecting the terms in (4.3) we can write

$$\sum_{n=1}^{N}\left(h_{F,n}^{S}+h_{A,n}^{S}\right)V_n=\sum_{n=1}^{N}h_{t,n}I_n \tag{4.4}$$

Applying mathematical operations, we can develop the expression

$$\sum_{n=1}^{N}V_n\iint_{S'}e_{t,m}\times\left(h_{F,n}^{S}+h_{A,n}^{S}\right)\bullet dS'=\sum_{n=1}^{N}I_n\iint_{S'}e_{t,m}\times h_{t,n}\bullet dS' \tag{4.5}$$

Applying the mode orthogonality relationships as described by (2.74)-(2.76), (4.5) leads us to the expression

$$\sum_{n=1}^{N}V_n\iint_{S'}e_{t,m}\times\left(h_{F,n}^{S}+h_{A,n}^{S}\right)\bullet dS'=I_m \tag{4.6}$$

Examination of (4.6) lends to a reformulation of the expression as

$$\mathbf{Y}_{in}\cdot\mathbf{V}=\mathbf{I} \tag{4.7}$$

where $\mathbf{Y}_{in}$ is the input admittance matrix defined as

$$\left(\mathbf{Y}_{in}\right)_{(m,n)}=\iint_{S'}e_{t,m}\times\left(h_{F,n}^{S}+h_{A,n}^{S}\right)\bullet dS' \tag{4.8}$$

4.2 Reflection Coefficient Formulation at the Aperture

The task of relating the aperture admittance matrix and the external input admittance matrix in terms of the reflection coefficient is derived. Initially, we can offer the expressions

$$\begin{aligned} \mathbf{V} &= \mathbf{a} + \mathbf{b} \\ \mathbf{I} &= \mathbf{Y}\left(\mathbf{a} - \mathbf{b}\right) \end{aligned} \tag{4.9}$$

We can establish the relationship of the input admittance matrix as

$$\mathbf{Y}_{in}\mathbf{V} = \mathbf{I} \tag{4.10}$$

Using (4.9) and (4.10) expands to

$$\mathbf{Y}_{in}\left(\mathbf{a} + \mathbf{b}\right) = \mathbf{Y}\left(\mathbf{a} - \mathbf{b}\right) \tag{4.11}$$

Collecting terms, we obtain

$$\left(\mathbf{Y}_{in} + \mathbf{Y}\right)\mathbf{b} = \left(\mathbf{Y} - \mathbf{Y}_{in}\right)\mathbf{a} \tag{4.12}$$

Further manipulation and we come to the expression

$$\mathbf{b} = \left(\mathbf{Y}_{in} + \mathbf{Y}\right)^{-1}\left(\mathbf{Y} - \mathbf{Y}_{in}\right)\mathbf{a} \tag{4.13}$$

Through the definition of the reflection coefficient we deliver the final expression for the reflection coefficient matrix at the aperture as

$$\mathbf{\Gamma}_{in} = \left(\mathbf{Y}_{in} + \mathbf{Y}\right)^{-1}\left(\mathbf{Y} - \mathbf{Y}_{in}\right) \tag{4.14}$$

4.3 Reflection Coefficient Formulation at the Input

The calculation of the admittance matrix allows for the subsequent solution of the reflection coefficient matrix. Referring again to Figure 4-1 Input Admittance terminated model., we will establish the following forward and backward traveling wave coefficient relationships

$$\mathbf{b}_1 = \mathbf{S}_{11}\mathbf{a}_1 + \mathbf{S}_{12}\mathbf{a}_2 \tag{4.15}$$

$$\mathbf{b}_2 = \mathbf{S}_{21}\mathbf{a}_1 + \mathbf{S}_{22}\mathbf{a}_2 \tag{4.16}$$

Relating the coefficient matrix to the equations can be expressed as

$$\mathbf{a}_2 = \boldsymbol{\Gamma}_{in}\mathbf{b}_2 \tag{4.17}$$

Applying (4.17) to (4.16), we get

$$\begin{aligned} \mathbf{b}_2 &= \mathbf{S}_{21}\mathbf{a}_1 + \mathbf{S}_{22}\boldsymbol{\Gamma}_{in}\mathbf{b}_2 \\ &= (\bar{\mathbf{I}} - \mathbf{S}_{22}\boldsymbol{\Gamma}_{in})^{-1}\mathbf{S}_{21}\mathbf{a}_1 \end{aligned} \tag{4.18}$$

Using (4.15), (4.17), and (4.18) it is shown that

$$\begin{aligned} \mathbf{b}_1 &= \mathbf{S}_{11}\mathbf{a}_1 + \mathbf{S}_{12}\boldsymbol{\Gamma}_{in}\mathbf{b}_2 \\ &= \mathbf{S}_{11}\mathbf{a}_1 + \mathbf{S}_{12}\boldsymbol{\Gamma}_{in}(\bar{\mathbf{I}} - \mathbf{S}_{22}\boldsymbol{\Gamma}_{in})^{-1}\mathbf{S}_{21}\mathbf{a}_1 \\ &= \left[\mathbf{S}_{11} + \mathbf{S}_{12}\boldsymbol{\Gamma}_{in}(\bar{\mathbf{I}} - \mathbf{S}_{22}\boldsymbol{\Gamma}_{in})^{-1}\mathbf{S}_{21}\right]\mathbf{a}_1 \end{aligned} \tag{4.19}$$

From which we obtain

$$\boldsymbol{\Gamma} = \mathbf{S}_{11} + \mathbf{S}_{12}\boldsymbol{\Gamma}_{in}(\bar{\mathbf{I}} - \mathbf{S}_{22}\boldsymbol{\Gamma}_{in})^{-1}\mathbf{S}_{21} \tag{4.20}$$

We can also express through (4.17) and (4.18)

$$\mathbf{a}_2 = \boldsymbol{\Gamma}_{in}(\bar{\mathbf{I}} - \mathbf{S}_{22}\boldsymbol{\Gamma}_{in})^{-1}\mathbf{S}_{21}\mathbf{a}_1 \tag{4.21}$$

The complete relationship is established for the forward and backward coefficients of wave propagation with respect to the reflection coefficient matrix.

4.4 Radiation Pattern Calculation

Simplification of calculating the integral expressions of the vector electric and magnetic potentials can be accomplished using far field observations [7,8]. The minimum distance to the far field region is represented by

$$r \geq \frac{2D}{\lambda} \tag{4.22}$$

where D is the largest dimension of the radiator or scatterer. Referencing [7] we can establish the approximation of the electric and magnetic vector potentials as

$$\mathbf{A} = \frac{\mu}{4\pi}\iint_S \mathbf{J}_{S'}\frac{e^{-jkR}}{R}\cdot dS' \simeq \frac{\mu e^{-jkr}}{4\pi r}\mathbf{N} \tag{4.23}$$

$$\mathbf{F} = \frac{\varepsilon}{4\pi}\iint_S \mathbf{M}_{S'}\frac{e^{-jkR}}{R}\cdot dS' \simeq \frac{\varepsilon e^{-jkr}}{4\pi r}\mathbf{L} \tag{4.24}$$

where

$$\mathbf{N} = \iint_S \mathbf{J}_{S'} e^{jk\mathbf{r}'\cdot\mathbf{a}_r} \cdot dS' \tag{4.25}$$

$$\mathbf{L} = \iint_S \mathbf{M}_{S'} e^{jk\mathbf{r}'\cdot\mathbf{a}_r} \cdot dS' \tag{4.26}$$

Due to the negligible contribution to $\mathbf{E}$ and $\mathbf{H}$ in the radial direction with respect to the contributions of θ and ϕ, we can express the following equations

$$E_\theta = Z_0 H_\phi = -\frac{jke^{-jkr}}{4\pi r}\left(L_\phi + Z_0 N_\theta\right) \tag{4.27}$$

$$E_r = 0 \tag{4.28}$$

$$E_\phi = -Z_0 H_\theta = \frac{jke^{-jkr}}{4\pi r}\left(L_\theta - Z_0 N_\phi\right) \tag{4.29}$$

$$H_r = 0 \tag{4.30}$$

The magnitude of the electric field can be calculated as

$$\begin{aligned} |\mathbf{E}| &= \sqrt{|E_\theta|^2 + |E_\phi|^2} \\ &= \frac{k}{4\pi r}\left(\left|L_\phi + Z_0 N_\theta\right|^2 + \left|L_\theta - Z_0 N_\phi\right|^2\right)^{\frac{1}{2}} \end{aligned} \tag{4.31}$$

The power can be represented by

$$\begin{aligned} P &= \frac{1}{2}\left(\mathbf{E}\times\mathbf{H}^*\right) \\ &= \frac{k^2}{32\pi^2 Z_0 r^2}\left(\left|L_\phi + Z_0 N_\theta\right|^2 + \left|L_\theta - Z_0 N_\phi\right|^2\right) \end{aligned} \tag{4.32}$$

To further consider the expansion of (4.25) and (4.26) with respect to the transverse components of θ and ϕ, the following can be derived for the cylindrical coordinate system:

$$\begin{aligned} N_\theta = \iint_S \Big\{ & J_{t'}(\mathbf{r}') \left[\cos\theta \sin\theta' \cos(\phi - \phi') - \sin\theta \cos\theta' \right] \\ & + J_{\phi'}(\mathbf{r}') \left[\cos\theta \sin(\phi - \phi') \right] \Big\} e^{jk\mathbf{r}'\cdot\mathbf{a}_r} dS' \end{aligned} \tag{4.33}$$

$$N_\phi = \iint_S \left\{ J_{t'}(\mathbf{r}') \left[-\sin\theta' \sin(\phi - \phi') \right] + J_{\phi'}(\mathbf{r}') \cos(\phi - \phi') \right\} e^{jk\mathbf{r}'\cdot\mathbf{a}_r} dS' \tag{4.34}$$

$$\begin{aligned} L_\theta = \iint_S \Big\{ & M_{t'}(\mathbf{r}') \left[\cos\theta \sin\theta' \cos(\phi - \phi') - \sin\theta \cos\theta' \right] \\ & + M_{\phi'}(\mathbf{r}') \left[\cos\theta \sin(\phi - \phi') \right] \Big\} e^{jk\mathbf{r}'\cdot\mathbf{a}_r} dS' \end{aligned} \tag{4.35}$$

$$L_\phi = \iint_S \left\{ M_{t'}(\mathbf{r}') \left[-\sin\theta' \sin(\phi - \phi') \right] + M_{\phi'}(\mathbf{r}') \cos(\phi - \phi') \right\} e^{jk\mathbf{r}'\cdot\mathbf{a}_r} dS' \tag{4.36}$$

To simplify the following mathematical derivations, we will define

$$G_0 = e^{jk\mathbf{r}'\cdot\mathbf{a}_r} \tag{4.37}$$

where

$$\begin{aligned} \mathbf{r}'\cdot\mathbf{a}_r &= \left(x'\mathbf{a}_x + y'\mathbf{a}_y + z'\mathbf{a}_z \right) \cdot \left(\sin\theta\cos\phi\mathbf{a}_x + \sin\theta\sin\phi\mathbf{a}_y + \cos\theta\mathbf{a}_z \right) \\ &= x'\sin\theta\cos\phi + y'\sin\theta\sin\phi + z'\cos\theta \\ &= \rho'\cos\phi'\sin\theta\cos\phi + \rho'\sin\phi'\sin\theta\sin\phi + z'\cos\theta \\ &= \rho'\sin\theta\cos(\phi' - \phi) + z'\cos\theta \end{aligned} \tag{4.38}$$

It follows that

$$G_0(\theta, \phi, \rho', \phi', z') = e^{jk\left[\rho'\sin\theta\cos(\phi' - \phi) + z'\cos\theta\right]} \tag{4.39}$$

Expressing the transverse currents as modal expressions, we write

$$\begin{aligned} J_{t'}\left(t',\phi'\right) &= J_{t'}\left(t'\right)\sin\left(m\phi'\right) \\ &= \left[\sum_n j_{t'_n}\left(t'\right)\cdot V_n\right]\sin\left(m\phi'\right) \end{aligned} \tag{4.40}$$

$$\begin{aligned} J_{\phi'}\left(t',\phi'\right) &= J_{\phi'}\left(t'\right)\cos\left(m\phi'\right) \\ &= \left[\sum_n j_{\phi'_n}\left(t'\right)\cdot V_n\right]\cos\left(m\phi'\right) \end{aligned} \tag{4.41}$$

$$\begin{aligned} M_{t'}\left(t',\phi'\right) &= M_{t'}\left(t'\right)\cos\left(m\phi'\right) \\ &= \left[\sum_n m_{t'_n}\left(t'\right)\cdot V_n\right]\cos\left(m\phi'\right) \end{aligned} \tag{4.42}$$

$$\begin{aligned} M_{\phi'}\left(t',\phi'\right) &= M_{\phi'}\left(t'\right)\sin\left(m\phi'\right) \\ &= \left[\sum_n m_{\phi'_n}\left(t'\right)\cdot V_n\right]\sin\left(m\phi'\right) \end{aligned} \tag{4.43}$$

It is now representative that

$$N_\theta\left(\theta,\phi\right) = N_\theta\left(\theta\right)\sin\left(m\phi\right) \tag{4.44}$$

$$N_\phi\left(\theta,\phi\right) = N_\phi\left(\theta\right)\cos\left(m\phi\right) \tag{4.45}$$

$$L_\phi\left(\theta,\phi\right) = L_\phi\left(\theta\right)\sin\left(m\phi\right) \tag{4.46}$$

$$L_\theta\left(\theta,\phi\right) = L_\theta\left(\theta\right)\cos\left(m\phi\right) \tag{4.47}$$

CHAPTER 5 NUMERICAL RESULTS

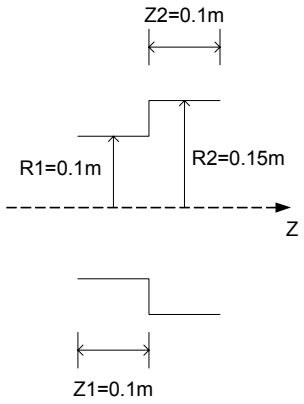

Figure 5-1 Step junction discontinuity.

A number of cases were modeled to test the components of the compiled program. Data is presented for component cases as well as for the comprehensive compiled program. The compiled program is named HATCH, an acronym for Harris Analysis Tool for Circular Horn fed structures; the legend will refer to the predicted data as HATCH.

5.1 Mode Matching Algorithm

The first component to be tested was the mode matching algorithm. A generally

accepted mode matching code, COSMIC, is used as a baseline for performance. Ansoft's HFSS package also represents baseline comparisons, as will be indicated in the legends. Figure 5-1 displays the first test case presented is a step discontinuity to support the theoretical development of chapter 2. Interestingly, when using HFSS with only one mode present in the software configuration, we noticed a large discrepancy in the results calculated between HFSS and the solutions of the HATCH mode matching and COSMIC mode matching. The results for the simulations of the three programs are shown in Figure 5-2 and Figure 5-3; the views are differing only in VSWR scale.

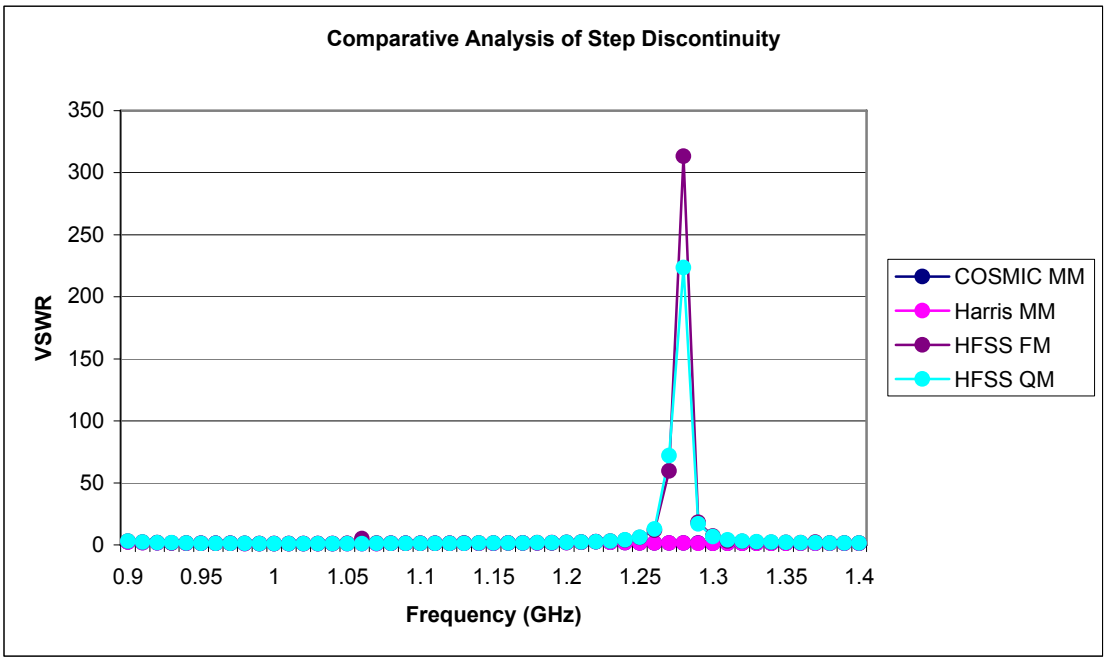

Figure 5-2 Step junction discontinuity model full view.

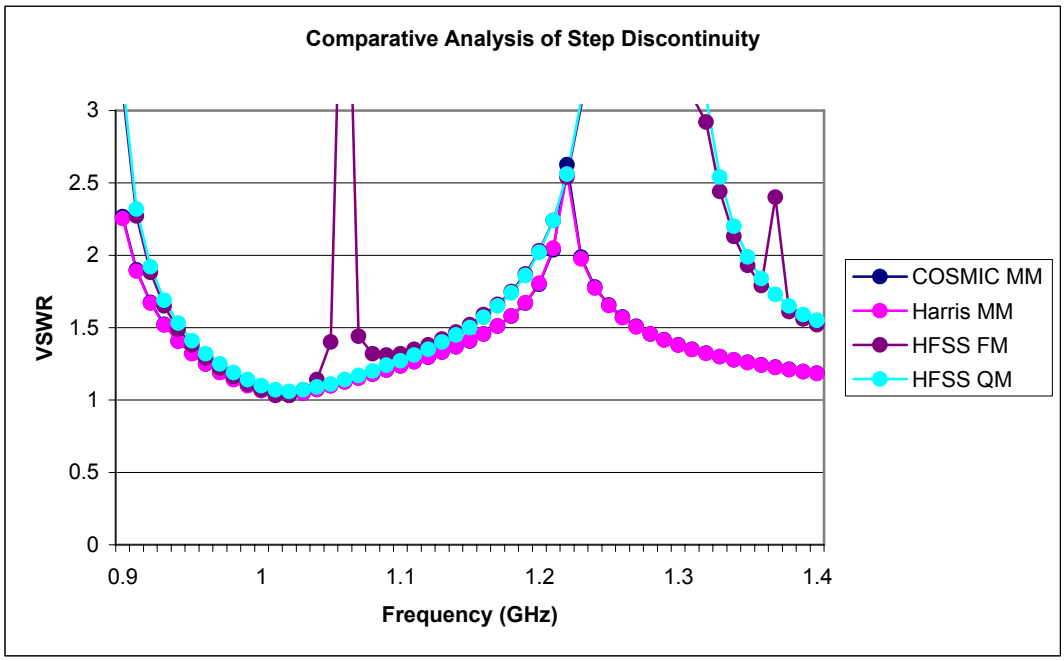

Figure 5-3 Step junction discontinuity fit view.

The FM and QM designation in the legend indicates full model and quarter models for the HFSS simulations. A large discrepancy is noted, as indicated previously; to adjust this discrepancy more modes were simulated using HFSS. There is a significant difference in the amount of computational time required for solution convergence between HFSS and the mode matching methods, as expected. The results for the modified simulation runs in HFSS are compared against the mode matching codes.

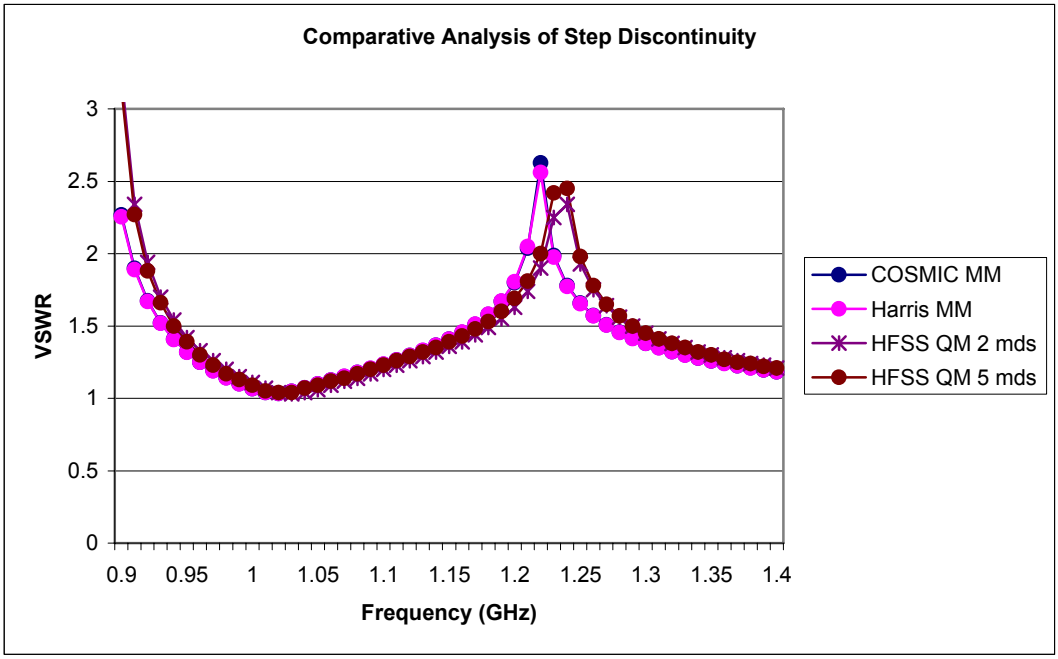

Figure 5-4 Step junction discontinuity comparison with added HFSS modes.

The comparison exhibits better correlation to the mode matching codes. The HATCH mode matching code correlates extremely well with an established mode matching code.

The second model to be simulated is shown in Figure 5-5, this model is representative of a corrugated horn that was developed at Harris Corporation. The primary purpose for this model is to validate the HATCH mode matching component through the use of a COSMIC baseline. The results of the simulated input file can be seen in Figure 5-6.

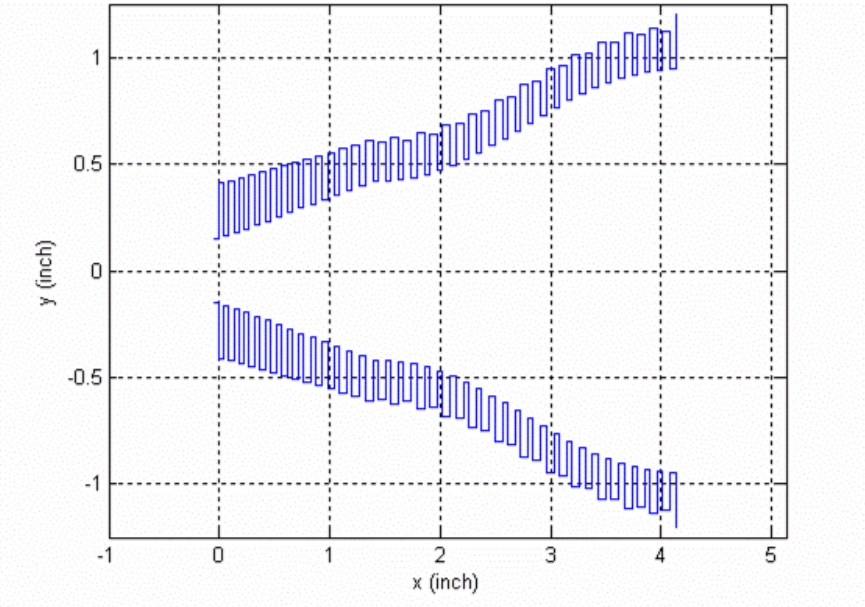

Figure 5-5 Corrugated Horn model.

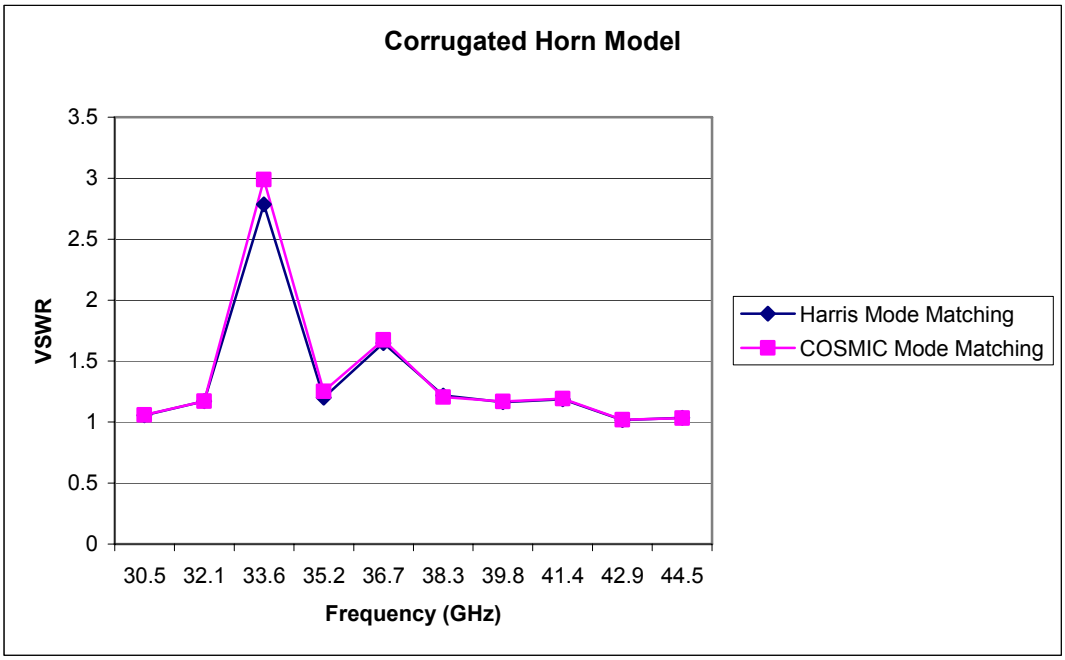

Figure 5-6 Corrugated horn comparison.

The correlation of the COSMIC and HATCH output is very close; the validation for the mode matching component of HATCH is considerate of complex structures.

5.2 Combined Solution Algorithm

The finite flange is the next model that is simulated as shown in Figure 5-7. HFSS and HATCH are used to comparatively simulate a finite flange on a circular waveguide with a conductor thickness of 0.01m, and the operational frequencies of the circular waveguide are 0.9 GHZ – 1.4 GHz.

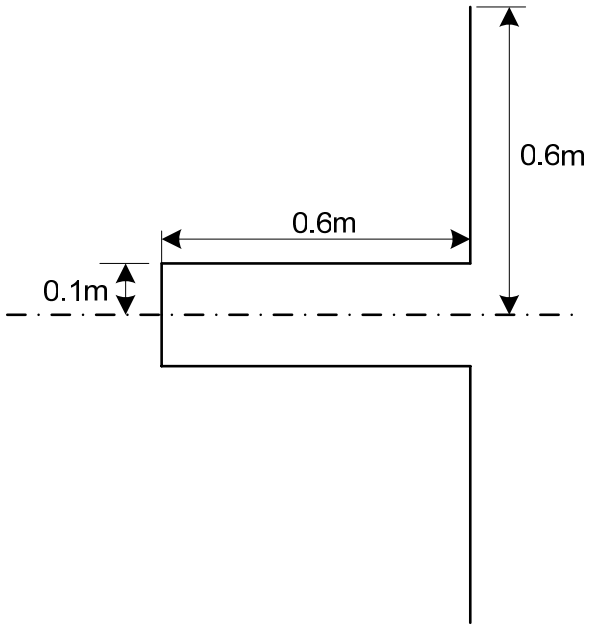

Figure 5-7 Finite flange model.

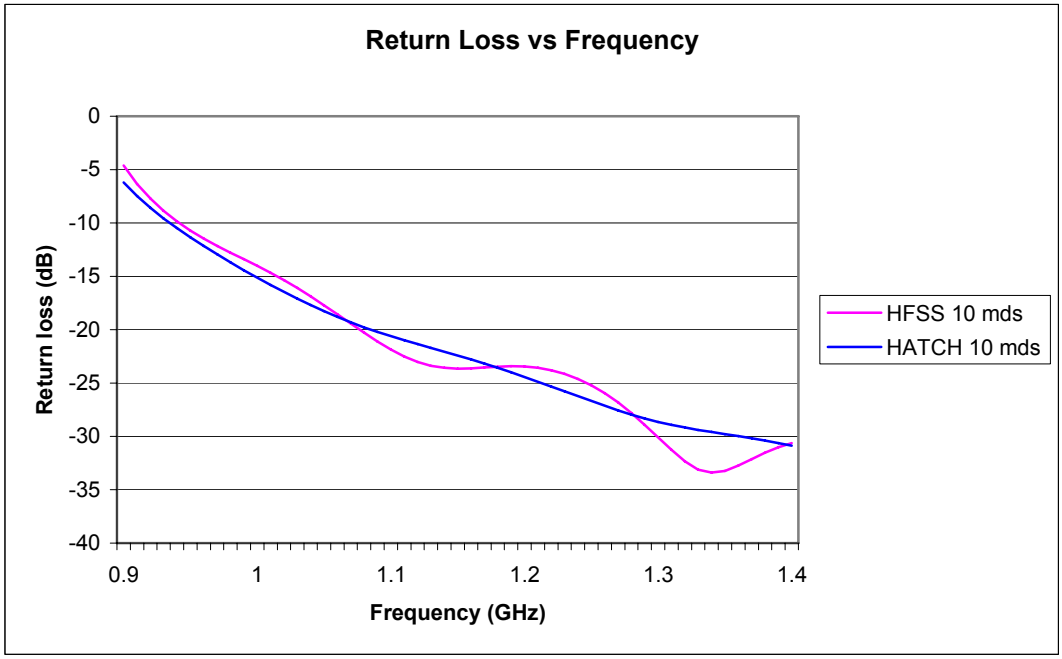

Figure 5-8 Return loss comparison of a 0.5m finite flange on a circular waveguide.

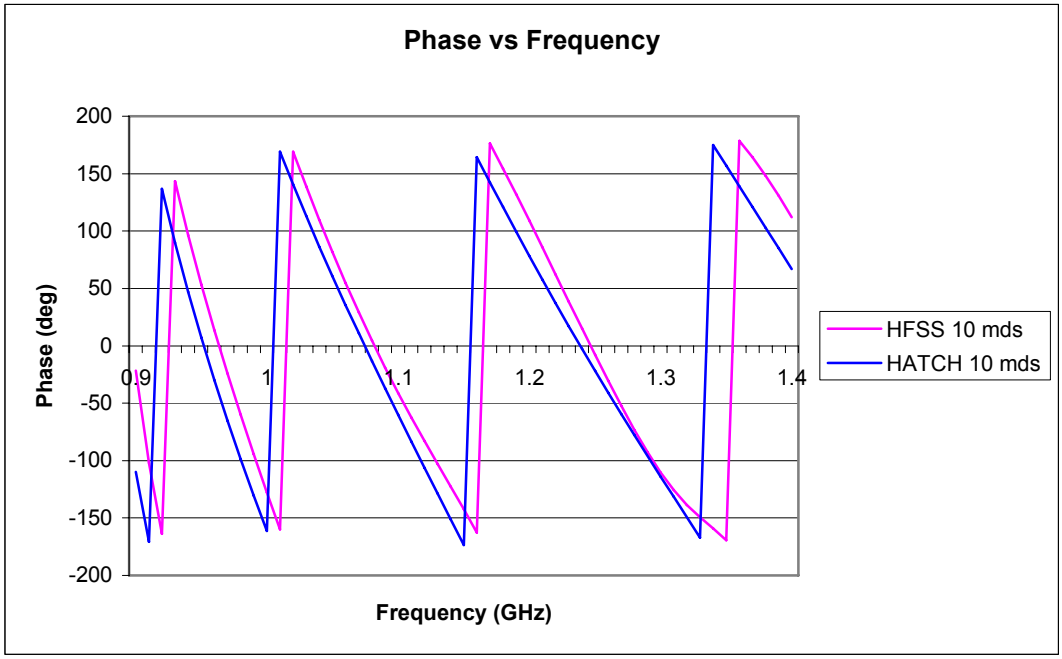

Figure 5-9 Phase comparison of a 0.5m finite flange on a circular waveguide.

The data predicted by HATCH is in close agreement with the predictions of HFSS. This measure validates the construct as input into HATCH for both return loss and phase.

A smooth walled circular horn is the next test model to be simulated with HATCH. Figure 5-10 shows the dimensions of a smooth horn model.

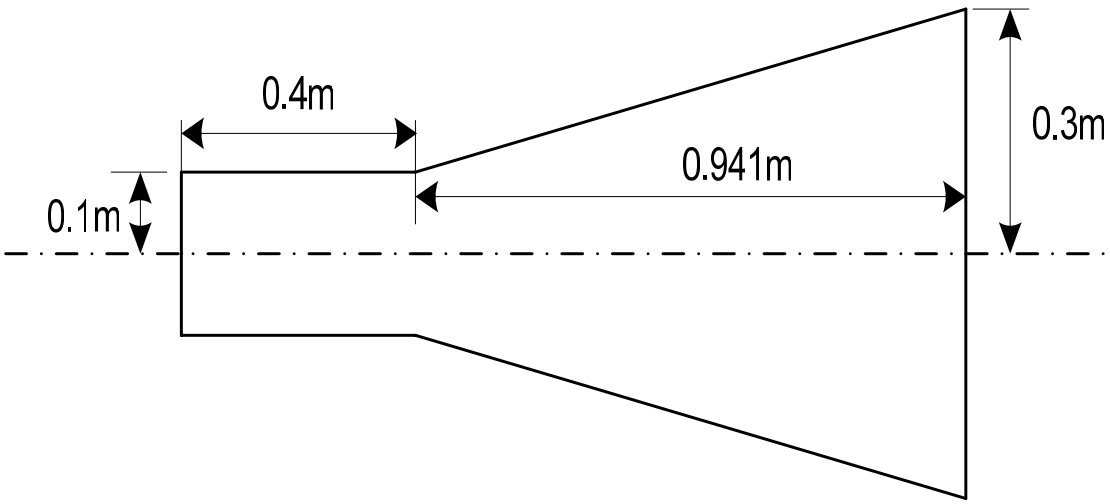

Figure 5-10 Cylindrical horn model.

The simulated results are shown in Figure 5-11 and Figure 5-12. The agreements in the two simulation methods validate the smooth horn model as treated with the HATCH program.

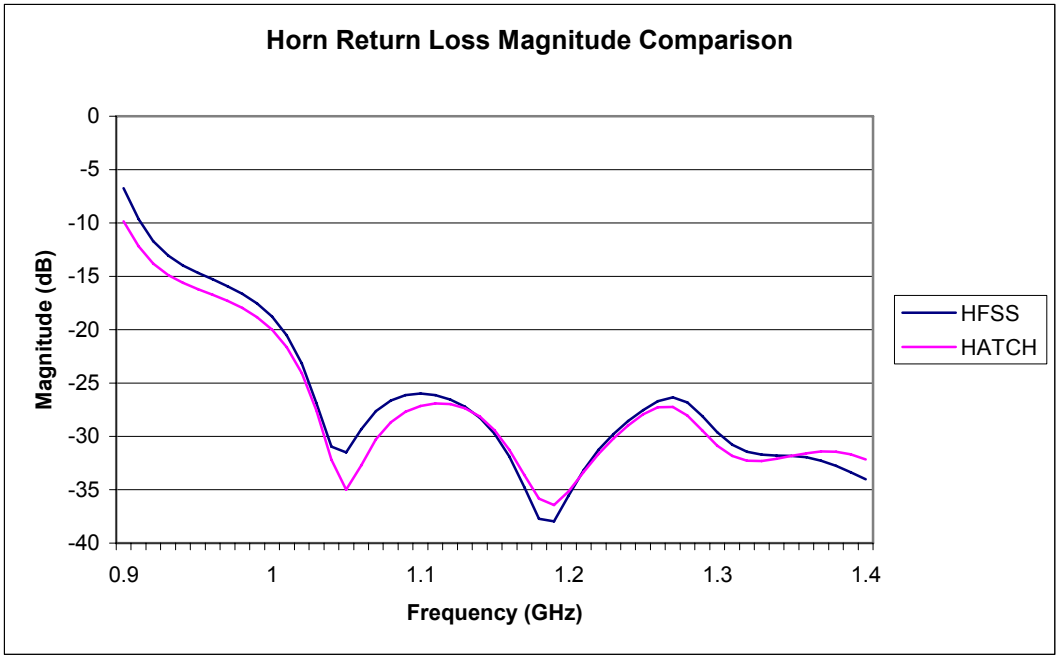

Figure 5-11 Return loss magnitude comparison for the smooth horn model.

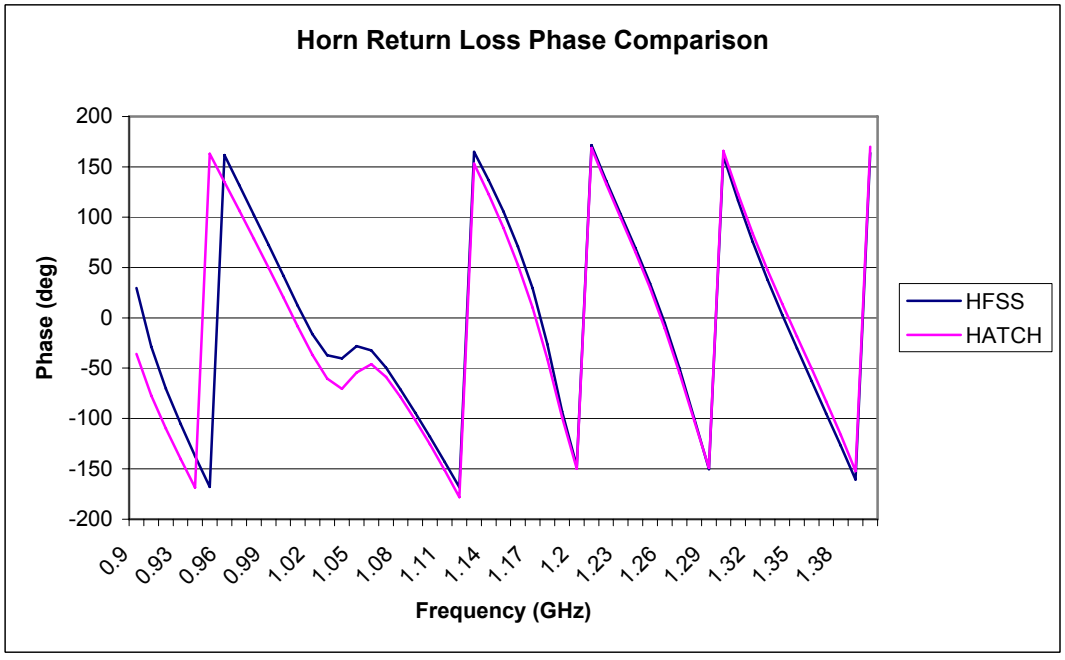

Figure 5-12 Return loss phase comparison for the smooth horn model.

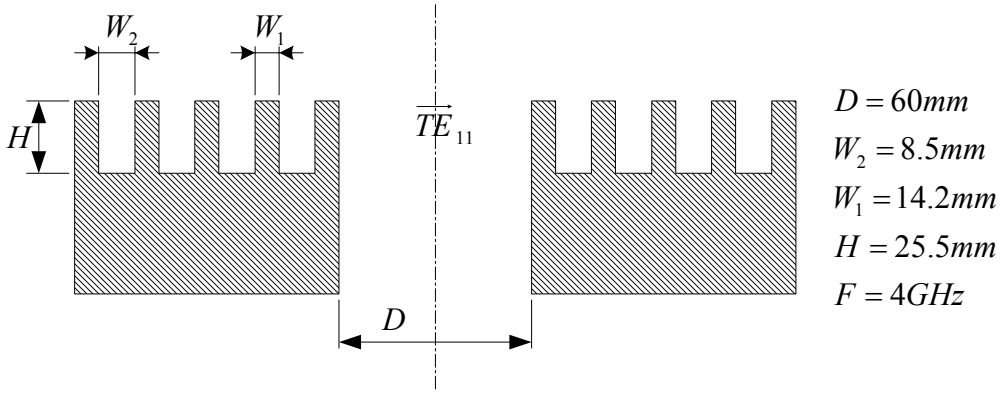

Figure 5-13 Complex feed model [74].

Figure 5-13 illustrates the next model that is simulated with HATCH, HFSS, and another BOR application developed by Ohio State University (OSU). The feed is simulated as shown, and an interesting occurrence can be seen in the magnitude of the return loss. The OSU BOR code is developed using EFIE; while there is a general reduction of the matrix and number of mathematical operations, the solution stability is contingent upon the degree of resonance that any closed structures present. Effectively, the structure must be open and thin PEC, and the degree to which the closed structure must be open is arbitrarily determined through iterative simulation. The advantage of using the CFIE method is the solution stability is inherent as the consideration of both electric and magnetic boundaries are treated in the formulation of the applied method. The radiation patterns for the linear electric and magnetic field intensities will be presented for this model, and the comparison is made between HATCH and the OSU BOR code.

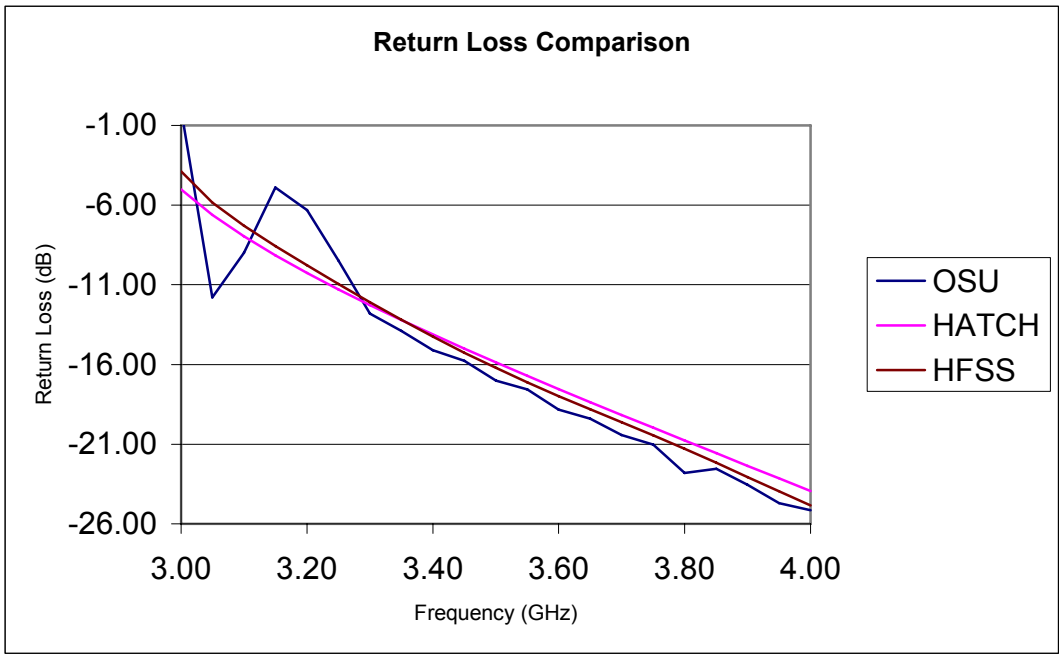

Figure 5-14 Return loss comparison for the complex feed horn.

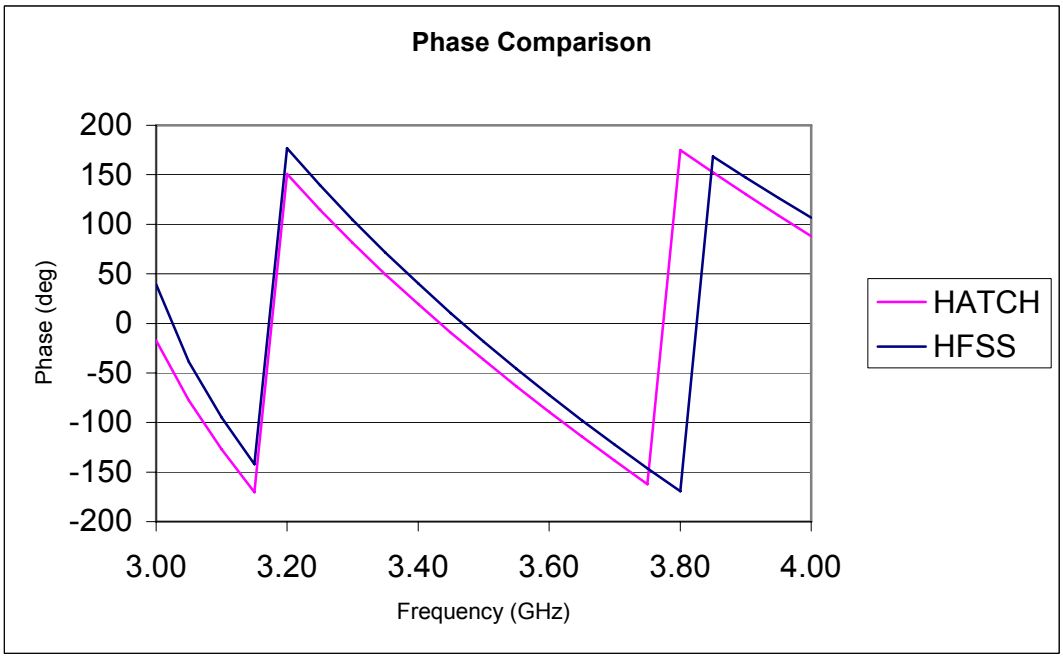

Figure 5-15 Phase comparison for the complex feed horn.

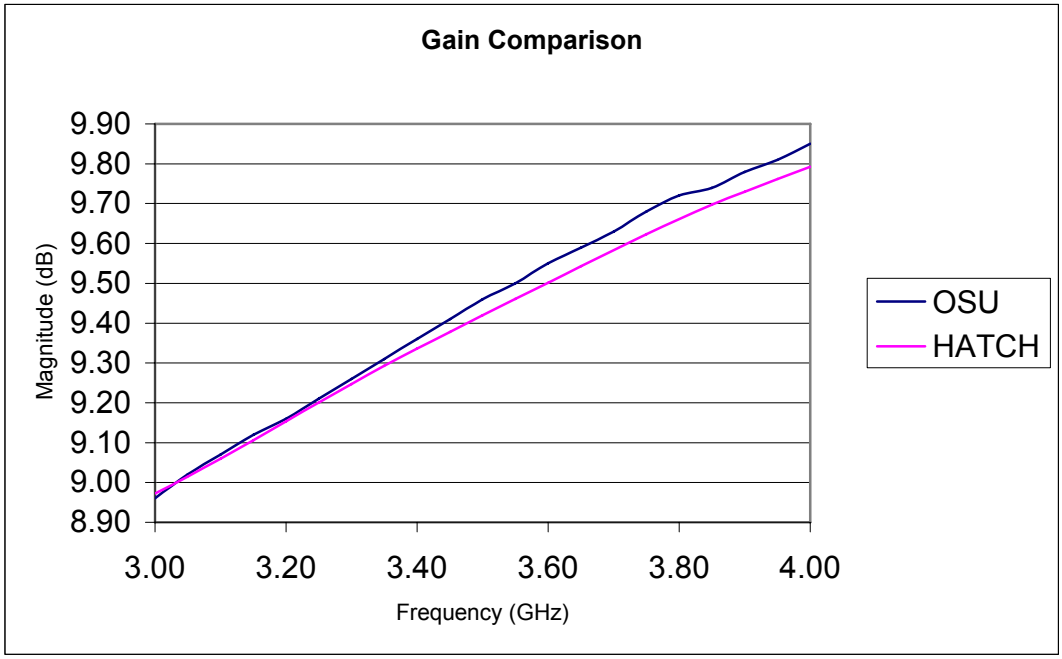

Figure 5-16 Gain comparison over frequency of the complex feed horn.

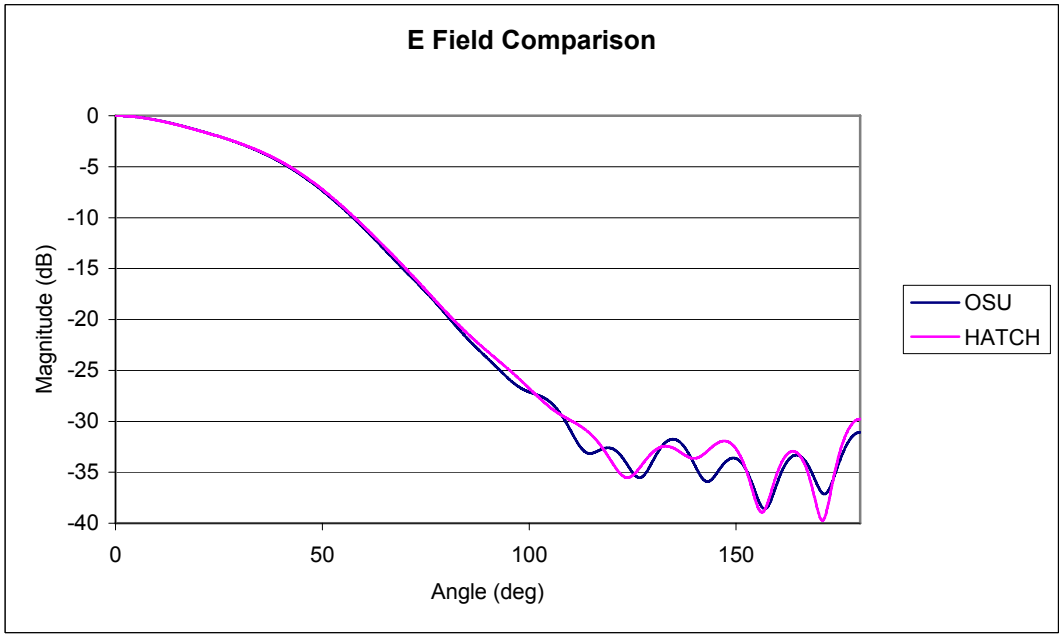

Figure 5-17 Linear electric field radiation pattern of the complex feed horn.

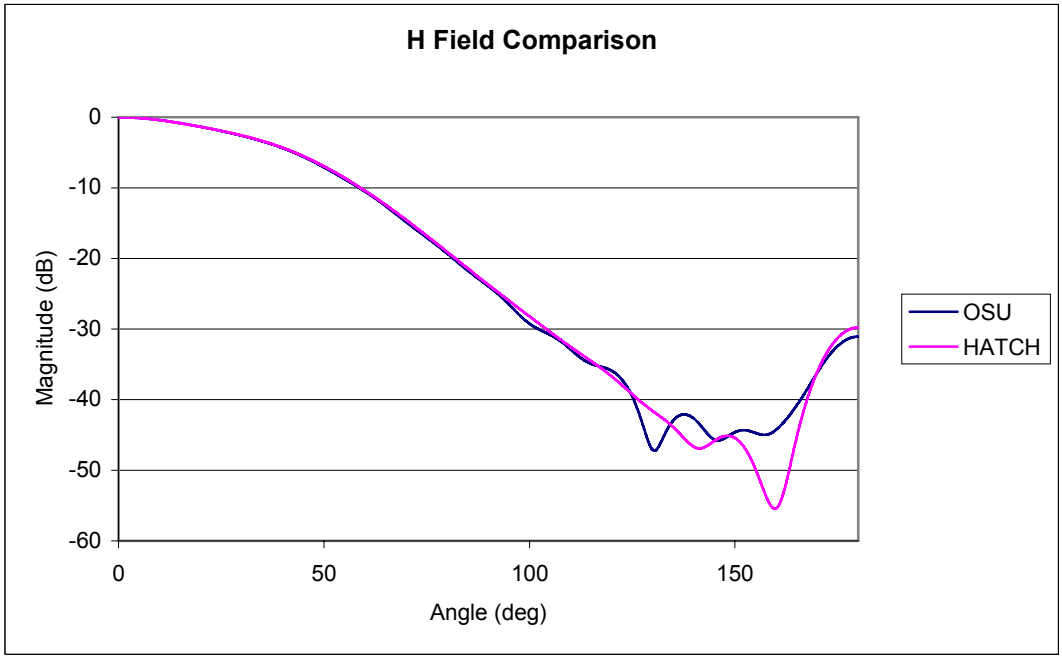

Figure 5-18 Linear magnetic field radiation pattern of the complex feed horn.

Figure 5-14 exhibits the return loss as estimated by HFSS, the OSU BOR code, and HATCH; it is evident that the return loss as delivered by the OSU BOR code is not consistent. The OSU BOR code is an example of the consideration that must be taken when treating the structure with the EFIE formulation. The structure as shown in Figure 5-13 is a closed structure; however, when creating an input file for the EFIE formulation, the structure must be an open structure that exhibits no resonant cavities. Therefore, to model a closed structure the input file must be an open approximation of the structure in order to get accurate results within a bandwidth of interest. Another impact due to the construct consideration when implementing the EFIE can be seen in the radiation patterns that are farther removed in angle from boresight.

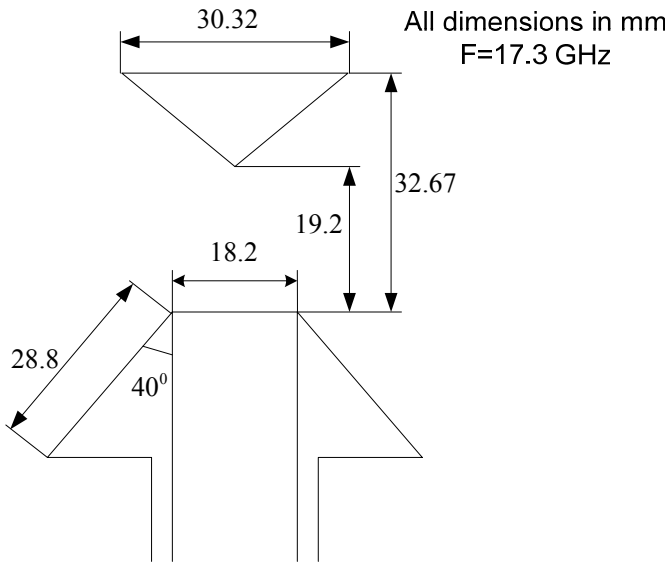

Figure 5-19 Simple multiple BOR model [74].

The model shown in Figure 5-19 is a simple construct of multiple bodies that will be simulated with the HATCH code. HFSS and the OSU BOR code are used to comparably simulate the model in order to acquire a consensus for solution. Figure 5-20 displays the return loss as estimated through the three code applications; it can be seen, as in the previous case of the complex feed, that the OSU BOR code is inconsistent with the other solutions due to the structural input into a code that utilizes the EFIE formulation.

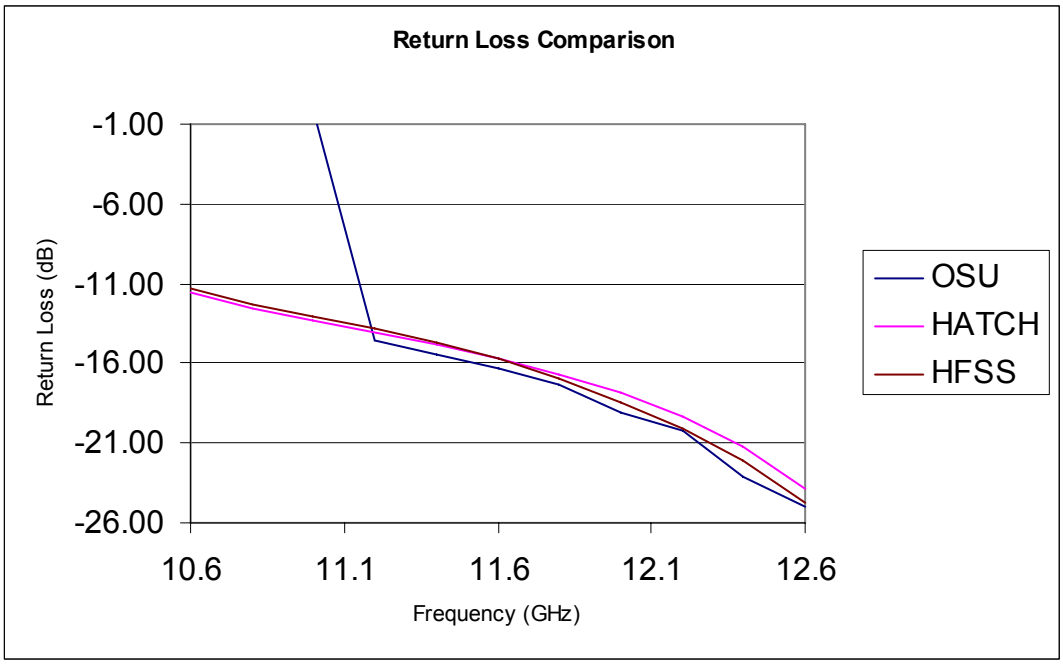

Figure 5-20 Return loss comparison for multiple BOR model.

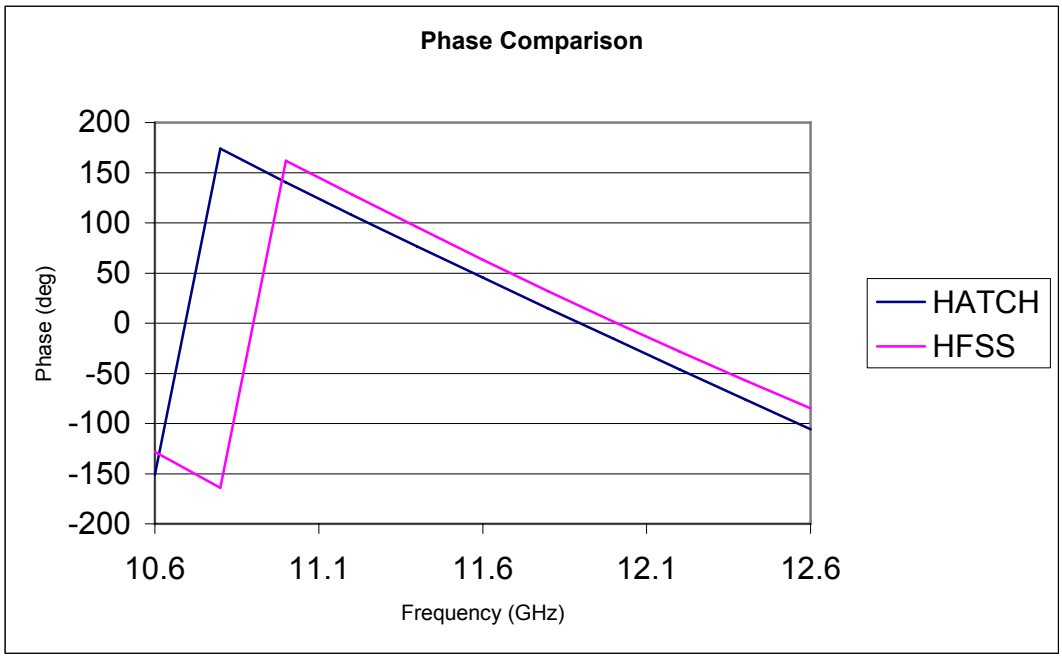

Figure 5-21 Phase comparison for multiple BOR model.

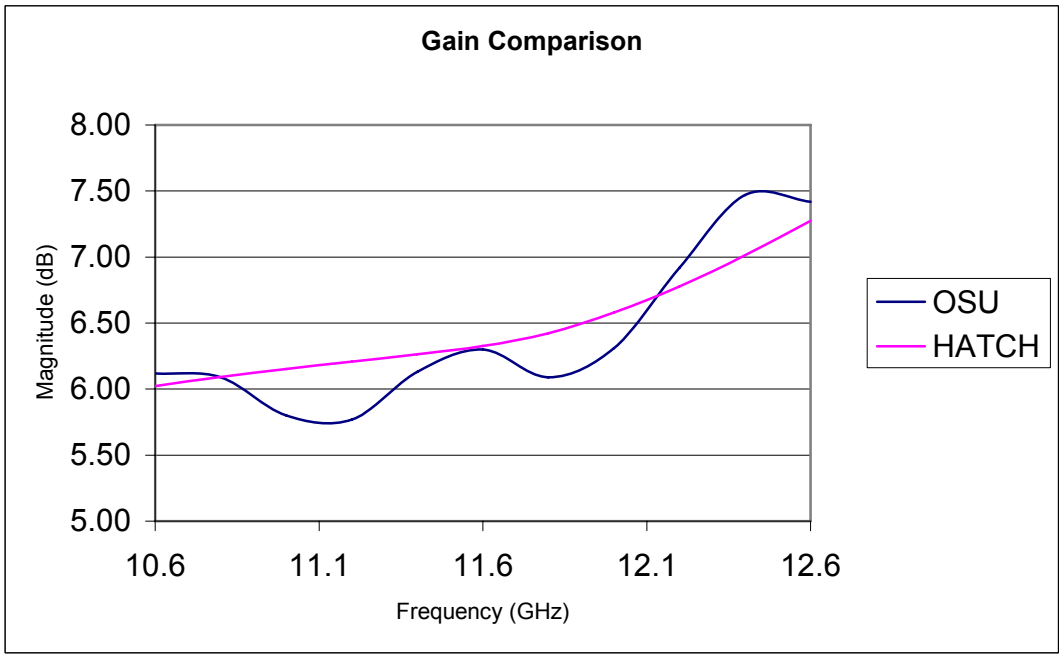

Figure 5-22 Gain comparison for multiple BOR model.

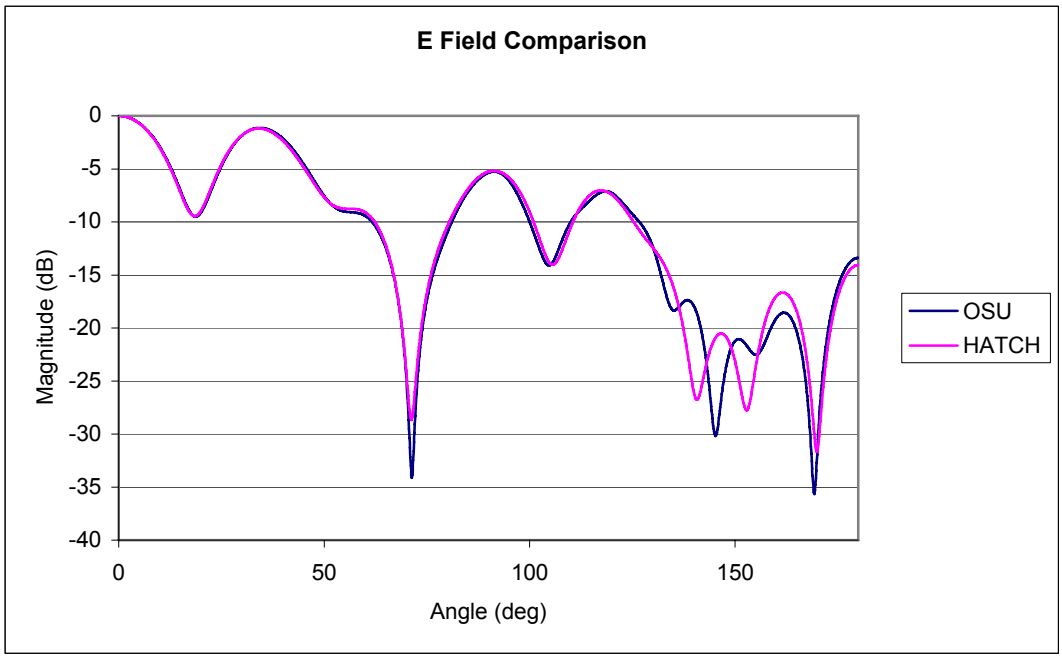

Figure 5-23 Electric field radiation pattern comparison for multiple BOR model.

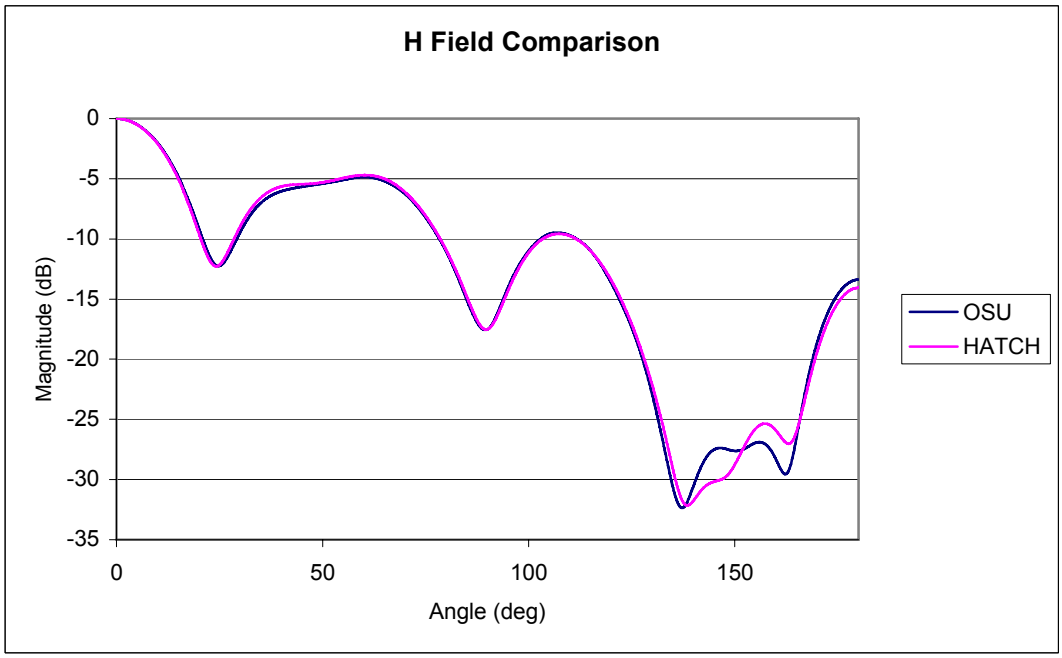

Figure 5-24 Magnetic field radiation comparison for multiple BOR model.

A corrugated horn was designed and fabricated at Harris Corporation; a comparison will be presented of the radiation response that was measured against the predicted radiation pattern that is generated by the HATCH code. Figure 5-25 and Figure 5-26 exhibit the predicted radiation patterns of the electric and magnetic fields, respectively, and the measured electric and magnetic field responses of the corrugated horn.

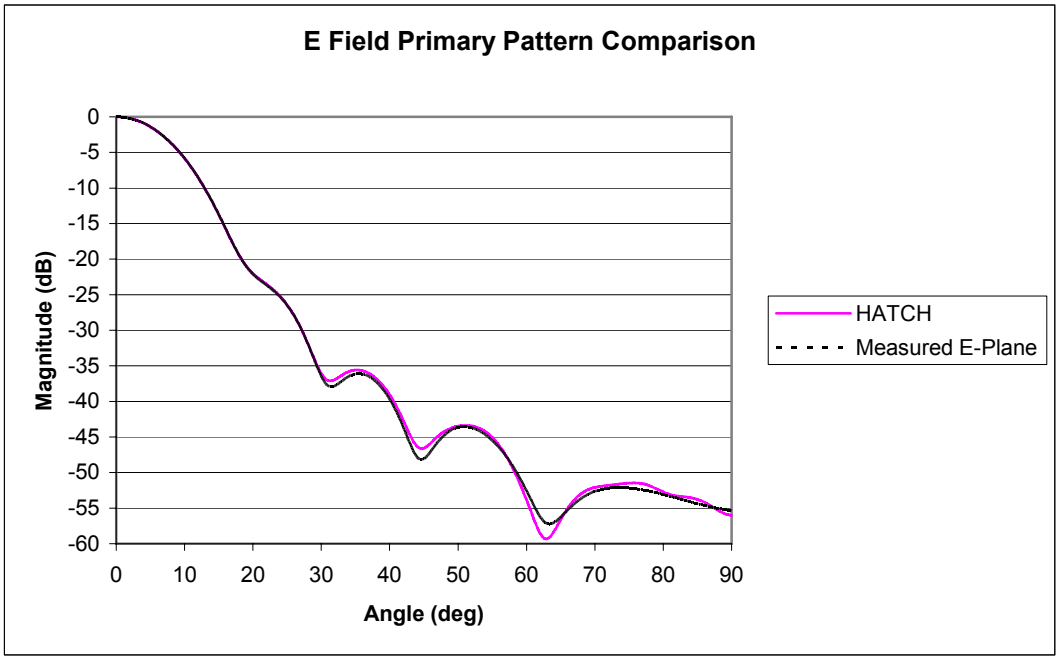

Figure 5-25 Electric field radiation pattern comparison of a corrugated feed.

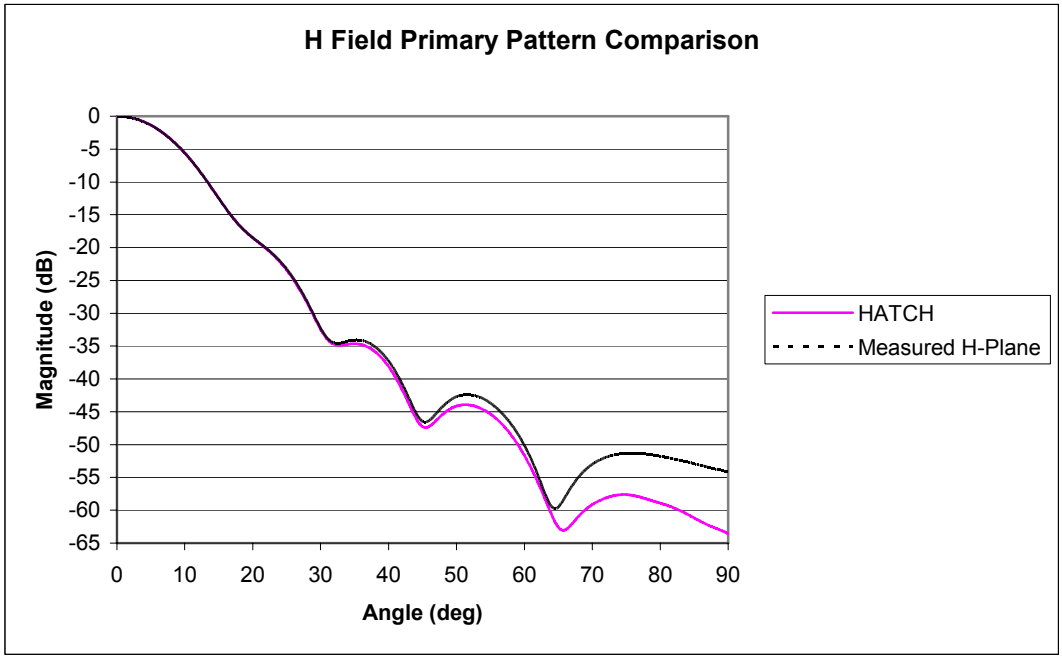

Figure 5-26 Magnetic field radiation pattern comparison of a corrugated feed.

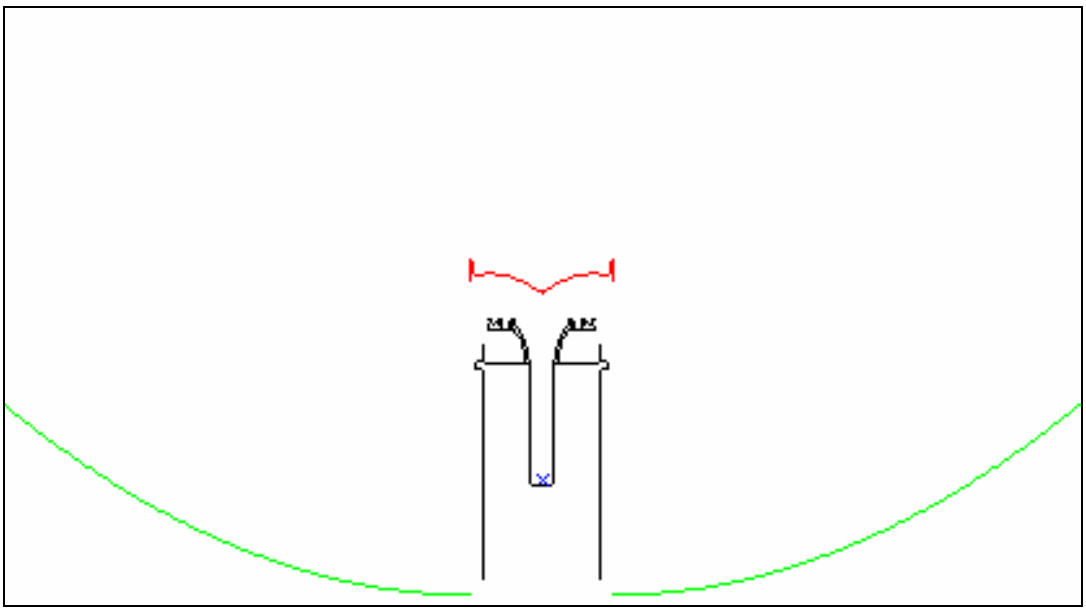

Figure 5-27 Complex structural ring focus geometry.

Figure 5-27 displays the next model to be considered using HATCH. This structure is a complex geometry of a patented focal ring antenna system (PATENT No. 6,831,613 Gothard et al.) that was designed and fabricated at Harris Corporation. The geometry was input to the HATCH code; the comparative electric and magnetic radiation patterns are shown in Figure 5-28 and Figure 5-29 respectively. The comparative results exhibit close correlation of the predicted and measured data.

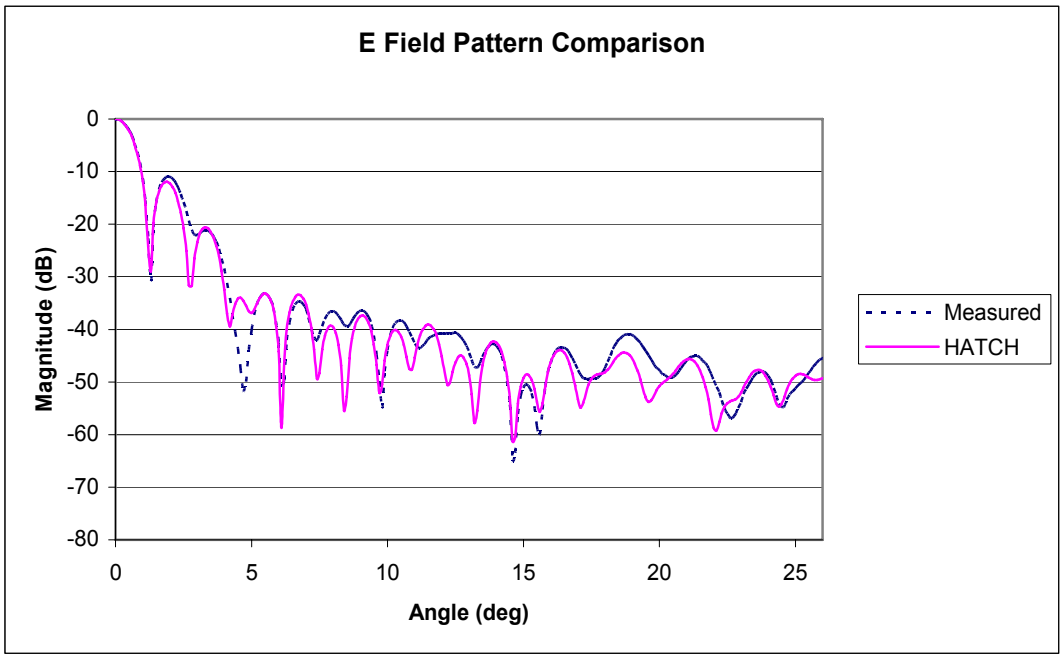

Figure 5-28 Comparative predicted and measured electric field patterns.

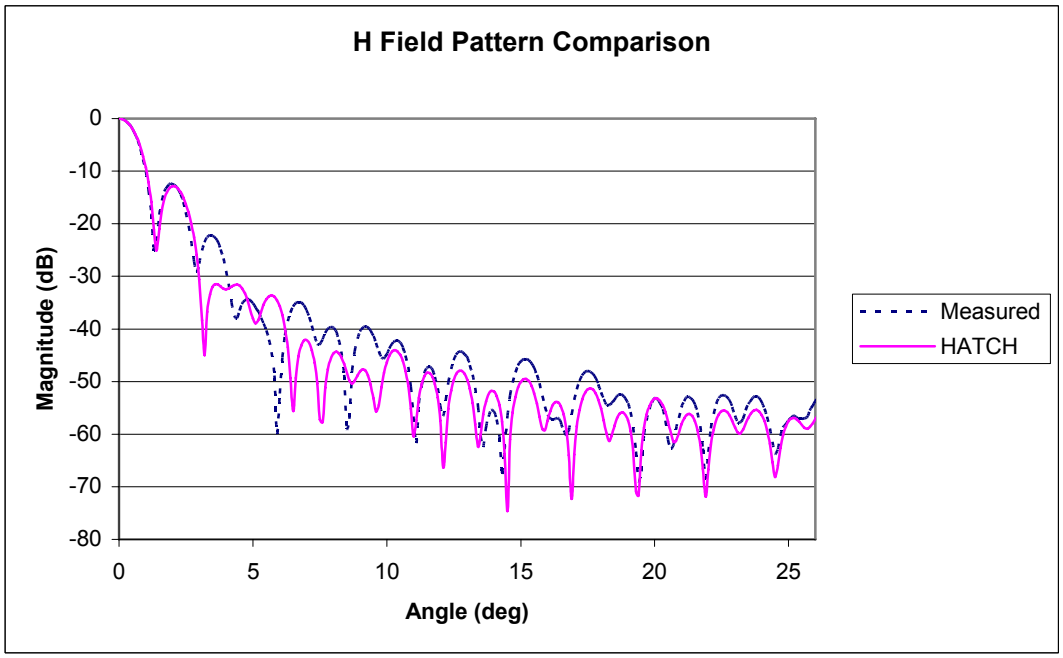

Figure 5-29 Comparative predicted and measured magnetic field patterns.

5.3 Benchmark Comparisons

Comparative benchmarking of solution times of the OSU BOR code, HFSS and HATCH is considered. The benchmarking was performed on a PC with a 2.0 GHz processor and 2GB of RAM. Table 5-1 exhibits the benchmarking results for solution times.

Table 5-1 Comparative benchmarking for selected geometries.

Geometry	HATCH	OSU BOR	HFSS
Figure 5-13	0.76s	0.99s	1512s
Figure 5-19	0.62s	2.04s	>>5700s
Figure 5-27	298s	105s	N/A

The benchmarking results exhibits the apparent advantage of using surface mesh solution methods as opposed to the volumetric mesh solution such as FEM with respect to solution time. The size of Figure 5-27 constrained the application to HATCH and the OSU BOR code. The difference between HATCH and the OSU BOR code in the last row of Table 5-1 has been attributed to the ϕ-direction integration. The radial distance influences the number of Gaussian points distributed in the phi direction; thus causing the solution time to increase with radial distance with respect to the OSU BOR code.

CHAPTER 6 CONCLUSION

A novel full wave analysis method to determine the scattering parameters and the radiation field intensities of arbitrary Body of Revolution (BOR) radiators consisting of impenetrable media was explored through derived components of modal analysis and the method of moments (MoM). Modal excitation was utilized to excite the structural feed; allowing for a more accurate measure of the scattering parameters of the total structure a opposed to the use of external excitation sources. The derivation of the mode matching method introduced a novel approach to achieving a frequency independent coupling matrix that reduced the computational requirements for iterations utilized in the solution of multi-step discontinuous junctions. An application of interpolation functions across a single element of the MoM's traditional basis function approach allowed for the ability to facilitate the meshing of complex structures. The combined field integral equation method was implemented in the analysis method to assure the mitigation of spurious solutions that can be problematic for electric field integral equation solutions that are predominant in many MoM based codes. The structures of interest represent bodies of revolution (BOR), which maintains that the structures must exhibit rotational symmetry about the longitudinal, or directional, axis. The complexity of the domain of structures that are treated with the analysis method was significantly reduced through the use of

BOR symmetry of the structure. The proposed method for the solution of structures included the comprehensive treatment of Boundary Value Problems (BVP's) through modal analysis, aperture treatment, and an application of the method of moments.

Solutions for BOR radiating structures were divided into two regions of analytical concern, the inner guided wave region and the outer radiating region. Modal analysis was used to determine the scattering matrix of the inner guided wave region. The method of mode matching was implemented to numerically solve the BVP's at each step discontinuity for a finite number of modal field distributions. The surface field equivalence principle was applied to treat the aperture in order to produce an equivalent problem that supplanted a source magnetic current density and an induced electric current density across the aperture that radiated in the presence of the outer structural material of the BOR radiator. An algorithm implementing the method of moments (MoM) was applied to solve integral equations that were defined to treat the surfaces of the BOR structure using electromagnetic boundary conditions. The application of the MoM developed the field intensities on the aperture with complete consideration of the outer structural boundaries of the BOR radiator. The field intensities on the aperture were related to the inner guided wave region through electromagnetic boundary conditions, and an admittance matrix was numerically calculated. The admittance matrix was then applied to the inner guided wave region's scattering matrix to determine the reflection and transmission coefficients at the input of the BOR radiator.

The implementation of the CFIE proved to be a more comprehensive solution method with respect to the EFIE implementation, as the consideration of resonant

structures present in closed body analysis was completely considered with CFIE, and can only be mitigated in the EFIE solution through the opening of the closed body structure to effectively force the resonance out of the band of consideration. The technique of opening the structure is iterative at best, and dependant upon the frequencies and structural complexities, may not be accurate with respect to the total design operational envelop. This is evident in the comparative results offered through the comparison of the OSU BOR code and the developed HATCH code.

With respect to the benchmarking of the solution times between HATCH and the OSU BOR code as presented in Table 5-1, an asymptotic treatment of the integration method used in the ϕ-direction can be implemented to reduce the time for solution as the model introduced to the HATCH code increases in the radial direction. Comparatively, the HATCH algorithm performs extremely well considering the increased matrix size when concerned with the solution of linear systems, and the increased integration that is inherent when applying the CFIE as opposed to the EFIE. The trade-off that has to be considered is the reduced matrix size/additional computation in integration and the assurance that spurious solutions will not affect design frequencies for models estimated using the EFIE solution method. Another consideration is the time required to iteratively estimate the input geometry for closed or curvilinear models when applying the EFIE method to ensure that there are no spurious solutions across the design frequencies, as this consideration does not need to be taken when applying the CFIE method.

The Ohio State University BOR code, as a component of the SATCOM

Workbench, Ansoft HFSS, CHAMP, and COSMIC are proprietary commercial codes that are utilized as comparative numerical methods employed to validate the accuracy of the developed HATCH code solution algorithm. The presented comparative analyses establish the HATCH correlation to accepted industry methods in producing accurate analysis of BOR structures.

LIST OF REFERENCES

[1] R. Mittra ed., *Computer Techniques for Electromagnetics,* Pergamon Press, 1973.

[2] A. Peterson, S. Ray, and R. Mittra, *Computational Methods for Electromagnetics*, IEEE Press, 1998.

[3] R. Booton, *Computational Methods for Electromagnetics and Microwaves*, John Wiley & Sons, 1992.

[4] R. Hamming, *Numerical Methods for Scientists and Engineers*, Dover, 1986.

[5] R. Harrington, *Time-Harmonic Electromagnetic Fields*, McGraw Hill, 1961.

[6] J. Kong, *Electromagnetic Wave Theory*, EMW Publishing, 2000.

[7] C. Balanis, *Advanced Engineering Electromagnetics*, John Wiley & Sons, 1989.

[8] C. Balanis, *Antenna Theory Analysis and Design*, John Wiley & Sons, 1982.

[9] W. Stutzman and G. Thiele, *Antenna Theory and Design,* John Wiley & Sons, 1998.

[10] D. Kerns and R. Beatty, *Basic Theory of Waveguide Junctions and Introductory Microwave Network Analysis*, Pergamon Press, 1967.

[11] C. Johnk, *Engineering Electromagnetic Fields and Waves,* John Wiley & Sons, 1988.

[12] D. Pozar, *Microwave Engineering*, John Wiley & Sons, 1998.

[13] P. Rizzi, *Microwave Engineering Passive Circuits*, Prentice Hall, 1988.

[14] M. Andreasen, "Scattering from bodies of revolution," *IEEE Transactions*, APS 13-2, pp. 303-310, March 1965.

[15] A. Mohsen and A. Abdelmageed, "Magnetic field integral equation for electromagnetic scattering by conducting bodies of revolution in layered media," *PIER 24,* pp.19-37, 1999.

[16] T. Durham, *Integral Equation Analysis of Composite Bodies of Revolution and Arbitrary Surfaces with Application to Cavity-Backed Antennas,* PhD Thesis, University of Central Florida, 1992.

[17] A. Glisson and C. Butler, "Analysis of a wire antenna in the presence of a body of revolution," *IEEE Transactions*, APS 28-5, pp.604-609, Sep 1980.

[18] J. Shaeffer and L. Medgyesi-Mitschang, "Radiation from wire antennas attached to bodies of revolution: The junction problem," *IEEE Transactions*, APS 29-3, pp. 479-487, May 1981.

[19] J. Shaeffer, "EM scattering from bodies of revolution with attached wires," *IEEE Transactions*, APS 30-3, pp. 426-431, May 1982.

[20] R. Pérez-Leal and M. Cátedra, "Input impedance of wire antennas attached on-axis to conducting bodies of revolution," *IEEE Transactions*, APS 36-9, pp. 1236-1243, Sep 1988.

[21] H. Schuman and D. Warren, "Aperture coupling in bodies of revolution," *IEEE Transactions*, APS 26-6, pp. 778-783, Nov 1978.

[22] C. Salema, C. Fernandes, and R. Jha, *Solid Dielectric Horn Antennas*, Artech House, 1998.

[23] A. Love, *Electromagnetic Horn Antennas,* IEEE Press Selected Reprint Series, IEEE Press, 1976.

[24] A. Love, *Horn* Antennas, McGraw Hill, 1993. Ch.15 of R. Johnson (ed.) *Antenna Engineering Handbook*.

[25] I. Shumljansky, *Horn Radiators of Complex Configuration*, World Scientific, 1993.

[26] P. Clarricoats and A. Olver, *Corrugated horns for microwave antennas*, Peter Peregrinus Ltd., 1984.

[27] A. Olver, P. Clarricoats, A. Kishk, and L. Shafai, *Microwave Horns and Feeds,* IEE Press, 1994.

[28] A. Wexler, "Solution of waveguide discontinuities by modal analysis," *IEEE Transactions*, MTT 15-9, pp. 508-517, Sep 1967.

[29] R. Collin, *Field Theory of Guided Waves*, IEEE Press, 1991.

[30] G. Conciauro, M. Guglielmi, and R. Sorrentino, *Advanced Modal Analysis CAD Techniques for Waveguide Components and Filters,* John Wiley & Sons, 2000.

[31] N. Marcuvitz, *Waveguide Handbook*, McGraw-Hill, 1951.

[32] N. Marcuvitz and J. Schwinger, "On the representation of the electric and magnetic fields produced by currents and discontinuities in wave guides," *Journal of Applied Physics*, Vol. 22, No. 6, pp. 806-819, June 1951.

[33] R. Harrington and J. Mautz, "A Generalized Network Formulation for Aperture Problems," *IEEE Transactions,* APS 24-6, pp. 870-873, Nov. 1976.

[34] A. Bhattacharyya and G. Gutotte, "A novel horn radiator with high aperture efficiency and low cross-polarization and applications in arrays and multibeam reflector antennas," *IEEE Transactions*, APS 52-11, pp. 2850-2859, November 2004.

[35] T. Wang, R. Harrington, and J. Mautz, "Electromagnetic scattering from an transmission through arditrary apertures in conducting bodies," *IEEE Transactions*, APS 38-11, pp. 1805-1814, Nov 1990.

[36] A. Bhattacharyya and G. Goyette, "Step-horn antenna with high aperture efficiency and low cross-polarisation,"*Electronic Letters*, Vol. 38, No. 24, pp. 1495-1496, Nov 2002.

[37] A. Glisson, "Equivalent current excitation for an aperture antenna embedded in an arbitrarily shaped impedance surface," *IEEE Transactions*, APS 50-7, pp. 966-970, July 2002.

[38] J. Uher, J. Bornemann, and U. Rosenberg, *Waveguide Components for Antenna Feed Systems*, Artech House, 1993.

[39] F. Alessandri, M. Mongiardo, and R. Sorrentino, "Rigorous mode matching analysis of mitered E-plane bends in rectangular waveguide," *IEEE Microwave and Guided Wave Letters* , Vol. 4-12, pp. 408 -410, December 1994 .

[40] P. Cornet, R. Duseaux, and J. Chandezon, "Wave propagation in curved waveguides of rectangular cross section," *IEEE Transactions*, MTT 47-7, pp. 965 -972, July 1999.

[41] S. Xu, X. Wu, W. Guo, and Z. Li, "Scattering characteristics of rectangular coaxial line discontinuities", *IEE Proceedings,* AP 142-3, pp. 257-264, June 1995.

[42] E. Kuhn and V. Hombach, "Computer-aided analysis of corrugated horns with axial or ring-loaded radial slots," *Proc. ICAP 83 part 1,* pp. 127-131, 1983.

[43] H. Flugel and E. Kuhn. "Computer-aided analysis and design of circular waveguide tapers," *IEEE Transactions,* MTT 36-2, pp. 332-336, Feb. 1988.

[44] S. Saad, J. Davies, and O. Davies, "Computer analysis of gradually tapered waveguide with arbitrary cross sections," *IEEE Transactions*, MTT 25-5, pp. 437-440, May 1977.

[45] L. Lewin, "On the resolution of a class of waveguide discontinuity problems by the use of singular integral equations," *IEEE Transaction*, MTT 9-4, pp. 321-332, July 1961.

[46] K. Liu, C. Balanis, C. Birtcher, and G. Barber, "Analysis of pyramidal horn antennas using moment methods," *IEEE Transactions*, APS 41-10, pp. 1379-1389, Oct 1993.

[47] R. Harrington, *Field Computation by Moment Method,* Robert E. Krieger Publishing, 1982.

[48] *Moment Methods in Antennas and Scattering*, R.C. Hansen ed., Artech House, 1990.

[49] J. Jin, *The Finite Element Method in Electromagnetics*, John Wiley & Sons, 2002.

[50] R. Bancroft, *Understanding Electromagnetic Scattering Using the Moment Method A Practical Approach,* Artech House, 1996.

[51] B. Kolundzija and A. Djordjevic, *Electromagnetic Modeling of Composite Metallic and Dielectric Structures,* Artech House, 2002.

[52] T. Eibert, "Iterative near-zone preconditioning of iterative method of moments electric field integral equation solutions," *IEEE Antennas and Wireless Propagation Letters*, Vol.2, No.7, pp. 101-102, 2003.

[53] D. Duffy, *Green's Functions with Applications*, Chapman & Hall/CRC, 2001.

[54] N. Morita, N. Kumagai, and J. Mautz, *Integral Equation Methods for Electromagnetics,* Artech House, 1990.

[55] J. Mautz and R. Harrington, "A combined-source solution for radiation and scattering from a perfectly conducting body," *IEEE Tranactions,* APS 27-4, pp. 445-454, July 1979.

[56] B. Jung and T. Sarkar, "A survey of various frequency domain integral equations for the analysis of scattering from three-dimensional dielectric objects," *PIER* 36, pp. 193-246, 2002.

[57] S. Rao, D. Wilton, A. Glisson, "Electromagnetic scattering by surfaces of arbitrary shape," *IEEE Transactions*, APS 30-3, pp. 409-418, May 1982.

[58] A. Greenbaum, *Iterative Methods for Solving Linear Systems,* SIAM, 1997.

[59] C. Kelley, *Iterative Methods for Linear and Non-Linear Equations,* SIAM,1995.

[60] H. Vorst, *Iterative Krylov Methods for Large Linear Systems,* Cambridge University Press, 2003.

[61] M. Cátedra, R. Torres, J. Basterrechea, and E. Gago, *The CG-FFT Method Application of Signal Processing Techniques to Electromagnetics,* Artech House, 1995.

[62] T. Sarkar and, E. Arvas, "On a Class of Finite Step Iterative Methods (Conjugate Directions) for the Solution of an Operator Equation Arising in Electromagnetics", *IEEE Transactions,* APS 33-10, pp. 1058-1066, Oct. 1985.

[63] B. Stupfel, "A fast-domain decomposition method for the solution of electromagnetic scattering by large objects," *IEEE Transactions*, APS 44-10, pp. 1375-1385, Oct 1996.

[64] B. Wohlmuth, *Discretization Methods and Iterative Solvers Based on Domain Decomposition*, Springer, 2001.

[65] A. Quarteroni and A. Valli, *Domain Decomposition Methods for Partial Differential Equations*, Oxford University Press, 1999.

[66] J. Liu and J. Jin, "A highly effective preconditioner for solving the finite element-boundary integral matrix equation of 3-D scattering," *IEEE Transactions*, APS 50-9, pp. 1212-1221, Sep 2002.

[67] J. Lee, R. Lee, and R. Burkholder, "Loop star basis functions and a robust preconditioner for EFIE scattering problems," *IEEE Transactions*, APS 51-8, pp. 1855-1863, Aug 2003.

[68] R. Coifman, V. Rokhlin, and S. Wandzura, "The fast multipole method for the wave equation: A pedestrian perscription," *IEEE Antennas and Propagation Magazine*, Vol. 35, No. 3, pp. 7-12, June 1993.

[69] W. Chew, J. Jin, E. Michielssen, and J. Song, Eds.,*Fast and Efficient Algorithms in Computational Electromagnetics*, Artech House, 2001.

[70] J. Song, C. Lu, W. Chew, "Multilevel fast multipole algorithm for electromagnetic scattering by large complex objects," *IEEE Transactions*, APS 45-10, pp. 1488-1493, Oct 1997.

[71] W. Pascher and R Pregla, "Analysis of rectangular waveguide discontinuities by the method of lines," *IEEE Transactions*, MTT 43-2, pp. 416-420, February 1995.

[72] P. Moller and R. Macphie, "On the graphical representation of electric field lines in waveguides," *IEEE Transactions,* MTT33-3, pp. 187-192 March 1985.

[73] N. Yeo, X. Nie, and L. Li, "A fast analysis of scattering and radiation of large microstrip antenna arrays," *IEEE Transactions*, APS 51-9, pp. 2218-2226, Sept 2003.

[74] M. Catedra, "A comparison between two kinds of equivalent currents to analyze conducting bodies with apertures using moment methods: Application to horns with symmetry of revolution," *IEEE Transactions,* APS 35-7, pp. 782-789, July 1987.